SHAW WEN SHEEN
Theoretical and Empirical Comparison of Water Chemistry and Karst Denudation in Conduit and Diffuse Aquifers, and Implications for Global Karst Denudation Models.
(Under the Direction of GEORGE A. BROOK)

Twelve months of data, from June, 1999 to May, 2000, show that under similar climatic conditions, mean water hardness (118 ppm) in the Lost Cove, Tennessee, conduit aquifer system was significantly lower than hardness (220 ppm) in the Pocket Branch, Georgia, diffuse aquifer system. Estimated long-term annual mean denudation is 39 mm/ka at Pocket Branch and 30 mm/ka at Lost Cove. This significant difference suggests that aquifer type needs to be given more attention in assessing global variations in water chemistry and denudation in karst terrains. This is because the difference in denudation due to aquifer type is as large as differences between cold, temperate and tropical regions due to differences in temperature and soil carbon dioxide. There are both relict and recent tufa deposits along Pocket Branch. Present deposition is influenced by algae with calcite tubes forming around each algal cell. Tufa is deposited at most times of the year except during high streamflow conditions when some erosion occurs. This suggests that in other parts of the world tufa deposition may also be determined by streamflow conditions not by climate alone. About 65% of tufa deposition occurred during the winter and spring wet season, with 35% being deposited in the summer and fall dry season. Relict tufas in Pocket Branch are of early-Holocene age. The large size of the relict tufa at Pocket Falls suggests that in the early to middle Holocene rainfall and ground water was more substantial than today. It is possible that increased summer (monsoonal) rainfall in this region caused massive tufa deposition at Pocket Falls in the past. Climate warming at the end of the Little Ice Age (ca. AD 1850) may explain whey there is tufa deposition at Pocket Branch today.

INDEX WORDS: Water Chemistry, Karst, Denudation, Tufa, Holocene,
Cumberland Plateau

THEORETICAL AND EMPIRICAL COMPARISON OF WATER CHEMISTRY AND KARST DENUDATION IN CONDUIT AND DIFFUSE AQUIFERS, AND IMPLICATIONS FOR GLOBAL KARST DENUDATION MODELS

by

SHAW WEN SHEEN
B.S., National Taiwan University, Taiwan, 1990
M.A., The University of Georgia, 1996

A Dissertation Submitted to the Graduate Faculty of The University of Georgia in Partial Fulfillment of the Requirements for the Degree

DOCTOR OF PHILOSOPHY

ATHENS, GEORGIA

2001

THEORETICAL AND EMPIRICAL COMPARISON OF WATER CHEMISTRY AND KARST DENUDATION IN CONDUIT AND DIFFUSE AQUIFERS, AND IMPLICATIONS FOR GLOBAL KARST DENUDATION MODELS

by

SHAW WEN SHEEN

Approved:

Major Professor: George A. Brook

Committee:
Thomas W. Hodler
David S. Leigh
Vernon G. Meentemeyer
L. Bruce Railsback

Electronic Version Approved:

Gordhan L. Patel
Dean of the Graduate School
The University of Georgia
December 2001

DEDICATION

I would like to dedicate this dissertation to my dear parents in Taiwan.

ACKNOWLEDGMENTS

I would like to acknowledge those who have helped in the completion of this dissertation. I am most indebted to my major professor, George Albert Brook, for the continuous research advice, field assistance and moral support that he gave through this dissertation work. Through eight years (1993 - 2001) of working closely with him, I am much influenced by him both in the field and in the classroom. I must say this "without your help I could not finish this work in time". Unfortunately, Dr. Brook has a serious accident during 2001 summer field work in Namibia. Get well soon, Dr. Brook!

This project is partially funded by an NSF Doctoral Dissertation Improvement Grant. I gratefully acknowledge financial support provided by the University of Georgia.

I would like to acknowledge Drs. Hodler, Leigh, Meentemeyer and Railsback for serving on my committee and giving needed advice on the completion of this work. I would like to thank professors, colleagues and friends: Dr. Lo (Geography), Dr. Kiefer (Brenau University), Dr. Dowd (Geology), Bill McClain (Geology), Dr. Culp (Center for Applied Isotope Studies), Fong Zhao Brook, Yueh-Tsern Shaw, Dr. Peng, Dr. Liu, Dr. Kai Wang, Dr. Xiaojun Yang (University of West Florida), Honglin Xiao, Byong-Woon Jun, Emily and Audrey. I also would like to thank my colleagues in the Department of Social Sciences Education, National Tainan Teachers College. Thanks especially to Dr. Wu and Professor Chu.

Finally, I would like to thank my lovely wife, Amy I-Hwei Wu.

TABLE OF CONTENTS

Page

CHAPTER 1

INTRODUCTION AND LITERATURE REVIEW

A karst landscape is one developed predominantly although not exclusively by the process of solution. The world's karst terrains contain a great diversity of landforms. Common karst forms in temperate climates contrast rather sharply with the typical karst topography of tropical climates. In tropical karst areas, residual hills, rather than the sinkholes so typical of temperate karst, dominate the topography. Climate has been regarded by some as the principal factor explaining the diversity of karst forms (Jakucs 1977; Jennings 1985; Trudgill 1985). Contrary to this view, Ford *et al.* (1988) suggest that the marked differences in landform between the doline karsts of many temperate areas and the cone and tower karst typical of many tropical areas are due to some combination of hydrogeologic setting and differential solution, and not to climate alone. Brook and Ford (1978) point out that recognition of labyrinth and associated tower karst in climates ranging from humid tropical to dry subarctic suggests that these styles are not primarily climate dependent. Perhaps the most compelling unanswered question in the field of karst studies is why humid tropical terrains are more accentuated, and more varied in landform style, than are the karst landscapes of temperate and cold environments. In order to answer this question, several studies have focused on the estimation of denudation rates in different climatic regions.

Corbel (1959) made a great impact on conventional thinking when he published results derived from the analysis of thousands of field samples. Corbel held the view that the rate of karst denudation was determined by climate, the greatest rates occurring in cold, humid climates and the lowest in hot, arid areas. In particular, Corbel claimed that the principal control of solution is temperature and that the cooler it is the greater will be the hardness of runoff water because CO_2 ,which is crucial in the dissolution of limestone, is more soluble at lower temperatures. Based on this argument, Corbel concluded that cold high mountains provide the most favorable environments for limestone solution. These conclusions were contrary to both morphological evidence and conventional wisdom that weathering processes in general are most rapid in hot humid conditions.

Smith and Atkinson (1976) attempted to determine if limestone terrains, and the erosion processes by which they are produced, are different in the various climatic belts of the world. They used two data sets: 231 reports on the mean hardness of spring and river waters in different regions of the world, and 134 estimates of the rate of solutional denudation. Smith and Atkinson (1976) found a trend in mean hardness from a minimum value in the arctic/alpine zone to a maximum in temperate regions with a slight decline in the tropical zone. This trend suggested that climate may influence water hardness, but it supports neither the hypothesis of Corbel nor that of his opponents, since the greatest values are found in temperate regions. Smith and Atkinson (1976) found erosion rates to be lowest in the tropical region and higher in the temperate zone, with the highest values in the arctic/alpine zone. Although these results tend to support Corbel’s hypothesis that the greatest erosion rates occur in the arctic/alpine regions, the differences between the means for each region are not statistically significant. Even today, karst geomorphologists are not sure if chemical denudation rates in tropical karst terrains, with the most spectacular landforms, are higher than in temperate and cold karst terrains.

A hypothesis that has been proposed to explain both the more varied nature of tropical karst and lower-than-expected denudation rates is that of Sweeting (1972). She has suggested that intense rains tend to form "conduit flow" underground drainage systems in karst while less intense rainfall tends to promote the development of "diffuse flow" aquifers. In conduit systems rainfall passes quickly underground via stream sinks and into caves. Flow velocities are comparable to surface rivers and so springs react quickly to intense storms. Usually, water runs off so quickly that it does not have time to equilibrate with soil CO_2, nor to reach saturation with respect to (w.r.t.) carbonate, and so waters have relatively low hardness. In diffuse systems the rainfall diffuses slowly through the soil and into relatively small cavities so that it moves gradually towards the spring outlet. The water is in contact with the soil and bedrock for a considerable period and so it picks up relatively more carbonate in solution. In addition, diffuse springs react much more slowly to storms because flow-through times from recharge to discharge are quite long. In reality, systems are never purely conduit or purely diffuse but fall into a range of types from predominantly conduit to predominantly diffuse, with intermediate conditions common.

If tropical areas are characterized by a greater abundance of conduit systems this might explain the lower rates of solution than in temperate areas where diffuse-flow aquifers may be more common. The problem with Sweeting’s suggestion, is that we really do not know enough about conduit and diffuse systems to fully assess them. Nor do we know if diffuse flow generates one suite of karst landforms while conduit flow generates another. If we knew how solutional denudation differs in "predominantly conduit" systems compared to "predominantly diffuse" systems we would be in a better position to assess the role of aquifer character (mainly conduit versus diffuse) on denudation rate and karst landform development.

The Solution Process and Karst Denudation

Solution occurs within the CO_2-water-carbonate system. Carbonate rocks (limestone and dolomite) dissolve in water into their constituent ions. The reaction is a function of temperature. The solubility of calcite in pure water is only 6 ppm at 10^0C. Most carbonate minerals are readily soluble in acid, and the acid most important in karst terrains is carbonic acid, formed by the dissolution of gaseous CO_2 in water. The solution of CO_2 from the gas phase takes place in two steps. First, CO_2 is transported across the gas-liquid interface to form aqueous CO_2 in solution. The dissolved CO_2 then reacts with water to form carbonic acid. The concentration of dissolved CO_2 increases with increasing CO_2 pressure in the gas phase that coexists with the aqueous solution. Carbonic acid dissociates in solution to form the bicarbonate ion, a little of which in turn dissociates to form the carbonate ion. Following Gillieson (1996), the solution of limestone and dolomite in karst terrains can be described by the equations:

$$CO_{2(g)} \rightleftharpoons CO_{2(aq)} \tag{1.1}$$

$$CO_{2(aq)} + H_2O \rightleftharpoons H_2CO_3^0 \tag{1.2}$$

$$H_2CO_3^0 \rightleftharpoons H^+ + HCO_3^- \tag{1.3}$$

$$CaCO_3 \text{ (limestone)} \rightleftharpoons Ca^{2+} + CO_3^{2-} \tag{1.4}$$

$$CaMg(CO_3)_2 \text{ (dolomite)} \rightleftharpoons Ca^{2+} + Mg^{2+} + 2CO_3^{2-} \tag{1.5}$$

$$H^+ + CO_3^{2-} \rightleftharpoons HCO_3^- \tag{1.6}$$

The last reaction (1.6), disturbs the equilibrium of (1.4) and (1.5) by removing CO_3^{2-} so that more carbonate must dissociate to restore the balance. In addition, the association of $H^+ + CO_3^{2-}$ disturbs the equilibrium of (1.3), promoting further dissociation. This in turn disturbs the equilibrium of (1.2) and ultimately (1.1), causing more CO_2 to dissolve in the water. These processes continue until the forward and reverse reaction rates are equal, at which point the system is in equilibrium and the solution is saturated w.r.t. limestone and dolomite. Combined, the equations give the often quoted dissolution equations for limestone and dolomite:

$CaCO_3$ (limestone) + $CO_{2(g)} + H_2O \rightleftharpoons Ca^{2+} + 2HCO_3^-$

$CaMg(CO_3)_2$ (dolomite) + $2CO_{2(g)} + 2H_2O \rightleftharpoons Ca^{2+} + Mg^{2+} + 4HCO_3^-$

The total amount of limestone and dolomite that can be dissolved at saturation equilibrium per unit volume of water is directly related to the CO_2 partial pressure of the air in contact with the water (either in the atmosphere or in the soil air). This determines the amount of CO_2 that can be dissolved in the water. Most studies suggest that soil CO_2 is crucial in the dissolution of carbonate rocks in karst terrains. Soil CO_2 acidifies the water, which then dissolves carbonate rocks. Carbon dioxide concentration in soils varies from 0.03 volume %, the atmospheric value, to 10 volume % (White, 1988). The solubility of CO_2 gas in water decreases as temperature increases. Although CO_2 is more soluble in cold water, the colder water makes the reaction proceed more slowly (Gillieson, 1996). Temperature also affects the dissolution of limestone and dolomite in karst terrains. Limestone and dolomite are more soluble in colder water. But the solution rates are faster in warmer water and the karst water will be close to the saturation state (White, 1990).

Palmer (1990) argued that whether water is in an "open" or a "closed" system influences the dissolution process. In an open system, as dissolution consumes aqueous CO_2, additional CO_2 is added to maintain an equilibrium state. In a closed system, the infiltrating water fills pore spaces, which cuts off the supply of gaseous CO_2. As further solution consumes dissolved CO_2, the equilibrium is approached at a lower CO_2 content than that of the original open system. As a result, the equilibrium concentration of dissolved carbonate is lower in a closed system than it would be in an open system.

Intermediate situations are also common as groundwater may alternate between open and closed systems along its path of flow (Palmer 1990).

The solutionally transported mass loss from karst basins, expressed as if it were removed uniformly from the land surface, is commonly known as "karst denudation" (Ford *et al.*, 1988). In 1984 White developed a global karst denudation model which assumed that an equilibrium is reached between infiltrating water and limestone under open system conditions.

$$D = \frac{100}{p \times 4^{1/3}} \times \left(\frac{K_C \times K_1 \times K_{CO2}}{K_2}\right)^{1/3} \times pCO_2^{\ 1/3} \times (P - E)$$

where D is the denudation rate in millimeters per thousand years for the system at equilibrium, pCO_2 is given in atmospheres, *p* is the density of limestone, P is precipitation in millimeters per year, E is evapotranspiration in millimeters per year, and K_C, K_1, K_{CO2}, and K_2 are chemical equilibrium constants for carbonate reactions (White 1984).

Aim of the Dissertation

The major aim of this dissertation is to use both a theoretical and empirical approach to assess water chemistry characteristics and karst denudation rates as an aid to interpreting karst landscape types. In particular, the objective is to assess the possible importance of aquifer type in determining denudation rates and erosion or deposition of carbonate. The dissertation consists of three major papers: Chapters 2, 3, and 4, which are followed by a conclusion chapter, Chapter 5, that brings together the findings of the three separate studies.

Chapter 2 is a theoretical study to estimate water hardness and karst denudation in different climatic zones under "open" and "closed" system conditions. Denudation rates in tropical, temperate, and arctic/alpine terrains are modeled using theoretical equations for the solution of limestone and dolomite. Theoretical denudation rates are calculated for CO_2 concentrations from $10^{-3.5}$ to $10^{-1.0}$ atmosphere (atm.), temperatures from 0°C to 30°C, and annual runoff from 500 to 3,000 mm. The Drake (1980) soil CO_2 and the Brook-Folkoff-Box (1983) soil CO_2 equations are used to develop global denudation models. The resulting data are used to assess the magnitude of karst denudation in the different climatic environments due only to aquifer type and to compare these differences with differences due to other factors.

Chapter 3 is an empirical study of a conduit karst region in Tennessee (Lost Cove) and a diffuse karst region in Georgia (Pocket Branch), both with very similar long-term climates. This chapter examines how water hardness and denudation in these two basins varied through a 12-month period and determines whether annual denudation is indeed higher in a diffuse system than in a conduit system. Temporal variations in chemical denudation (bimonthly and seasonally) are also examined, as are factors controlling this distribution of erosion. Differences in denudation between the two areas, due to aquifer type alone, are compared with theoretical estimates outlined in Chapter 2. The chapter concludes by assessing whether the difference in denudation due to aquifer type is high enough to explain denudation values from tropical karst areas that are lower than rates from temperate and colder environments.

Chapter 4 is a second empirical study to examine controls on present-day tufa deposition in a diffuse aquifer system, namely Pocket Branch in Georgia, USA. This valley contains the only known tufa in the State of Georgia. As denudation in a diffuse system is reduced where tufa is deposited, this chapter attempts to determine how tufa deposition affects denudation, why deposition occurs where it does, and what factors control its magnitude throughout the year.

The final chapter, Chapter 5, brings together the findings of Chapters 2 - 4 by comparing theory with empirical results. In particular, an attempt is made to place the impact of aquifer type on denudation in a global perspective. Can it explain why there is so much overlap in denudation rates in different climatic environments, and is the difference in denudation between conduit-flow and diffuse-flow aquifers substantial enough to warrant consideration of aquifer type in any assessment of global denudation patterns?

REFERENCES

Brook, GA and Ford DC. 1978. The origin of labyrinth and tower karst and the climatic conditions necessary for their development. *Nature* **275**: 492-6.

Brook, GA, Folkoff, ME and Box, EO. 1983. A world model of soil carbon dioxide. *Earth Surface Processes and Landforms* **8**:79-88.

Corbel, J. 1959. Erosion en terrain calcaire. *Ann. Geog.* **68**: 97-120

Drake, JJ. 1980. The effect of soil activity on the chemistry of carbonate groundwater. *Water Resources Research* **16**: 381-6.

Ford, DC, Palmer, AN and White, WB. 1988. Landform development: karst. In *Hydrogeology,* eds. Back, W, Rosenshein, JS and Seaber PR, 401-12. Boulder, Colo: Geological Society of America, The Geology of North America Vol. O-2.

Gillieson, D. 1996. *Cave: Processes, Development and Management*. Oxford, UK: Blackwell.

Jakucs, L. 1977. *Morphogenetics of Karst Regions*. New York: John Wiley & Sons.

Jennings, JN. 1985. *Karst Geomorphology*. Oxford, UK: Basil Blackwell.

Palmer, AN. 1990. Groundwater processes in karst terranes. In *Groundwater geomorphology: The role of subsurface water in earth-surface processes and landforms*, eds. Higgins, CG and Coates, DR, 177-209. Boulder, Colo: Geological Society of America, Geological Society of America Special Paper 252.

Smith, DI and Atkinson, TC. 1976. Process, landforms and climate in limestone regions. In *Geomorphology and climate,* ed. Derbyshire, E, 367-409. New York: John Wiley.

Sweeting, MM. 1972. *Karst Landforms*. London: Macmillan.

Trudgill, S. 1985. *Limestone Geomorphology*. London: Longman.

White, WB. 1984. Rate process: Chemical kinetics and karst landform development. In *Groundwater as a geomorphic agent,* ed. LaFleur, RG, 227-48. Boston: Allen and Unwin.

White, WB. 1988. *Geomorphology and Hydrology of Karst Terrains*. New York: Oxford University Press.

White, WB. 1990. Surface and near-surface karst landforms. In *Groundwater geomorphology: The role of subsurface water in earth-surface processes and landforms*, eds. Higgins, CG and Coates, DR, 157-75. Boulder, Colo: Geological Society of America, Geological Society of America Special Paper 252.

CHAPTER 2

A WORLD MODEL OF CHEMICAL MODEL OF CHEMICAL DENUDATION IN KARST TERRAINS[*]

---

[*] Sheen,S.-W. (2000) “A World Model of Chemical Denudation in Karst Terrains”. *Professional Geographer* 52(3): 397-406.

Abstract

In this paper, I develop global karst chemical denudation models using chemical equilibrium equations. Theoretical karst chemical denudation rates are calculated as soil carbon dioxide concentration varies from $10^{-3.5}$ atm to $10^{-1.0}$ atm, temperature varies from 0°C to 30°C, and annual runoff varies from 500 mm to 3,000 mm. Both open and closed karst solution systems are examined. The Drake (1980) and the Brook-Folkoff-Box (1983) soil pCO_2 equations are used to develop chemical denudation models for different carbonate rocks (limestone and dolomite), climate (tropical, temperate, and arctic/alpine terrains), and karst solution type (open and close systems). The major conclusion is that the karst solution type, least known in the past karst studies, is an important factor to controlling chemical denudation rates. Key Words: karst, chemical denudation, open system, closed system.

Introduction

A karst landscape is one developed predominantly by a solution process. The most common rocks making karst landforms are limestone and dolomite. Perhaps the most compelling unanswered question in the field of karst studies is why humid tropical karst terrains are more accentuated than are the karst landscapes of temperate and colder environments. In order to answer this question, most karst studies focus on the estimation of karst chemical denudation rates in different climatic settings (Williams and Dowling 1979; Gunn 1981; Crowther 1984; Day 1984; Zambo and Ford 1997). However, karst geomorphologists are still not sure if tropical karst terrains with the most spectacular landforms have the higher chemical denudation rates than temperate and cold karst terrains (Sweeting 1972; Jakucs 1977; Jennings 1985; Trudgill 1985; White 1988; Ford and Williams 1989).

The solution of limestone and dolomite in karst terrains are generally explained by the equations:

$$CaCO_3 \text{ (limestone)} + CO_2 + H_2O \rightleftharpoons Ca^{2+} + 2HCO_3^-$$

$$CaMg(CO_3)_2 \text{ (dolomite)} + 2CO_2 + 2H_2O \rightleftharpoons Ca^{2+} + Mg^{2+} + 4HCO_3^-$$

The total amount of limestone and dolomite that can be dissolved at saturation equilibrium per unit volume of water is a direct function of the carbon dioxide partial pressure of the air in contact with the water (either in the atmosphere or in the soil air) as this determines the amount of carbon dioxide that can dissolve in the water. It is an inverse function of the water temperature because carbon dioxide is more soluble in colder water (Ford and Williams 1989). Temperature also affects the dissolution of limestone and dolomite in karst terrains. Limestone and dolomite are more soluble in colder water. But the solution rates are faster in warmer water and the karst water will be close to the saturation state (White 1990).

White (1984) developed a global karst chemical denudation model which assumed that an equilibrium is reached between infiltrating water and limestone under open system conditions.

$$D = \frac{100}{p \times 4^{1/3}} \times \left(\frac{K_C \times K_1 \times K_{CO2}}{K_2}\right)^{1/3} \times pCO_2^{\ 1/3} \times (P - E)$$

where D is the denudation rate in millimeters per thousand years for the system at equilibrium, pCO_2 is given in atmospheres, *p* is the density of limestone, P is precipitation in millimeters per year, E is evapotranspiration in millimeters per year, and K_C, K_1, K_{CO2}, and K_2 are chemical equilibrium constants for carbonate reactions (White 1988).

In an open system, as dissolution consumes aqueous carbon dioxide, additional carbon dioxide is added to maintain an equilibrium state (Palmer 1990). However, both open and closed systems occur in karst terrains (Drake and Ford 1981; Ford and Drake 1982; Ford et al. 1988; Palmer 1990; White 1990). In a closed system, the infiltrating water fills pore spaces, what cuts off the supply of gaseous carbon dioxide. As further solution consumes dissolved carbon dioxide, the equilibrium is approached at a lower carbon dioxide content than that of the original open system. As a result, the equilibrium concentration of dissolved carbonate is lower than it would have been in an open system. Intermediate situations are also common: groundwater may alternate between open and closed systems along its path of flow (Palmer 1990). Therefore, open and closed system conditions are needed to be considered in modeling karst chemical denudation. However, White's (1984) model only examined an open system condition.

The aim of this paper is to develop global chemical denudation models for both open and closed karst systems in order to compare the chemical denudation rates in tropical, temperate, and arctic/alpine terrains. This global model improves the White (1984) equation by

(1) considering both ions and ion pairs in the karst system (e.g., $H_2CO_3^*$ (= $CO_{2(aqueous)}$ + $H_2CO_3^0$), HCO_3^-, CO_3^{2-}, H^+, OH^-, Ca^{2+}, $CaHCO_3^+$, $CaCO_3^0$, Mg^{2+}, $MgHCO_3^+$, $MgCO_3^0$) (Stumm and Morgan 1996),

(2) accurately considering the electrical neutrality (i.e., limestone system: mH^+ (molality of hydrogen ion) + 2 × mCa^{2+} (2 × molality of calcium ion) + $mCaHCO_3^+$ (molality of $CaHCO_3^+$) = mOH^- (molality of OH^-) + $mHCO_3^-$ (molality of HCO_3^-) + 2 × mCO_3^{2-} (2 × molality of CO_3^{2-}) and dolomite system: $mH^+ + 2 \times mCa^{2+} + mCaHCO_3^+ + 2 \times mMg^{2+} + mMgHCO_3^+ = mOH^- + mHCO_3^- + 2 \times mCO_3^{2-}$),

(3) calculating ion activities using the extended Debye-Huckel equation (e.g., aCa^{2+} (activity of calcium cation) = mCa^{2+} (molality of calcium cation) × rCa^{2+} (activity coefficient of calcium cation) (Stumm and Morgan 1996),

(4) considering the activity of water (Wigley 1977), and

(5) calculating groundwater hardness (i.e., limestone system: water hardness (ppm, as $CaCO_3$) = mCa × 100.09 × 1000 mg/L, and dolomite system: water hardness (ppm, as $CaCO_3$) = (mCa + mMg) × 100.09 × 1000 mg/L).

The study consists of two parts: theoretical karst chemical denudation models and global models of chemical denudation in karst terrains. First theoretical chemical denudation rates are calculated as carbon dioxide concentration varies from $10^{-3.5}$ atm to $10^{-1.0}$ atm, temperature varies from 0°C to 30°C, and annual runoff varies from 500 to 3,000 mm for both open and closed systems. The theoretical model is based on three variables: temperature, soil pCO_2, and runoff. Drake (1980) and Brook et al. (1983) developed soil CO_2 concentration models using climate variables. In the second part the Drake soil CO_2 concentration equation (1980) and the Brook-Folkoff-Box soil CO_2

concentration equation (1983) are used to develop global karst chemical denudation under open and closed system conditions.

Methods

The karst denudation equation is (Ford and Williams 1989):

$$D = 0.001 \times R \times \frac{H}{p}$$

where D is the karst denudation rate (mm/1000 years), R is annual runoff (mm), H is water hardness in groundwater (mg/L, as $CaCO_3$), and *p* is the density of carbonate rocks (g/cm^3). In this study the density of limestone (calcite) is assumed to be 2.71 g/cm^3, and the density of dolomite 2.85 g/cm^3 (Ford and Williams 1989).

Using chemical equilibrium equations (Stumm and Morgan 1996), Fortran programs are developed to calculate water hardness values in an equilibrium state. In an open limestone system, seven equilibrium equations are considered.

$$CO_{2(g)} + H_2O \rightleftarrows H_2CO_3^*$$

$$H_2CO_3^* \rightleftarrows H^+ + HCO_3^-$$

$$HCO_3^- \rightleftarrows H^+ + CO_3^{2-}$$

$$H_2O \rightleftarrows H^+ + OH^-$$

$$CaCO_{3(calcite)} \rightleftarrows Ca^{2+} + CO_3^{2-}$$

$$Ca^{2+} + HCO_3^- \rightleftarrows CaHCO_3^+$$

$$Ca^{2+} + CO_3^{2-} \rightleftarrows CaCO_3^0$$

There are eight unknown variables: $H_2CO_3^*$, HCO_3^-, CO_3^{2-}, H^+, OH^-, Ca^{2+}, $CaHCO_3^+$, and $CaCO_3^0$. There are eight equations (K_{CO2}, K_1, K_2, K_W (equilibrium constant of water), K_C (equilibrium constant of limestone), K_{CaHCO3}, K_{CaCO3}, and electroneutrality) used to solve for these variables (Morse and Mackenzie 1990; Stumm and Morgan 1996).

In a closed limestone system, a soil water system is considered first.

$CO_{2(g)} + H_2O \rightleftharpoons H_2CO_3^*$

$H_2CO_3^* \rightleftharpoons H^+ + HCO_3^-$

$HCO_3^- \rightleftharpoons H^+ + CO_3^{2-}$

$H_2O \rightleftharpoons H^+ + OH^-$

Then, this equilibrated water reacts with limestone to reach a new equilibrium in a closed system. In this closed limestone system, six equilibrium equations are considered.

$H_2CO_3^* \rightleftharpoons H^+ + HCO_3^-$

$HCO_3^- \rightleftharpoons H^+ + CO_3^{2-}$

$H_2O \rightleftharpoons H^+ + OH^-$

$CaCO_{3(calcite)} \rightleftharpoons Ca^{2+} + CO_3^{2-}$

$Ca^{2+} + HCO_3^- \rightleftharpoons CaHCO_3^+$

$Ca^{2+} + CO_3^{2-} \rightleftharpoons CaCO_3^0$

There are eight unknown variables: $H_2CO_3^*$, HCO_3^-, CO_3^{2-}, H^+, OH^-, Ca^{2+}, $CaHCO_3^+$, and $CaCO_3^0$. There are eight equations (K_1, K_2, K_W, K_C, K_{CaHCO3}, K_{CaCO3}, electroneutrality, and new total dissolved carbon = old total dissolved carbon + total dissolved calcium) used to solve for these variables. Figure 2.1 shows water hardness values in open and closed equilibrium limestone systems as pCO_2 varies from $10^{-3.5}$ atm to $10^{-1.0}$ atm and temperature varies from 0°C to 30°C.

In an open equilibrium dolomite system, nine equilibrium equations are considered.

$CO_{2(g)} + H_2O \rightleftharpoons H_2CO_3^*$

$H_2CO_3^* \rightleftharpoons H^+ + HCO_3^-$

$HCO_3^- \rightleftharpoons H^+ + CO_3^{2-}$

$H_2O \rightleftharpoons H^+ + OH^-$

$CaMg(CO_3)_{2(dolomite)} \rightleftharpoons Ca^{2+} + Mg^{2+} + 2CO_3^{2-}$

$Ca^{2+} + HCO_3^- \rightleftharpoons CaHCO_3^+$

$Ca^{2+} + CO_3^{2-} \rightleftharpoons CaCO_3^0$

$Mg^{2+} + HCO_3^- \rightleftharpoons MgHCO_3^+$

$Mg^{2+} + CO_3^{2-} \rightleftharpoons MgCO_3^0$

There are 11 unknown variables: $H_2CO_3^*$, HCO_3^-, CO_3^{2-}, H^+, OH^-, Ca^{2+}, $CaHCO_3^+$, $CaCO_3^0$, Mg^{2+}, $MgHCO_3^+$, and $MgCO_3^0$. There are 11 equations (K_{CO2}, K_1, K_2, K_W, K_D (equilibrium constant of dolomites), K_{CaHCO3}, K_{CaCO3}, K_{MgHCO3}, K_{MgCO3}, electroneutrality, and total dissolved calcium = total dissolved magnesium) used to solve for these 11 variables.

In a closed equilibrium dolomite system, a soil water system is considered first.

$CO_{2(g)} + H_2O \rightleftharpoons H_2CO_3^*$

$H_2CO_3^* \rightleftharpoons H^+ + HCO_3^-$

$HCO_3^- \rightleftharpoons H^+ + CO_3^{2-}$

$H_2O \rightleftharpoons H^+ + OH^-$

This equilibrated water then reacts with dolomite to reach a new equilibrium in a closed system. In this closed equilibrium dolomite system, eight equilibrium equations are considered.

$H_2CO_3^* \rightleftharpoons H^+ + HCO_3^-$

$HCO_3^- \rightleftharpoons H^+ + CO_3^{2-}$

$H_2O \rightleftharpoons H^+ + OH^-$

$CaMg(CO_3)_{2(dolomite)} \rightleftharpoons Ca^{2+} + Mg^{2+} + 2CO_3^{2-}$

$Ca^{2+} + HCO_3^- \rightleftharpoons CaHCO_3^+$

$Ca^{2+} + CO_3^{2-} \rightleftharpoons CaCO_3^0$

$Mg^{2+} + HCO_3^- \rightleftharpoons MgHCO_3^+$

$Mg^{2+} + CO_3^{2-} \rightleftharpoons MgCO_3^0$

There are 11 unknown variables: $H_2CO_3^*$, HCO_3^-, CO_3^{2-}, H^+, OH^-, Ca^{2+}, $CaHCO_3^+$, $CaCO_3^0$, Mg^{2+}, $MgHCO_3^+$, and $MgCO_3^0$. There are 11 equations (K_1, K_2, K_W, K_D, K_{CaHCO3}, K_{CaCO3}, K_{MgHCO3}, K_{MgCO3}, electroneutrality, total dissolved calcium = total dissolved Mg, and new total dissolved carbon = old total dissolved carbon + 2 × total dissolved calcium) used to solve for these 11 variables. The water hardness values in the dolomite system are shown in Figure 2.2. Global models between karst chemical denudation rates and runoff values were then developed for different climatic conditions (tropical, temperate, and arctic/alpine areas) under both open and closed systems.

Results

Theoretical Chemical Denudation in Karst Terrains

The theoretical water hardness values for both open and closed karst systems were calculated using the chemical equilibrium equations (Figs. 2.1 and 2.2). Theoretical chemical denudation rates were then calculated from the calculated water hardness values using the runoff values assumed to range from 500 to 3,000 mm. Chemical denudation rates (mm/1000 years) were calculated in limestone under open and closed equilibrium systems for the temperature values = 0°C, 15°C, and 30°C, the pCO_2 values = $10^{-3.5}$, $10^{-2.0}$, and $10^{-1.0}$ atm, and the runoff values = 500, 1,000, 2,000, and 3,000 mm/year (Figs. 2.3 and 2.4). Chemical denudation rates in dolomite under open and closed equilibrium systems were also calculated for the same temperature, pCO_2 and runoff values (Figs. 2.5 and 2.6). These results indicate that the chemical denudation in karst terrains is controlled by five major variables: soil CO_2 concentration, temperature, dissolution type (open system vs. closed system), carbonate rock type (limestone vs. dolomite), and runoff.

Soil CO_2 concentration, temperature, and dissolution type determine the water hardness from the solution of carbonate rocks. Karst terrains with higher soil CO_2 concentrations and lower temperatures will produce greater chemical denudation rates than other areas with lower soil CO_2 concentrations and higher temperatures. Dissolution types also affect chemical denudation rates. Chemical denudation values are higher under open systems and lower under closed systems. Higher runoff will produce greater chemical denudation. These results are based on the assumption that the karst system reaches an equilibrium state. Disequilibrium systems occur in the real world (Ford et al. 1988; Palmer 1990). Especially, dolomite takes longer time than limestone to reach an equilibrium state (White 1984). Therefore, using chemical equilibrium equations, karst chemical denudation rates at an equilibrium state can be estimated by assuming soil carbon dioxide concentration, temperature, solution type, carbonate rock type, and runoff. The results also indicate that the karst solution type, least known in past studies, can be an important factor to controlling chemical denudation.

A World Model of Karst Chemical Denudation

Global chemical denudation models were developed for both open and closed systems in karst terrains. The Drake (1980) and the Brook-Folkoff-Box (1983) soil pCO_2 equations were used to develop a world model of groundwater hardness in karst terrains under an equilibrium state.

The Global Chemical Denudation Models Using the Drake (1980) Soil pCO_2 Equation

Drake (1980) developed a soil pCO_2 model:

$$\mathrm{Log}_{10}(pCO_2^{*}) = -1.97 + 0.04 \times T$$

$$pCO_{2(soil)} = \{(0.21 - pCO_{2(soil)})/0.21\} \times pCO_2^{*}$$

where T is the annual average air temperature or groundwater temperature (°C). The global model of chemical denudation is based on the assumption that the annual temperature is 25°C in tropical karst, 15°C in temperate karst, and 5°C in arctic/alpine karst (Christopherson 1997). Soil pCO_2 concentration values are then calculated for these three climatic regions using the Drake (1980) equation and the water hardness values are computed for both limestone and dolomite terrains under open and closed dissolution types using chemical equilibrium equations.

Table 2.1 indicates that the water hardness values in an open solution type are greater than those in a closed solution type. The water hardness in tropical limestone terrains under open solution systems is about 1.75 times the value under closed solution systems, the water hardness in temperate limestone terrains under open solution systems is about 2.13 times the value under closed solution systems, and the water hardness in arctic/alpine limestone terrains under open solution systems is about 2.76 times the value under closed solution systems.

Figures 2.7 and 2.8 show the global karst chemical denudation rates in limestone and dolomite terrains under open and closed systems as the runoff values increase from 500 to 3,000 mm/year. The karst chemical denudation rates are larger in open systems and smaller in closed systems. For 2,000 mm annual runoff value, the chemical denudation rates of limestone terrains are from 201 mm/kyrs (arctic/alpine regions) to 249 mm/kyrs (tropical regions) under open systems and 72 mm/kyrs (arctic/alpine regions) to 143 mm/kyrs (tropical regions) under closed systems. For 2,000 mm annual runoff value, the chemical denudation rates of dolomite terrains are from 248 mm/kyrs (arctic/alpine regions) to 267 mm/kyrs (tropical regions) under open systems and 67 mm/kyrs (arctic/alpine regions) to 135 mm/kyrs (tropical regions) under closed systems.

The relationships between the karst chemical denudation rates and the runoff are produced for tropical, temperate, and arctic/alpine karst landscapes (Table 2.2). This indicates that the dissolution type is an important factor to control karst chemical denudation. Also under the same dissolution type and the same runoff, chemical denudation rates are the largest in tropical karst terrains and the least in arctic/alpine karst terrains.

The Global Chemical Denudation Models Using the Brook-Folkoff-Box (1983) Soil pCO_2 Equation

Brook et al. (1983) developed a soil pCO_2 model:

$$\log_{10}(pCO_{2(soil)}) = -3.47 + 2.09 \times (1 - e^{-0.00172 \times AET})$$

where $pCO_{2(soil)}$ is the mean growing season soil pCO_2, and AET is the mean annual actual evapotranspiration (mm). This study assumed actual evapotranspiration to be 1,500 mm in tropical karst, 900 mm in temperate karst, and 300 mm in arctic/alpine karst (Christopherson 1997). Soil pCO_2 concentration values are computed for these three climatic regions using the Brook-Folkoff-Box (1983) equation and the water hardness values are calculated for both limestone and dolomite karst terrains under open and closed conditions.

Table 2.3 indicates that the water hardness in tropical limestone karst under open systems is about 2.55 times the value under closed systems, the water hardness in temperate limestone terrains under open systems is about 3.28 times the value under closed systems, and the water hardness value in arctic/alpine limestone terrains under open solution systems is about 6.90 times the value under closed systems.

Figures 2.9 and 2.10 show the global karst chemical denudation rates in limestone and dolomite karst terrains under open and closed systems as the runoff values increase from 500 to 3,000 mm/year. For 2,000 mm annual runoff value, the chemical denudation rates of the limestone karst are from 102 mm/kyrs (arctic/alpine regions) to 179 mm/kyrs (tropical regions) under open systems and 14 mm/kyrs (arctic/alpine regions) to 70 mm/kyrs (tropical regions) under closed systems. For 2,000 mm annual runoff value, the chemical denudation rates of the dolomite terrains are from 124 mm/kyrs (arctic/alpine regions) to 191 mm/kyrs (tropical regions) under open systems and 15 mm/kyrs (arctic/alpine regions) to 63 mm/kyrs (tropical regions) under closed systems.

The relationship between karst chemical denudation rates and runoff is developed for these three climatic regions. Table 2.4 indicates that under open systems, the chemical denudation rates are about the same in both tropical and temperate karst terrains and both rates are higher than those in arctic/alpine karst. A comparison between Table 2.2 and Table 2.4 indicates that karst chemical denudation rates calculated from the Brook-Folkoff-Box (1983) soil pCO_2 equation are less than those calculated from the Drake (1980) soil pCO_2 equation which predicts the higher soil carbon dioxide concentration levels.

Discussion

Smith and Atkinson (1976) developed global empirical karst chemical denudation regression equations from 134 estimates of dissolution rates around the world:

$Y = 0.063 \times X + 5.7$ in tropical karst

$Y = 0.055 \times X + 7.9$ in temperate karst

$Y = 0.036 \times X + 7.4$ in arctic/alpine karst

where Y is the karst chemical denudation (mm/kyrs), and X is the annual runoff (mm). In this study I have developed several global models of karst chemical denudation for different carbonate rock (limestone vs. dolomite) and different solution systems (open system vs. closed system) using the Drake (1980) and the Brook-Folkoff-Box (1983) soil pCO_2 equations (Tables 2.2 and 2.4). In order to obtain a simpler global chemical denudation model this study averages these chemical denudation models. Using the Drake (1980) equation, the global chemical denudation models are:

$Y = 0.0992 \times X$ in tropical karst

$Y = 0.0869 \times X$ in temperate karst

$Y = 0.0734 \times X$ in arctic/alpine karst

where Y is the karst chemical denudation (mm/kyrs), and X is the annual runoff (mm). Using the Brook-Folkoff-Box equation, the global chemical denudation models are:

$Y = 0.0629 \times X$ in tropical karst

$Y = 0.0566 \times X$ in temperate karst

$Y = 0.0319 \times X$ in arctic/alpine karst

where Y is the karst chemical denudation (mm/kyrs), and X is the annual runoff (mm). A comparison of both global models developed in this paper, with the empirical model of Smith and Atkinson (1976) indicates that the karst chemical denudation rates calculated using the Brook-Folkoff-Box (1983) equation are very similar to those estimated by the regression equations developed by Smith and Atkinson (1976) (Fig. 2.11).

I conclude that more accurate chemical denudation rates in global karst terrains can be estimated if climate, carbonate rock type, solution type, and runoff are more precisely known. Also tropical karst terrains with the most dramatic landforms could be produced by the higher chemical denudation potential, higher temperature (faster chemical reaction to reach equilibrium states), and higher runoff.

Conclusions

This study has shown the following three conclusions. First, chemical denudation in karst terrains are controlled by five major variables: soil CO_2 concentration, temperature, dissolution type (open system vs. closed system), carbonate rock type (limestone vs. dolomite), and runoff. The differences in chemical denudation rates between tropical, temperate and arctic/alpine karst are controlled by these factors.

Second, both the Drake (1980) and the Brook-Folkoff-Box (1983) equations develop a global relationship between climate and soil pCO_2. Using these equations, global karst chemical denudation rates can be modeled. The results show tropical karst has a greater chemical denudation potential than temperate and arctic/alpine karst. The spectacular tropical karst can be produced by higher temperature (faster chemical reaction to reach equilibrium states), higher soil carbon dioxide concentration, and higher runoff.

Third, the solution type (open system vs. closed system) is an important factor to controlling the water chemistry and chemical denudation in karst terrains. The open system has a higher chemical denudation potential than the close system. In the future more field studies need to be done to examine the solution types in karst terrains of different climatic regions.

Literature Cited

Brook,George A., Folkoff,Michael E., and Box,Elgene O. 1983. A world model of soil carbon dioxide. *Earth Surface Processes and Landforms* 8:79-88.

Christopherson,Robert W. 1997. *Geosystems: An Introduction to Physical Geography*. 3rd ed. Upper Saddle River, NJ: Prentice Hall.

Crowther,J. 1984. Soil carbon dioxide and weathering potentials in tropical karst terrain, peninsular Malaysia: a preliminary model. *Earth Surface Processes and Landforms* 9:397-407.

Day,Michael 1984. Carbonate erosion rates in southwestern Wisconsin. *Physical Geography* 5(2):142-9.

Drake,John J. 1980. The effect of soil activity on the chemistry of carbonate groundwater. *Water Resources Research* 16: 381-6.

Drake,John J., and Ford,Derek C. 1981. Karst solution: a global model for groundwater solute concentrations. *Transactions, Japanese Geomorphological Union* 2(2):223-230.

Ford,Derek C., and Drake,John J. 1982. Spatial and temporal variations in karst solution rates: the structure of variability. In *Space and time in geomorphology*, ed. C.E. Thorn, 147-170. London: Allen & Unwin.

Ford,Derek C., Palmer,Arthur N., and White,William B. 1988. Landform development: karst. In *Hydrogeology,* eds. W. Back, J.S. Rosenshein, and P.R. Seaber, 401-12. Boulder, Colo: Geological Society of America, The Geology of North America Vol. O-2.

Ford,Derek C., and Williams,Paul W. 1989. *Karst Geomorphology and Hydrology*. London: Chapman & Hall.

Gunn,John 1981. Limestone solution rates and processes in the Waitomo District, New Zealand. *Earth Surface Processes and Landforms* 6: 427-45.

Jakucs,Laszlo 1977. *Morphogenetics of Karst Regions*. New York: John Wiley & Sons.

Jennings,Joseph N. 1985. *Karst Geomorphology*. Oxford, UK: Basil Blackwell.

Morse,John W., and Mackenzie,Fred T. 1990. *Geochemistry of Sedimentary Carbonates*. Amsterdam: Elsevier.

Palmer,Arthur N. 1990. Groundwater processes in karst terranes. In *Groundwater geomorphology: The role of subsurface water in earth-surface processes and landforms*, eds. C.G. Higgins and D.R. Coates, 177-209. Boulder, Colo: Geological Society of America, Geological Society of America Special Paper 252.

Smith,David I. and Atkinson,Timothy C. 1976. Process, landforms and climate in limestone regions. In *Geomorphology and climate*, ed. E. Derbyshire, 367-409. New York: John Wiley.

Stumm,Werner, and Morgan,James J. 1996. *Aquatic Chemistry*. 3rd ed. New York: John Wiley & Sons, Inc.

Sweeting,Marjorie M. 1972. *Karst Landforms*. London: Macmillan.

Trudgill,Stephen 1985. *Limestone Geomorphology*. London: Longman.

White,William B. 1984. Rate process: Chemical kinetics and karst landform development. In *Groundwater as a geomorphic agent*, ed. R.G. LaFleur, 227-48. Boston: Allen and Unwin.

White,William B. 1988. *Geomorphology and Hydrology of Karst Terrains*. New York: Oxford University Press.

White,William B. 1990. Surface and near-surface karst landforms. In *Groundwater geomorphology: The role of subsurface water in earth-surface processes and landforms*, eds. C.G. Higgins and D.R. Coates, 157-75. Boulder, Colo: Geological Society of America, Geological Society of America Special Paper 252.

Wigley,T.M.L 1977. *Watspec: A Computer Program for Determining the Equilibrium Speciation of Aqueous Solutions*. British Geomorphological Research Group Technical Bulletin No. 20. London.

Williams,Paul W., and Dowling,Ross K. 1979. Solution of marble in the karst of the Pikikiruna Range, northwest Nelson, New Zealand. *Earth Surface Processes* 4:15-36.

Zambo,L. and Ford,Derek C. 1997. Limestone dissolution processes in Beke Doline Aggtelek National Park, Hungary. *Earth Surface Processes and Landforms* 22:531-543.

Table 2.1 *Water Hardness in Open and Closed Equilibrium Systems Using the Drake (1980) Soil* pCO_2 *Equation.*

	water hardness (ppm, as $CaCO_3$)
Limestone terrains	
Open system	
Tropical karst	338
Temperate karst	309
Arctic/alpine karst	272
Closed system	
Tropical karst	193
Temperate karst	145
Arctic/alpine karst	98
Dolomite terrains	
Open system	
Tropical karst	412
Temperate karst	402
Arctic/alpine karst	383
Closed system	
Tropical karst	208
Temperate karst	154
Arctic/alpine karst	103

Table 2.2 *Models of Global Karst Chemical Denudation Using the Drake (1980) Soil $p\mathrm{CO}_2$ Equation.*

Limestone terrains			
	Open system		
		Tropical karst	Y[*] $= 0.1247 \times X$[**]
		Temperate karst	$Y = 0.1142 \times X$
		Arctic/apine karst	$Y = 0.1004 \times X$
	Closed system		
		Tropical karst	$Y = 0.0713 \times X$
		Temperate karst	$Y = 0.0536 \times X$
		Arctic/alpine karst	$Y = 0.0362 \times X$
Dolomite terrains			
	Open system		
		Tropical karst	$Y = 0.1333 \times X$
		Temperate karst	$Y = 0.1299 \times X$
		Arctic/alpine karst	$Y = 0.1238 \times X$
	Closed system		
		Tropical karst	$Y = 0.0673 \times X$
		Temperate karst	$Y = 0.0499 \times X$
		Arctic/alpine karst	$Y = 0.0333 \times X$

[*] Y: karst chemical denudation rate (mm/1000 years)

[**] X: annual runoff (mm)

Table 2.3 *Water Hardness in Open and Closed Equilibrium Systems Using the Brook-Folkoff-Box (1983) Soil* pCO_2 *Equation.*

	water hardness (ppm, as $CaCO_3$)
Limestone terrains	
Open system	
Tropical karst	242
Temperate karst	226
Arctic/alpine karst	138
Closed system	
Tropical karst	95
Temperate karst	69
Arctic/alpine karst	20
Dolomite terrains	
Open system	
Tropical karst	295
Temperate karst	292
Arctic/alpine karst	192
Closed system	
Tropical karst	98
Temperate karst	71
Arctic/alpine karst	24

Table 2.4 *Models of Global Karst Chemical Denudation Using the Brook-Folkoff-Box (1983) Soil* pCO_2 *Equation.*

Limestone terrains	
Open system	
Tropical karst	$Y^{*} = 0.0894 \times X^{**}$
Temperate karst	$Y = 0.0832 \times X$
Arctic/alpine karst	$Y = 0.0508 \times X$
Closed system	
Tropical karst	$Y = 0.0350 \times X$
Temperate karst	$Y = 0.0255 \times X$
Arctic/alpine karst	$Y = 0.0072 \times X$
Dolomite terrains	
Open system	
Tropical karst	$Y = 0.0954 \times X$
Temperate karst	$Y = 0.0944 \times X$
Arctic/alpine karst	$Y = 0.0621 \times X$
Closed system	
Tropical karst	$Y = 0.0317 \times X$
Temperate karst	$Y = 0.0231 \times X$
Arctic/alpine karst	$Y = 0.0076 \times X$

[*] Y: karst chemical denudation rate (mm/1000 years)

[**] X: annual runoff (mm)

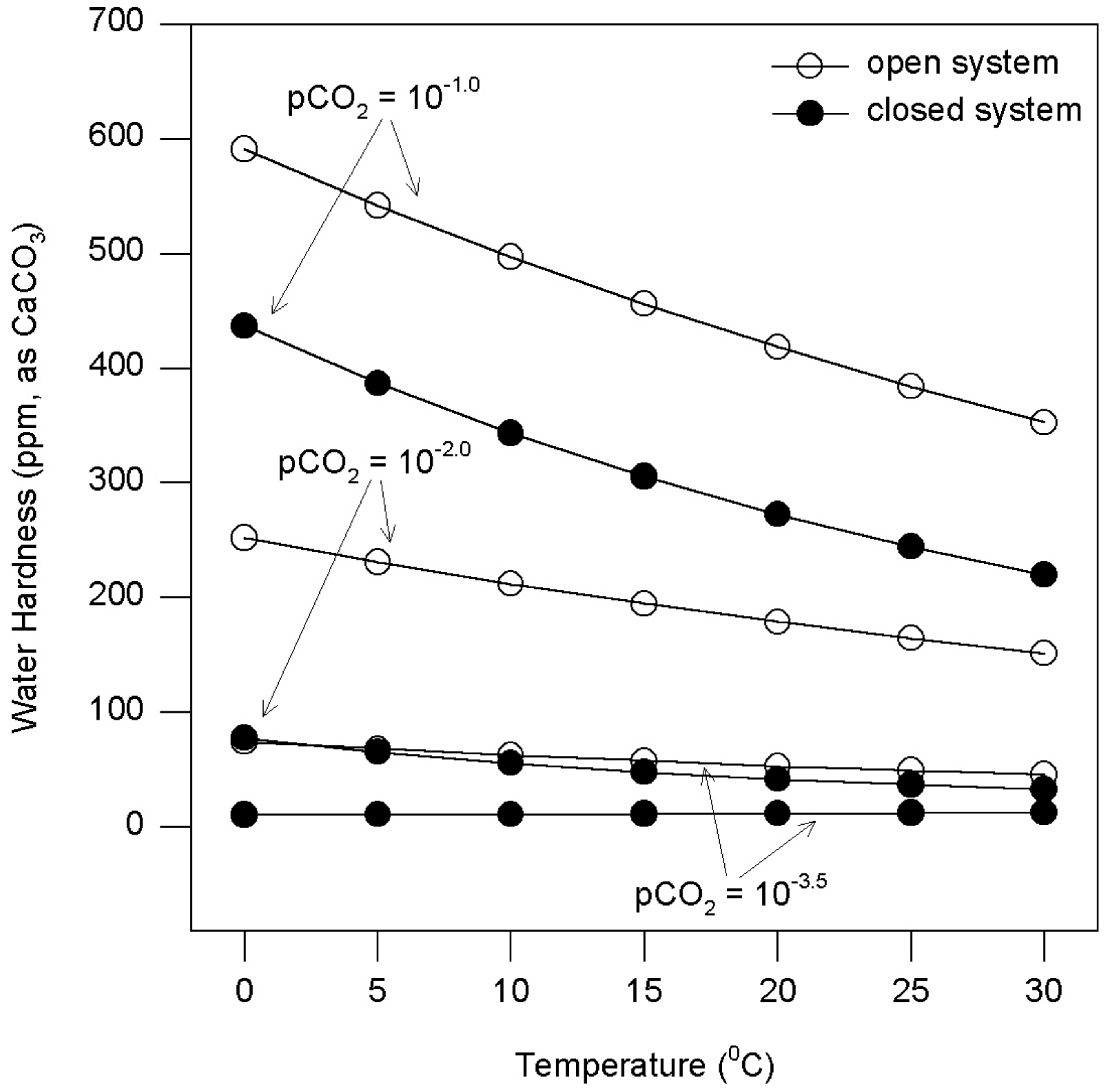

Figure 2.1: Water hardness in open and closed equilibrium limestone systems.

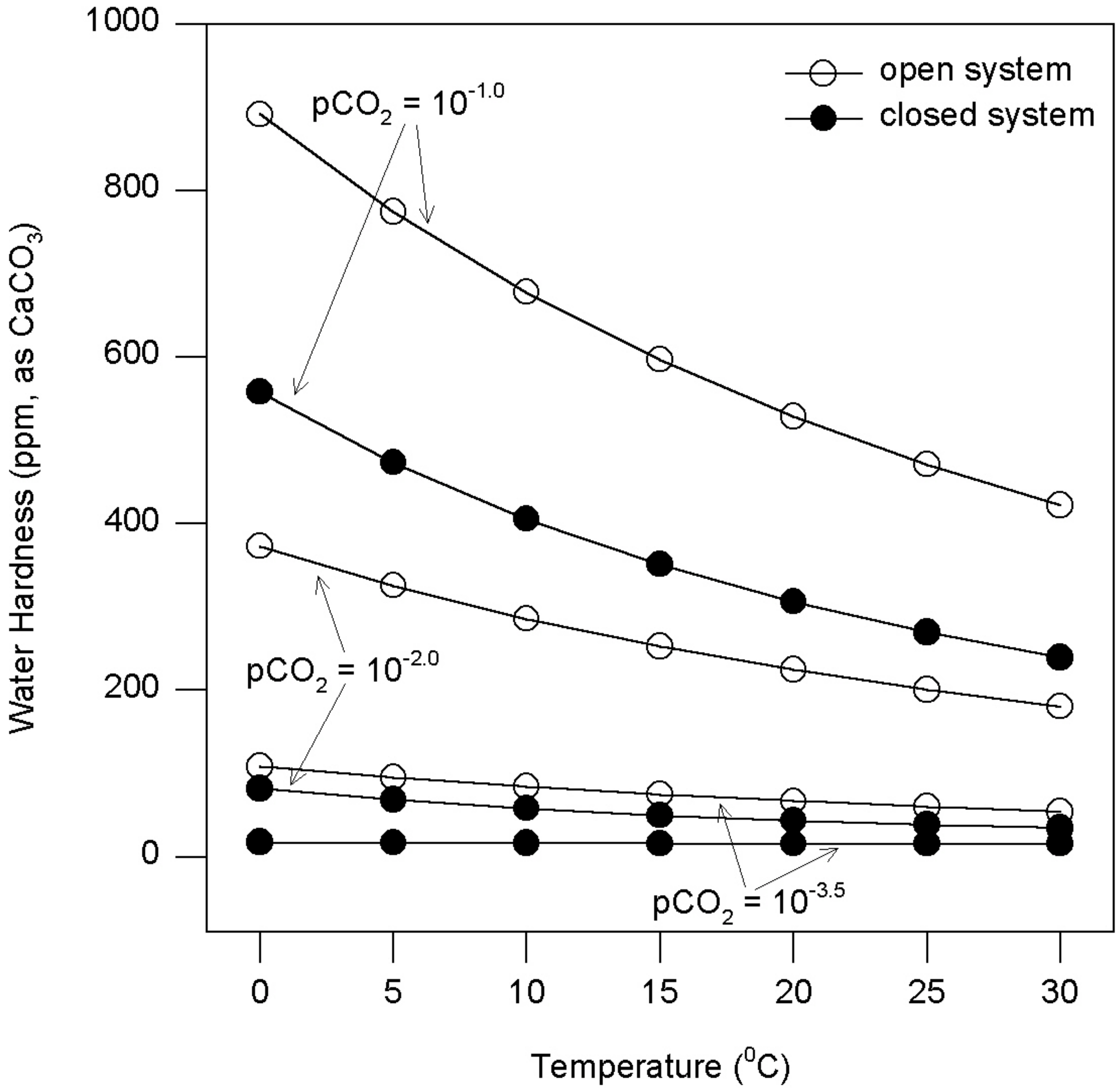

Figure 2.2: Water hardness in open and closed equilibrium dolomite systems.

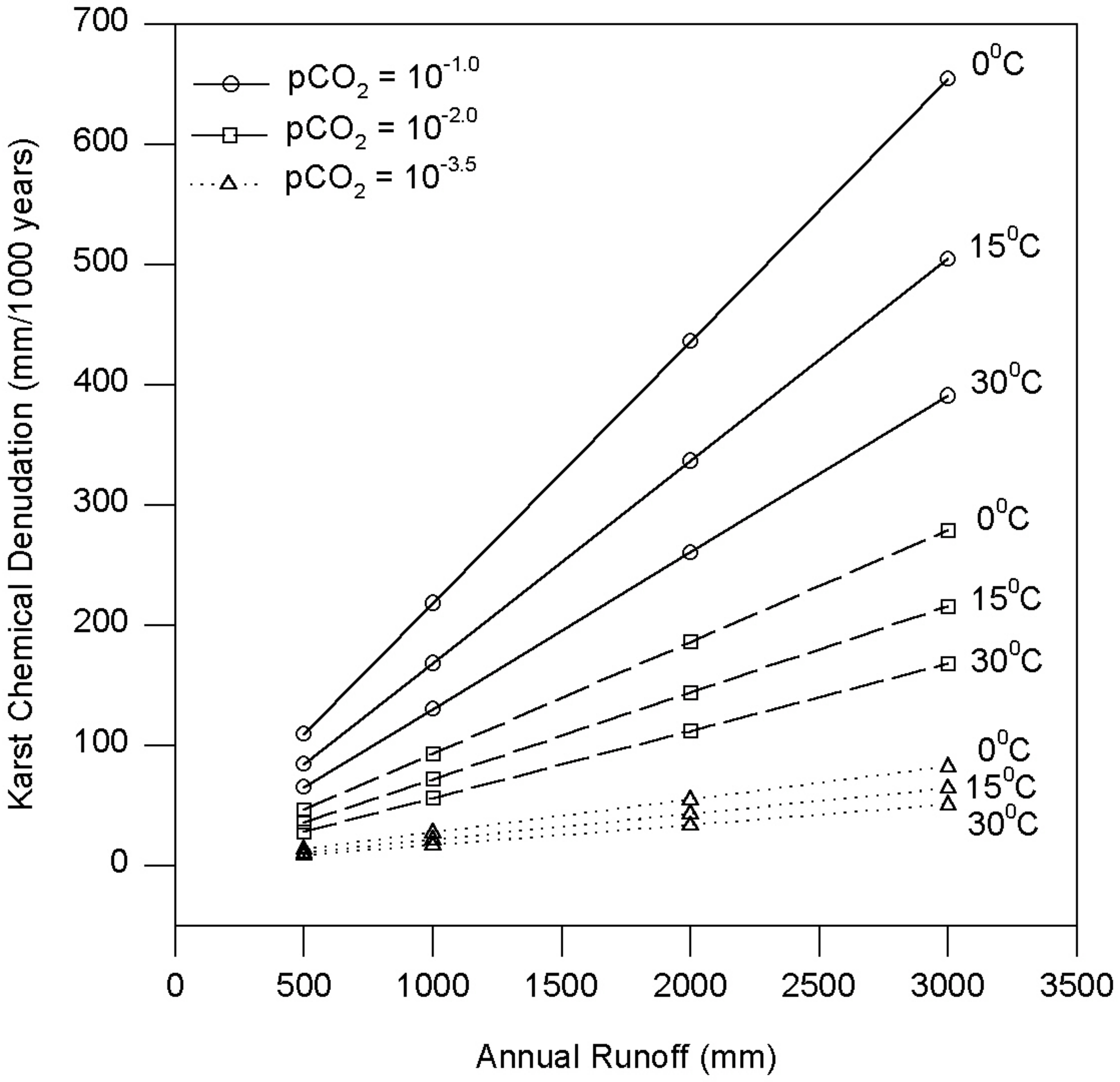

Figure 2.3: Theoretical karst chemical denudation rates in an open limestone equilibrium system.

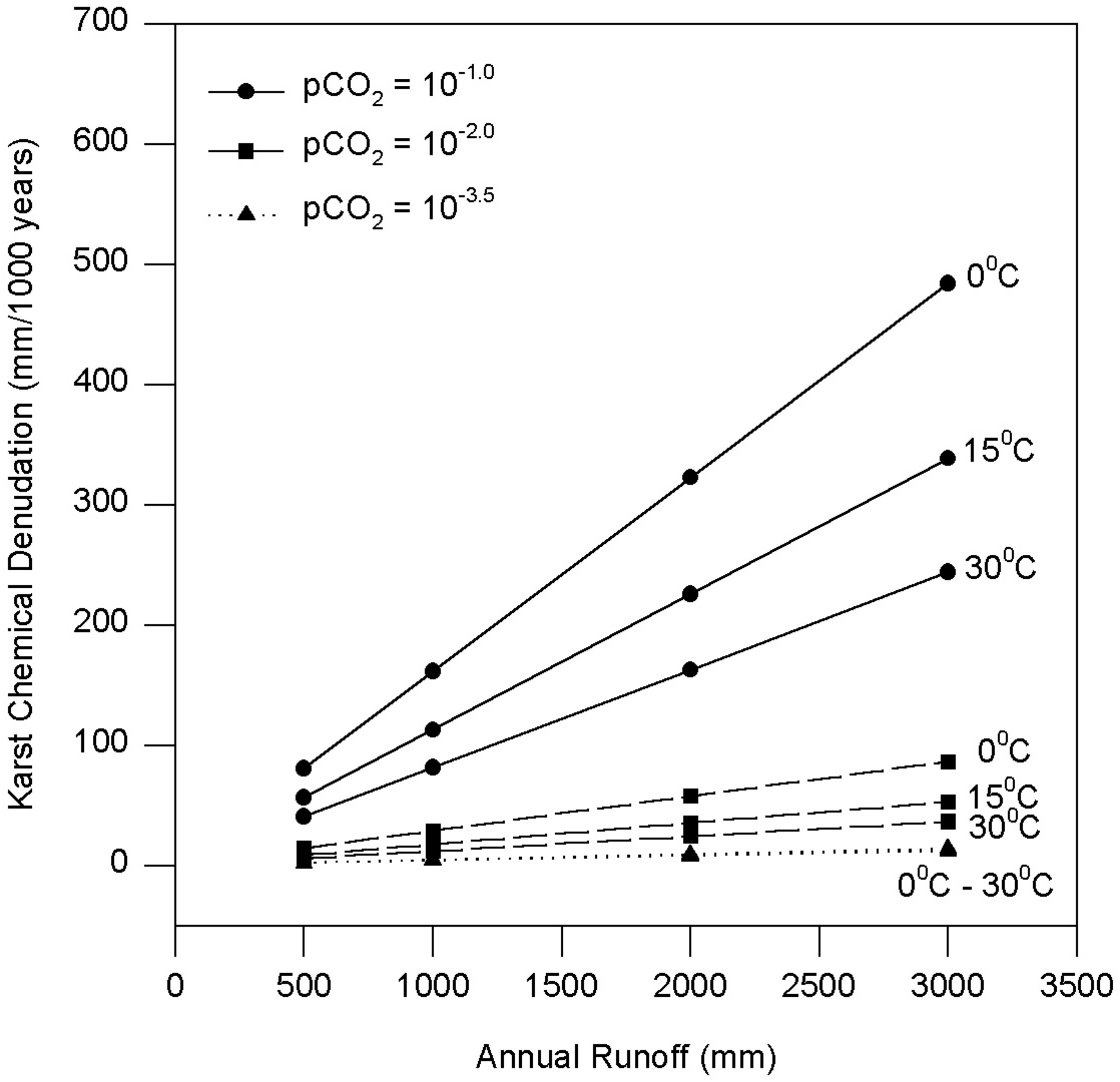

Figure 2.4: Theoretical karst chemical denudation rates in a closed limestone equilibrium system.

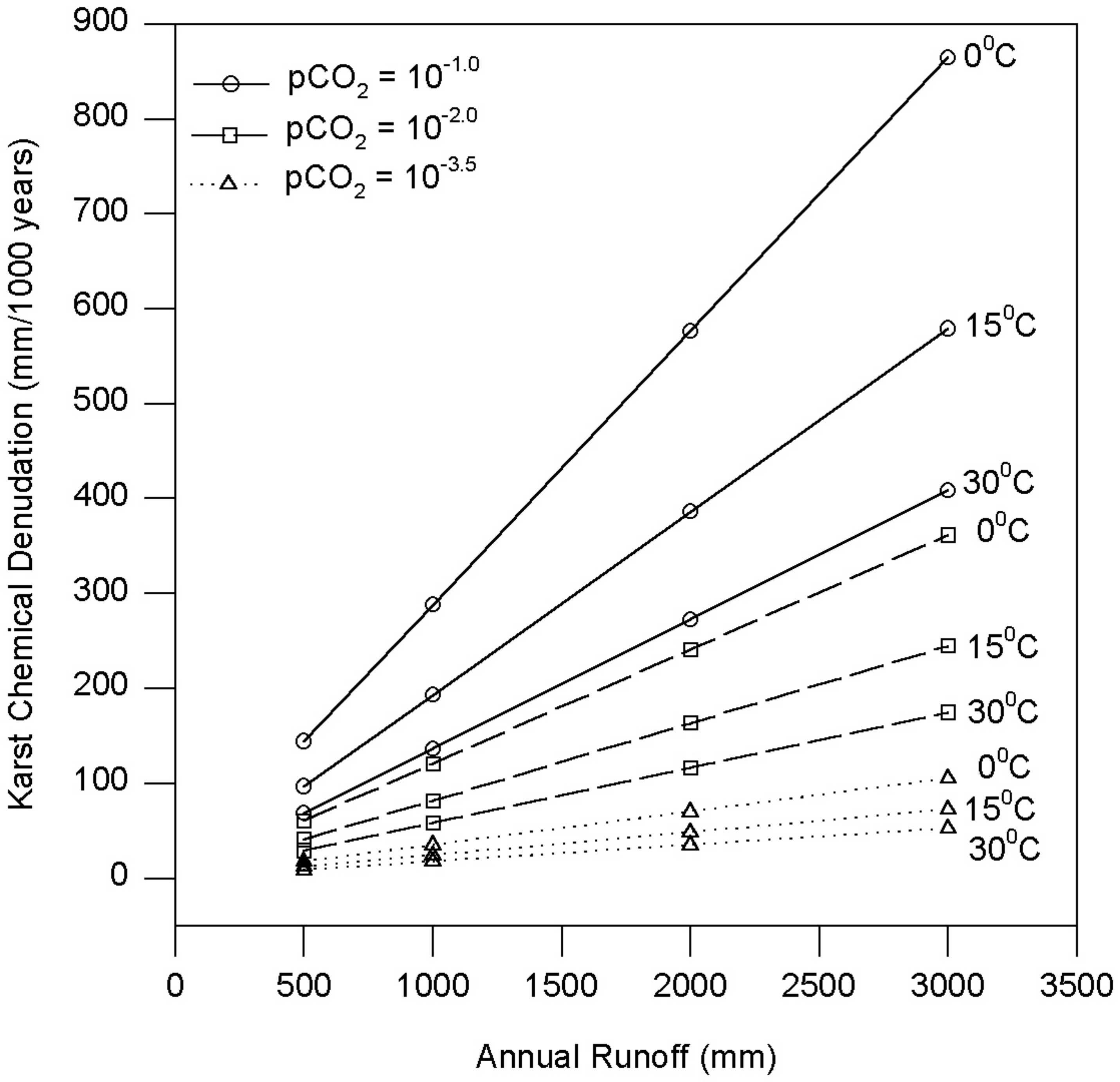

Figure 2.5: Theoretical karst chemical denudation rates in an open dolomite equilibrium system.

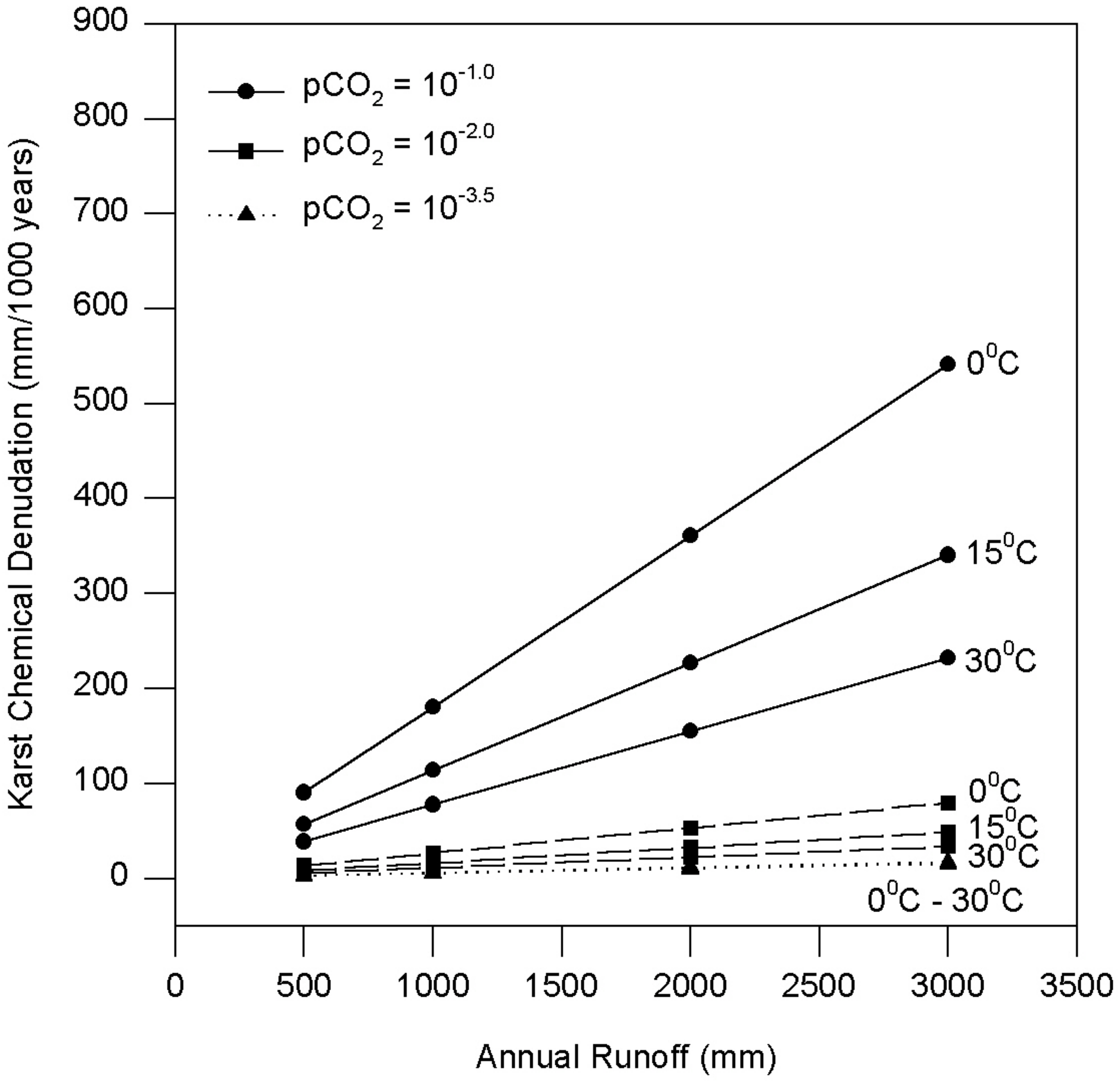

Figure 2.6: Theoretical karst chemical denudation rates in a closed dolomite equilibrium system.

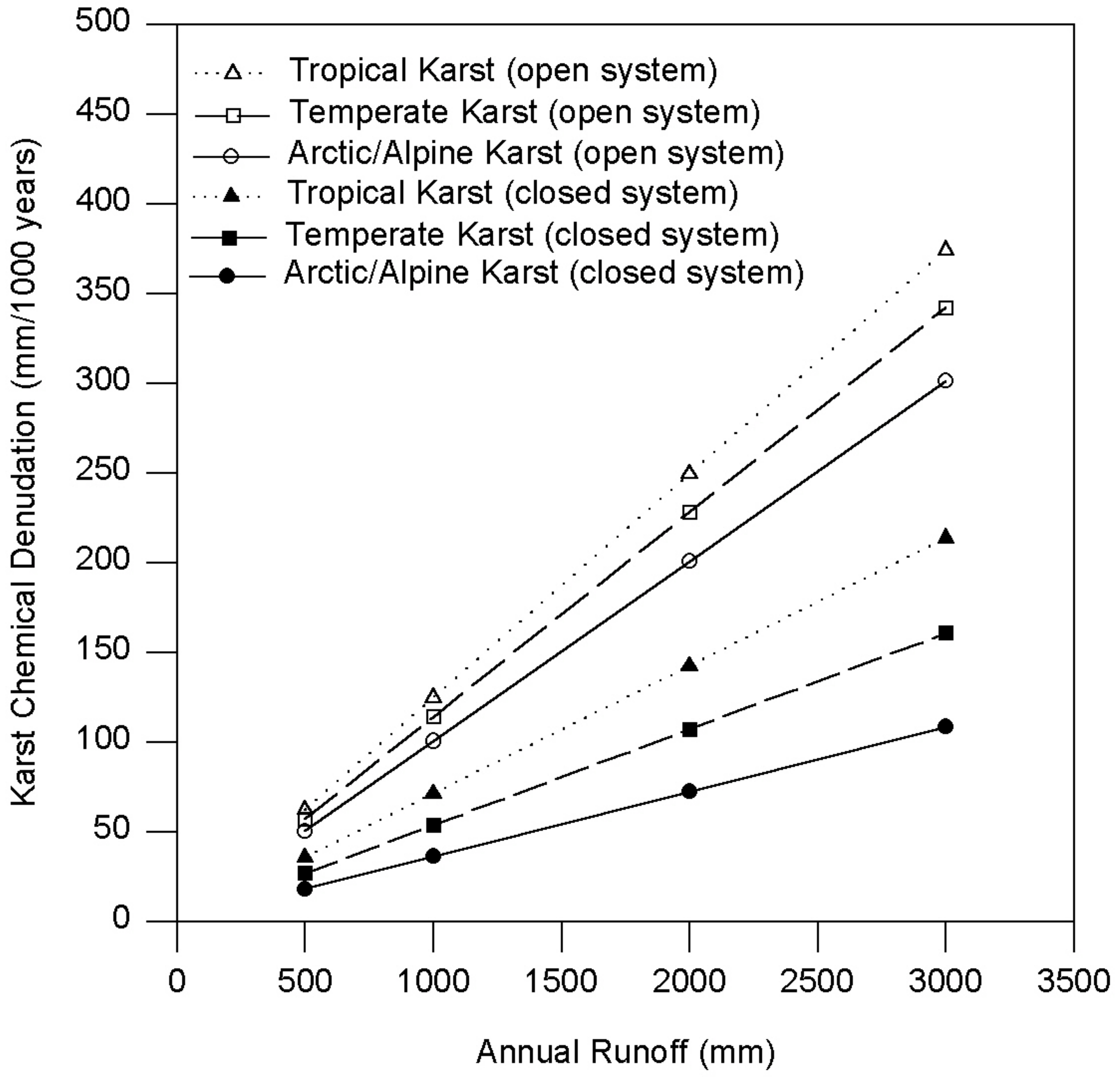

Figure 2.7: Global karst chemical denudation rates in open and closed limestone equilibium systems using the Drake (1980) soil pCO_2 equation.

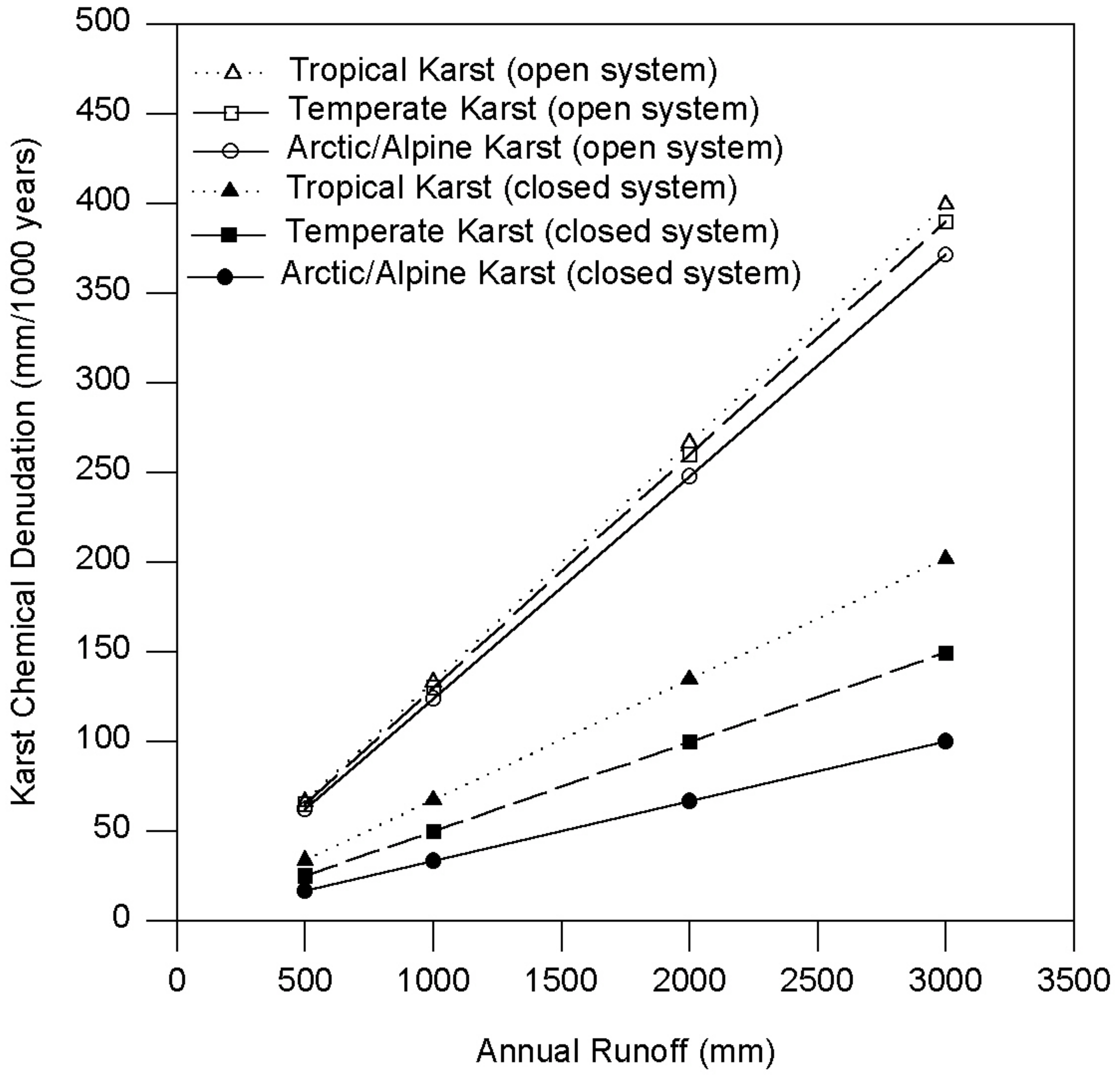

Figure 2.8: Global karst chemical denudation rates in open and closed dolomite equilibium systems using the Drake (1980) soil pCO_2 equation.

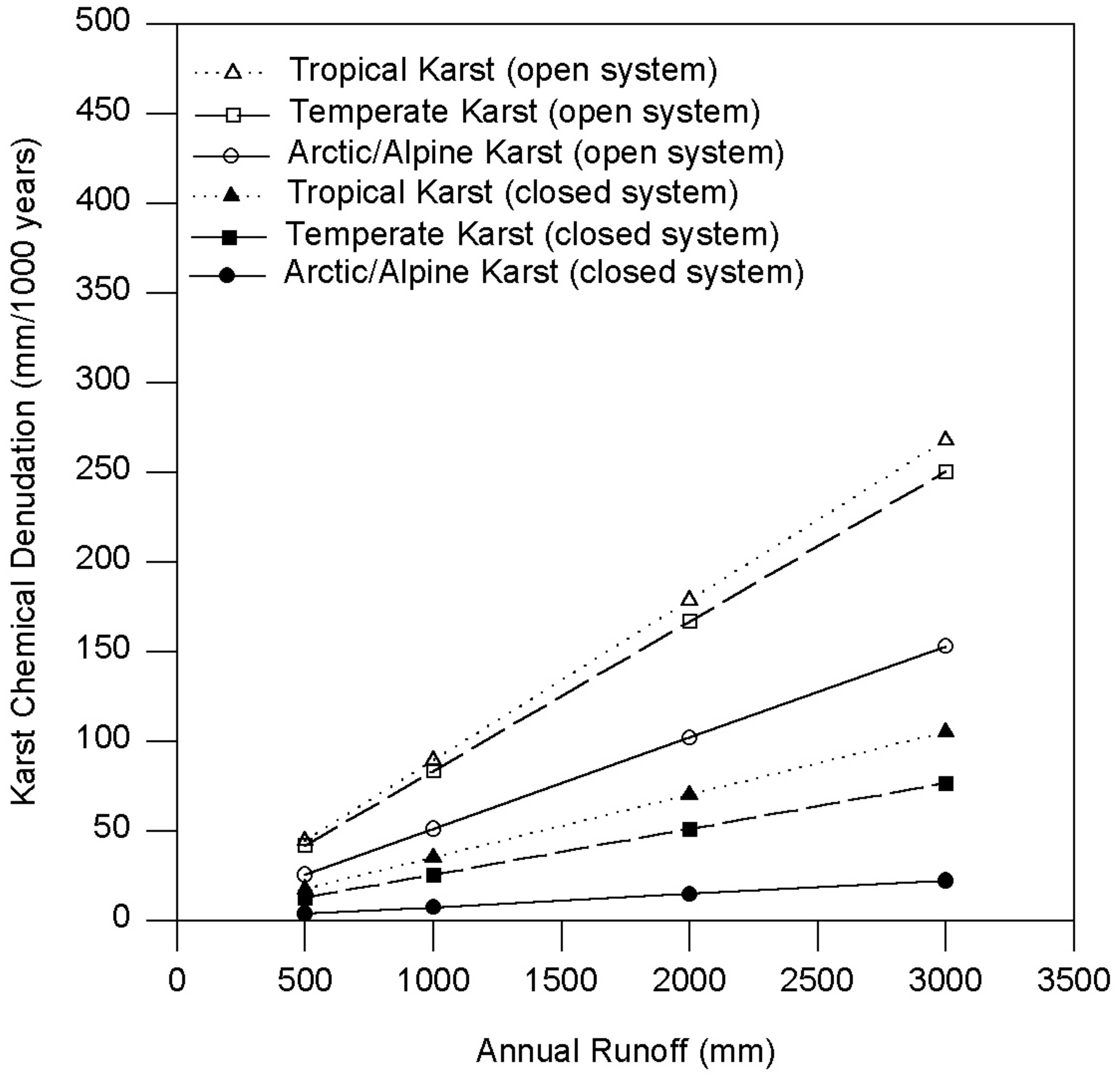

Figure 2.9: Global karst chemical denudation rates in open and closed limestone equilibium systems using the Brook-Folkoff-Box (1983) soil pCO_2 equation.

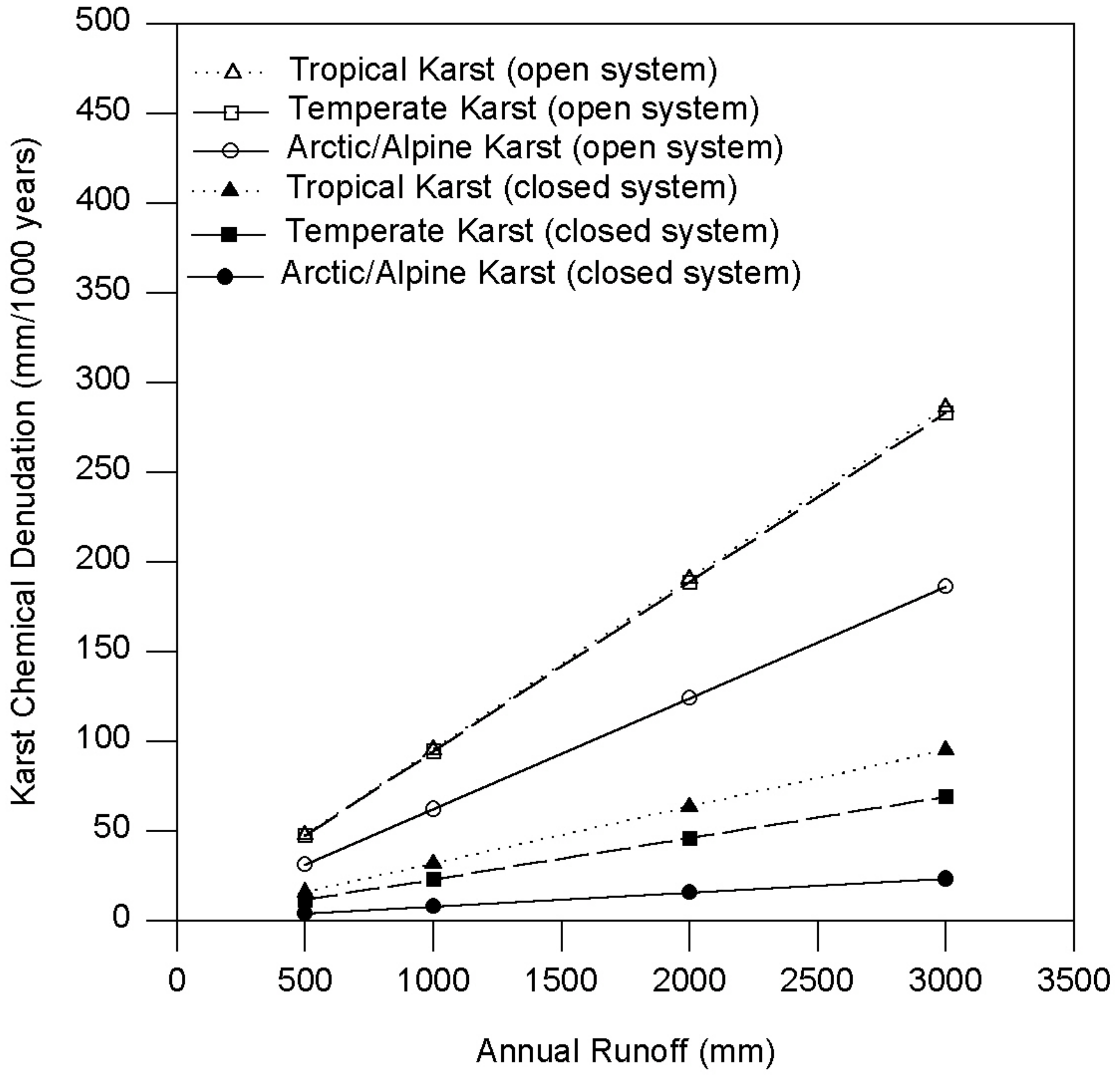

Figure 2.10: Global karst chemical denudation rates in open and closed dolomite equilibium systems using the Brook-Folkoff-Box (1983) soil pCO_2 equation.

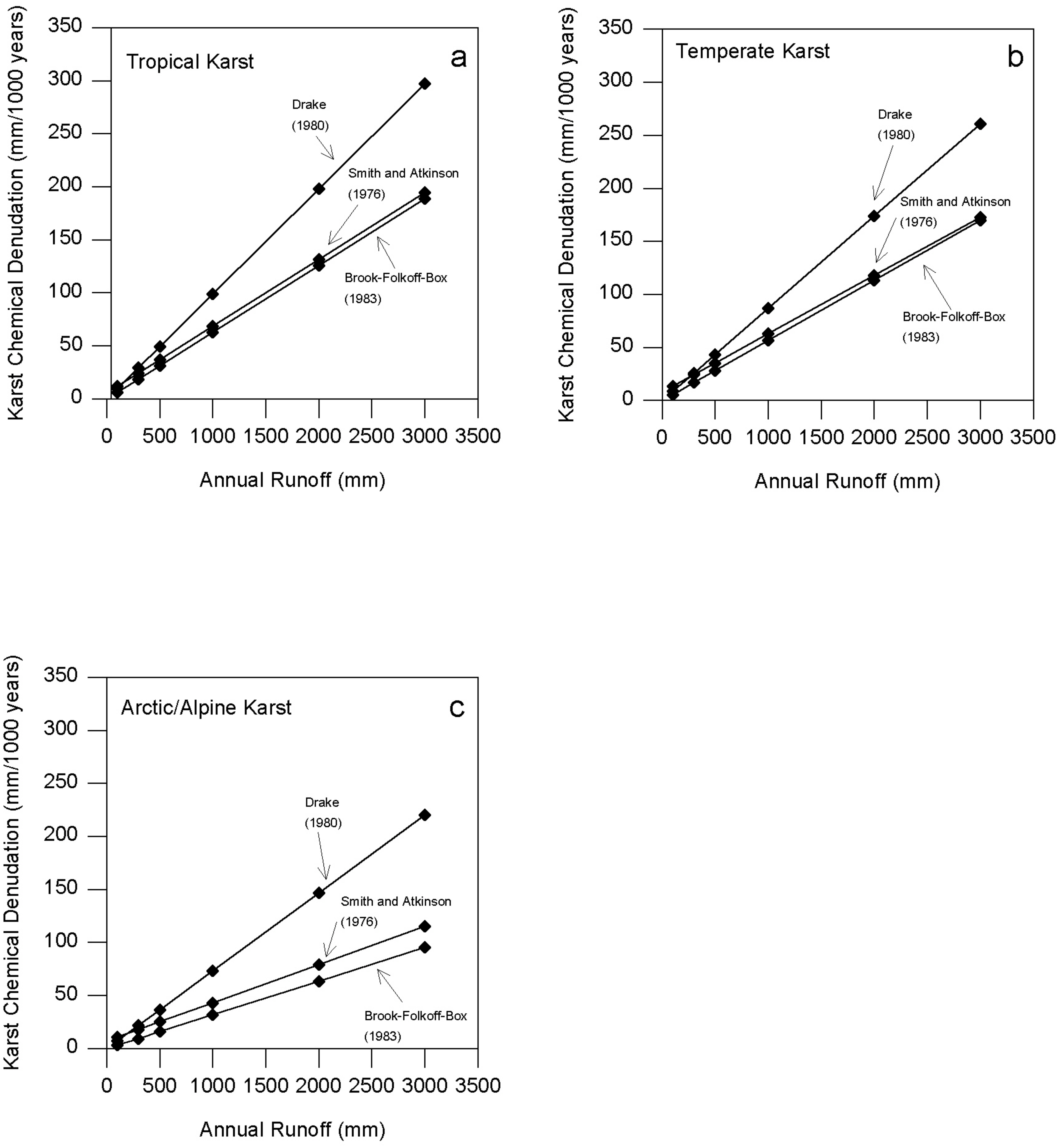

Figure 2.11: Comparison of global karst chemical denudation models in (a) tropical, (b) temperate, and (c) arctic/alpine karst terrains.

CHAPTER 3

COMPARISON OF WATER CHEMISTRY AND KARST DENUDATION IN CONDUIT AND DIFFUSE AQUIFERS WITH SIMILAR CLIMATE, AND IMPLICATIONS FOR GLOBAL KARST DENUDATION MODELS: LOST COVE, TENNESSEE AND POCKET BRANCH, GEORGIA[*]

---

[*] Sheen, S.-W. and G.A. Brook 2001. To be submitted to *Earth Surface Processes and Landforms.*

ABSTRACT

Twelve months of data, from June, 1999 to May, 2000, show that under similar climatic conditions, mean water hardness (118 ppm) in the Lost Cove conduit aquifer system was significantly lower than hardness (220 ppm) in the Pocket Branch diffuse aquifer system. Estimated long-term annual mean solutional denudation is 38.8 mm/ka at Pocket Branch and 29.9 mm/ka at Lost Cove. This significant difference suggests that aquifer type needs to be given more attention in assessing global variations in water chemistry and denudation in karst terrains. This is because the difference in denudation due to aquifer type is as large as differences between cold, temperate and tropical regions due to differences in temperature and soil carbon dioxide. At Lost Cove, 76% of karst denudation occurs in the cool/wet season (winter and spring) and 24% in the warm/dry season (summer and fall); at Pocket Branch, these figures are 83% and 17%. This emphasizes the importance of runoff rather than temperature and soil carbon dioxide in determining denudation rates. Key Words: water chemistry, karst, denudation, Cumberland Plateau.

INTRODUCTION

In karst landscapes, the dominant factor in landform evolution is the dissolution of carbonate rocks. There is a great diversity of form within the world's karst terrains. Common karst landforms in humid temperate climates contrast rather sharply with the typical karst topography of humid tropical climates. In tropical karst areas, residual hills, rather than the sinkholes so typical of temperate karst, dominate the topography. Such differences in landform type have led many to regard climate as the principal factor controlling the diversity of karst forms.

Contrary to this view, Ford *et al.* (1988) suggested that the marked differences in landforms between the doline karsts of many temperate areas and the cone and tower karst typical of many tropical areas are due to some combination of hydrogeologic setting and differential solution, and not to climate alone. Brook and Ford (1978) argued that recognition of labyrinth and associated tower karst in climates ranging from humid tropical to dry subarctic suggests that these styles are not primarily climate dependent. Therefore, a major unanswered question in karst studies is why humid tropical terrains are more accentuated than the karst landscapes of temperate and cold environments. In order to answer this question, many studies have focused on the estimation of denudation rates in different climatic regions. However, even today, karst geomorphologists are not sure if tropical karst terrains, which host the world's most spectacular solutional landforms, have higher chemical denudation rates than temperate and cold regions.

Adams and Swinnerton (1937) argued that karst denudation in humid tropical areas should be higher than elsewhere because of high soil CO_2 levels, high temperatures and abundant water. Few questioned the arguments (e.g. Jakucs, 1977). However, Corbel (1959) made a great impact on conventional thinking when he published results derived from thousands of water samples collected in the field. Corbel held the view that the rate of karst denudation was determined by climate, the greatest rates occurring in cold and humid climates and the lowest in hot and arid areas. In particular, Corbel claimed that the principal control of solution is temperature and that the cooler it is the greater will be the hardness of runoff water because carbon dioxide is more soluble at lower temperatures (Smith and Atkinson, 1976). Based on this argument, Corbel concluded that cold, high mountains provide the most favorable environments for limestone solution (Ford and Williams, 1989). These conclusions were contrary to both morphological evidence and conventional wisdom that weathering processes in general are most rapid in hot and humid conditions because of higher soil carbon dioxide levels (due to a denser, more active vegetation and year-round growth) and more rapid chemical reactions (due to higher temperatures).

Smith and Atkinson (1976) attempted to determine if limestone terrains, and the dissolution processes by which they are produced, are different in the various climatic belts of the world. They used two data sets, 231 values of mean water hardness in different regions of the world, and 134 denudation rates. They found a trend in mean hardness from a minimum value in the cold zone to a maximum in the temperate region with slightly lower levels in the tropical zone. This trend indicates that climate may well exert some control upon water hardness, but it supports neither the hypothesis of Corbel nor that of his opponents, since the greatest values are found in the temperate group. Smith and Atkinson (1976) also found that denudation rates were lowest in the tropical region, higher in the temperate zone, and highest in the cold zone. Although these results tend to support Corbel’s hypothesis that the greatest denudation rates occur in cold regions, regional differences are not statistically significant and the validity of Corbel’s data have been considered suspect. Therefore, the role of climate in determining karst denudation remains uncertain.

In an attempt to explain why denudation is not always highest in humid tropical karsts, Sweeting (1972) suggested that intense rains, which are more common in tropical areas, may promote a higher proportion of conduit flow in karst aquifers while less intense rainfall, more typical of cold and temperate areas, may produce more diffuse flow. In conduit flow rainfall passes quickly underground. Usually water runs off so quickly that it does not have time to equilibrate with soil CO_2, nor to reach saturation with respect to (w.r.t.) carbonate, and so waters have relatively low hardness. In diffuse flow the rainfall diffuses slowly through the soil and into relatively small cavities so that it moves gradually towards the spring outlet. The water is in contact with the soil and bedrock for a considerable period and so it picks up relatively more carbonate in solution. Sweeting postulated that if tropical areas are characterized by a greater abundance of conduit flow this might explain lower rates of solution than in temperate areas where diffuse-flow aquifers may be more common. In reality, systems are never purely conduit or purely diffuse but fall into a range of types from "predominantly conduit" to "predominantly diffuse", with intermediate conditions being the most common. However, to date, we really do not know enough about conduit and diffuse systems, and about their world-wide distribution, to fully assess their roles in karst development. Nor do we know if diffuse flow has a tendency to produce one type of karst landform and conduit flow another.

Sheen (2000) developed global karst chemical denudation models using chemical equilibrium equations for conditions of “open” and “closed” system solution. In an open system, as dissolution consumes aqueous carbon dioxide, additional carbon dioxide is added to maintain an equilibrium state (Palmer, 1990). In a closed system, the infiltrating water fills pore spaces, and this cuts off the supply of gaseous carbon dioxide. As further solution consumes the dissolved carbon dioxide, an equilibrium is approached at a lower carbon dioxide content than that of the original open system. As a result, the equilibrium concentration of dissolved carbonate is lower than it would have been in an open system (Palmer, 1990). Sheen (2000) calculated theoretical values of water hardness for soil CO_2 concentrations varying from $10^{-3.5}$ to $10^{-1.0}$ atm. and temperatures of 0 to 30 °C (Sheen, 2000) and concluded that the path of karst solution, which is not taken into consideration in estimating global solution characteristics, is, in fact, an important control of karst denudation.

Sweeting (1972) and Sheen (2000) have both suggested that aquifer type is extremely important in determining karst denudation. The aim of this study is to test this idea through an empirical study of two karst areas of similar climate, one (Lost Cove, Tennessee) dominated by conduit (closed system) groundwater flow and the other (Pocket Branch, Georgia) by diffuse (open system) groundwater flow. The study has several objectives. The first is to examine how denudation in the two basins varies annually and seasonally and determine whether annual denudation is indeed higher in the diffuse system than in the conduit system. A second objective is to determine if the magnitude of difference in denudation is significant relative to differences in denudation between cold, temperate and tropical areas due to temperature and soil CO_2 characteristics. A third objective of the study is to examine when (in which season) and why most of the chemical denudation occurs in each area.

THE STUDY AREAS

Lost Cove

Lost Cove is a doline of drainage area less than 100 km^2, that is located in the Cumberland Plateau of south-central Tennessee at about 550 m above sea level (Fig. 3.1). The Cove is drained by Lost Creek which eventually sinks at “The Big Sink” (TBS) in the southeast section of the Cove (Fig. 3.2). From The Big Sink the water flows underground in Buggytop Cave eventually emerging at the cave entrance, as Buggytop Cave Spring (BCS), which is located at the head of Crow Creek. Underground drainage is predominantly in large conduits.

The Lost Cove area is underlain by essentially horizontally bedded upper Mississippian limestones and shales (St. Louis Limestone, Monteagle Limestone, Hartselle Formation, Bangor Limestone, and Pennington Formation) and lower Pennsylvanian shales and sandstones (Raccoon Mountain Formation, Warren Point Sandstone, Signal Point Shale, Sewanee Conglomerate, and Whitewell Shale) (Moore, 1983). The plateau above 520 m elevation is capped by lower Pennsylvanian sandstones. The slopes and floor of Lost Cove are in upper Mississippian limestones.

The Buggytop Cave Spring resurgence is perched upon strata near the top of the St. Louis Limestone, consisting of a very fine-grained, medium- to thick-bedded silty and dolomitic limestone and dolomite (Crawford, 1992). The floor of the Crow Creek valley is on the St. Louis Limestone. Above lies the Monteagle Limestone, a very fine- to coarse-grained, and thin- to very thick-bedded, fossiliferous, oolitic limestone. It contains some dolomitic and cherty beds in the lower half and some thin shale beds near the top. The formation ranges in thickness from 58 m to 88 m. The floor of Lost Cove is in the Monteagle Limestone. Above the Monteagle is the Hartselle Formation at 317 m - 335 m elevation, and 18 m thick. The Hartselle is a significant hydrological barrier, as it consists of beds of shale, limestone, and sandstone. The saddle between Lost Cove and the Crow Creek valley is capped by the Hartselle Formation (Crawford, 1992). Above the Hartselle is the Bangor Limestone from 335 m to 396 m elevation and 61 m thick. It is a very fine- to very coarse-grained, thin- to very thick-bedded, fossiliferous, oolitic limestone with some silty and dolomitic beds. Above the carbonate units, the youngest Mississippian age rock is the Pennington Formation at 396 m - 518 m elevation. It is 122 m thick and consists of beds of shale and dolomite. The Pennington also contains several limestone beds. The rim of Lost Cove is in lower Pennsylvanian clastic rocks.

Pocket Branch

Pocket Branch in Pigeon Mountain, northwest Georgia, has a drainage area less than 10 km^2, underground drainage is dominated by diffuse flow (Fig. 3.1). The headward sections of Pocket Branch are characterized by a series of dry valleys and flow from them rarely reaches the middle section of the drainage basin. However, in the middle reaches of Pocket Branch there is a perennial karst spring, Pocket Branch Spring (PBS), which produces stream flow in the middle and lower parts of the drainage basin. After about 100 m the spring flow passes over Pocket Falls, a 20 m high waterfall perched on Fort Payne Chert (Fig. 3.3). During the summer the spring flow sinks about 50 m from the spring outlet (ST1), about 50 m from the waterfall. At the base of Pocket Falls there is a second perennial spring, Pocket Falls Spring (PFS), which discharges deep ground water as well as water from PBS that sinks at ST1. There are both active and relict freshwater calcareous tufa deposits at and immediately below the Pocket Falls waterfall.

Pigeon Mountain is the eastern front of the Cumberland Plateau and forms the western boundary of the Valley and Ridge Province. It has rolling hills and shallow valleys except where downcutting streams have formed canyons (Cressler, 1981). Pigeon Mountain rises about 400 m above the adjacent valleys. The area is underlain by essentially horizontally bedded Pennsylvanian and Mississippian clastics and carbonates. The mountain slopes are almost entirely in Mississippian-age limestones and cherts, except for shale near the top of the sequence. At about 600 m elevation the mountain is capped by sandstones and shales of Pennsylvanian age. As both Lost Cove and Pigeon Mountain are part of the Cumberland Plateau, they have very similar geological characteristics.

CLIMATE OF THE STUDY AREAS

Lost Cove and Pocket Branch have a humid subtropical climate (Köppen Cfa). Climate data were collected from June 1999 to May 2000 from both areas for use and comparison with discharge and chemistry information. Air temperature was measured every 15 minutes to a resolution of 0.4°C using HOBO temperature dataloggers (Onset Computer Corp.). BoxCar Pro for Windows (Onset Computer Corp.) software installed in a laptop computer was used to retrieve stored data. Precipitation was recorded using a tipping bucket rain gauge, Rain Collector II, connected to a HOBO Event Rainfall Logger (Onset Computer Corp.). The self-emptying design of the Rain Collector II allowed rainfall to be measured in 0.25 mm increments. The datalogger recorded cumulative rainfall curves for rainfall events. The climate of the two study areas was very similar during the year of study except that rainfall at Lost Cove (1308 mm) was significantly higher than at Pocket Branch (965 mm). The mean temperature at Lost Cove was 16.0°C, and at Pocket Branch 15.8°C.

In order to determine if our year of study was warmer/colder or wetter/drier than normal, we compared long-term climate data at nearby climate stations with climate data for the period June 1999-May 2000. The nearest climate station to Lost Cove is Bridgeport (204 m a.s.l.), 24 km away, where June 1999-May 2000 was warmer (+1.3°C) than the long-term mean annual temperature of 14.5°C, and also drier (-280 mm) than the average precipitation of 1509 mm (Fig. 3.4, Table 3.1). The nearest climate station to Pocket Branch is LaFayette (244 m a.s.l.), 5 km away, where the mean annual temperature is 14.4°C and the average annual precipitation 1464 mm. Compared to these long-term values, June 1999-May 2000 was 0.9°C warmer (15.3°C), and 260 mm drier (1205 mm).

Also, during the study year, about 60% of precipitation (788 mm) at Lost Cove fell in winter and spring and 40% (520 mm) in summer and fall; equivalent figures for Bridgeport over the same period were 63% (774 mm) and 37% (455 mm), with long-term values at Bridgeport being 57% (855 mm) and 43% (654 mm). At Pocket Branch 61% (589 mm) of precipitation during the study year was in winter and spring and 39% (376 mm) in summer and fall, compared to 63% (760 mm) and 37% (445 mm) at LaFayette, with long-term values at LaFayette being 55% (801 mm) and 45% (664 mm). These data suggest that Bridgeport and LaFayette were 200 mm and 220 mm drier than normal in summer and fall, and 80 mm and 40 mm drier in winter and spring, respectively.

These comparisons clearly indicate that our study year was somewhat warmer and quite a bit drier than the long-term averages for the two study sites. This must be taken into account when considering long-term chemical characteristics and denudation in the two areas. In order to estimate long-term temperature and precipitation at Lost Cove and Pocket Branch, regression relationships were developed between long-term monthly temperature and precipitation, and monthly temperature and precipitation in the period June 1999-May 2000, for Bridgeport and LaFayette (Fig. 3.5). The regression equations for Bridgeport were used to estimate long-term temperature (15.0°C) and precipitation (1515 mm) at Lost Cove, and the regression equations for LaFayette the long-term temperature (14.8°C) and precipitation (1146 mm) at Pocket Branch. The estimated long-term annual mean temperature values at Lost Cove and Pocket Branch are 1°C cooler than the annual mean temperatures during the study year. The estimated long-term annual precipitation values for Lost Cove and Pocket Branch are both 1.2 times the annual precipitation during the study year. These data indicate that Lost Cove and Pocket Branch were 160 mm and 150 mm drier than long-term estimates in summer and fall, and 45 mm and 30 mm in winter and spring, respectively.

STREAM DISCHARGE AND DRAINAGE BASIN RUNOFF

In order to examine relationships between water chemistry and runoff, stream discharge was monitored at Buggytop Cave Spring in Lost Cove, and downstream of Pocket Branch Spring and Pocket Falls Spring in Pocket Branch (Figs. 3.2 and 3.3). Stream width was measured by tape and stream velocity using a flow meter (Global Water). In order to develop rating curves linking stream depth and discharge, stream dimensions and stream velocity were measured on several occasions at times of different discharge.

A Enmos pressure transducer (Environmental Monitoring Systems), linked to a data logger, was placed in a stilling well in the Buggytop Cave Spring outflow to record depths from 0 to 3 m at a resolution of 1.5 cm. Water level was recorded every 10 minutes. At 2-3 week intervals the memory module was removed from the datalogger and replaced. The datalogger, as well as one 12V and 2 alkaline 9V batteries for power, were stored in a waterproof box. In the laboratory a data reader was used to retrieve the data from memory modules.

At Pocket Branch, a Enmos pressure transducer was used to record stream depths from June to October and a PDCR 1830 pressure transducer (Druck) linked to a CR10X datalogger (Campbell Scientific) was used to record depths from November to May. PC208W Datalogger Support Software (Campbell Scientific), installed in a laptop computer, was used to retrieve data stored in the datalogger. The PDCR 1830 pressure transducer can measure depths of 0 to 3.5 m with a resolution of 0.03 cm.

Average monthly stream discharge from the Lost Cove drainage basin exiting via Buggytop Cave Spring was highest in March (2.28 m^3/s) and lowest in August (0.18 m^3/s) (Fig. 3.4). The annual mean stream discharge was 1.01 m^3/s, the seasonal average being 0.52 m^3/s in summer, 0.39 m^3/s in fall, 1.50 m^3/s in winter, and 1.65 m^3/s in spring (Table 3.2). Spring discharge during the wet season (winter and spring) was 3.5 times that in the dry season (summer and fall).

The monthly mean stream discharge of Pocket Branch and Pocket Falls Spring was highest in March (0.22 m^3/s) and lowest in September (0.01 m^3/s) (Fig. 3.4). Average annual discharge was 0.09 m^3/s, 0.03 m^3/s in summer, 0.04 m^3/s in fall, 0.14 m^3/s in winter and 0.16 m^3/s in spring (Table 3.2). Discharge in the wet season was 4.3 times that in the dry season.

In order to calculate denudation rates in the study areas, June 1999-May 2000 and long-term runoff were estimated. Because of the complexity of underground drainage in karst terrains, it is impossible to know the exact drainage areas for Buggytop Cave Spring and for Pocket Branch and Pocket Falls Spring. However, topographic map analysis indicates that both drainage areas are small. The Lost Cove drainage system appears to be less than 100 km^2 in area, and the Pocket Branch diffuse system less than 10 km^2. Also, in the period June 1999-May 2000, there was no significant lag between precipitation and streamflow in either area, indicating rapid ground water flow-through times. Based on this finding, June 1999-May 2000 and long-term runoff for Lost Cove and Pocket Branch, were estimated using long-term precipitation/runoff ratios derived from Bridgeport and LaFayette climate data and runoff at nearby U.S. Geological Survey stream gaging stations

The closest stream gaging station to Bridgeport is Crow Creek, in Bass, Alabama (183 m a.s.l.), and the closest to LaFayette is Lookout Creek, near New England, Georgia (202 m a.s.l.) (Fig. 3.1). Long-term annual runoff at Crow Creek is 768 mm, 78% occurring in the wet season, and 22% in the dry season (Table 3.2). Long-term annual runoff at Lookout Creek is 618 mm, 80% occurring in the wet season, and 20% in the dry season.

Comparison of long-term annual rainfall (1509 mm) at Bridgeport and annual runoff (768 mm) at Crow Creek indicates that 51% of annual rainfall becomes runoff. In summer, fall, winter, and spring, runoff is 16%, 36%, 73%, and 68% of precipitation. If these rainfall/runoff percentages hold for our June 1999 - May 2000 and long-term estimates of annual and seasonal rainfall at Lost Cove, this means that in the period June 1999 to May 2000 annual runoff was 670 mm. Summer, fall, winter, and spring runoff were 54 mm, 66 mm, 199 mm, and 351 mm, respectively (Table 3.2). Long-term annual runoff at Lost Cove is 763 mm, 77% (587 mm) occurring in the wet season and 23% (176 mm) in the dry season.

Comparison of long-term annual rainfall (1465 mm) at LaFayette and annual runoff (618 mm) at Lookout Creek indicates that 42% of annual precipitation becomes runoff. In summer, fall, winter and spring, runoff is 15%, 22%, 65% and 58% of precipitation. Applying these rainfall/runoff percentages to our June 1999-May 2000, and long-term annual and seasonal precipitation estimates for Pocket Branch, gives a June 1999- May 2000 annual runoff of 427 mm with runoff during summer and fall, and during winter and spring, being 69 mm, and 358 mm, respectively. Long-term annual runoff at Pocket Branch is 480 mm, 80% occurring in the wet season and 20% in the dry season.

WATER CHEMISTRY

Water chemistry in the two study areas was investigated at 2-3 week intervals over the 12- month period June 1999 to May 2000, at 2 monitoring sites in Lost Cove, and at two sites in Pocket Branch (Figs. 3.6 and 3.7). Water pH and temperature were measured in the field using a Cole-Parmer Digi-Sense pH and temperature meter using pH buffers 7 and 10 for calibration. Alkalinity was measured in the laboratory, within 24 hours of returning from the field, by titration with 0.02 N hydrochloric acid to an end point pH 4.5. Major cation concentrations, including Ca^{2+}, Mg^{2+}, K^{+}, and Na^{+} ,were determined by Inductively Coupled Plasma Spectroscopy (ICP) analysis (Chemical Analysis Laboratory, University of Georgia). Total water hardness was calculated by addition of calcium and magnesium concentrations. Measured water chemistry data were analyzed using the program PHREEQC (Parkhurst, 1995) which estimates the partial pressure of the dissolved carbon dioxide (pCO_2) and the saturation index with respect to calcite (SI_c).

In order to examine temporal variations, the chemical data were averaged into 6 bimonthly values (June/July, August/September, October/November, December/January, February/March, and April/May) and 4 seasonal values (summer: June-August, fall: September-November, winter: December-February, and spring: March-May) (Table 3.3).

Temporal Variations at Lost Cove

Thirty seven water samples were collected on 20 sampling dates: 17 at The Big Sink (TBS) and 20 at Buggytop Cave Spring (BCS) (Figs. 3.2 and 3.8). Variations in water temperature at TBS and BCS clearly parallel variations in air temperature in Lost Cove although the range in temperature is somewhat dampened. As a result, water temperature at TBS and BCS was highest in summer (14.9°C and 14.2°C) and lowest in winter (11.2°C and 10.3°C). Significantly, water temperatures at TBS and BCS are virtually identical (BS: mean=13.2°C, range=10.1-15.6°C; CS: mean=12.6°C, range=10.0-15.3°C) (Table 3.4), indicating only a very slight cooling as water passes from The Big Sink through Buggytop Cave to Buggytop Cave Spring. Water temperatures at TBS and BCS reached a maximum in summer (14.9°C and 14.2°C) and a minimum in winter (11.2°C and 10.3°C). Thus water temperature in Lost Cove is influenced by air temperature and by passage through the cooler rocks surrounding Buggytop Cave.

In karst areas pCO_2, pH and SI_c are usually related as gain or loss of CO_2 changes water acidity and thus its ability to dissolve carbonate. As Fig. 3.8 displays, pCO_2 at these sites broadly parallels seasonal changes in temperature and spring discharge, particularly the latter. This is understandable in a conduit-flow system as soil CO_2 is higher in the spring and summer (Davis and Brook, 1993; Kiefer, 1990; Dyer and Brook, 1991), but increased discharge limits the amount of CO_2 that can be picked up by runoff waters by reducing contact time with the soil air, and often also by providing too much water for equilibrium to be attained with the relatively small amount of gas in the soil. So, at high soil CO_2 and low discharge, such as occurs in summer and fall at Lost Cove, water pCO_2 is high. By contrast, at low pCO_2 and high discharge, such as in winter and spring at Lost Cove, it is low. A further important observation is that throughout the year pCO_2 at TBS (mean = $10^{-2.48}$ atm.) was higher than at BCS (mean = $10^{-2.75}$ atm.). This shows that pCO_2 at TBS and BCS was influenced by soil CO_2, which is itself positively correlated with air temperature, and by degassing of CO_2 en route through Buggytop Cave.

Temporal changes in pH at TBS and BCS are inversely related to changes in pCO_2 with values consistently higher at TBS (mean=7.5, range=7.2-7.9) than at BCS (mean=7.8, range=7.5-8.1) throughout the year (Table IV). Although there are clear relationships between SI_c at TBS and BCS, and pCO_2 and pH at these two sites, there are also differences. In particular, it appears that SI_c is heavily influenced by short-term and long-term variations in discharge at BCS with increases in SI_c being associated with decreases in discharge. Also, SI_c at BCS is noticeably higher than at TBS throughout the year as degassing of CO_2 from water en route from TBS to BCS causes an increase in water saturation. At no time during our study did water at TBS (mean SI_c = -0.43, range -0.64 to -0.22) reach saturation, while that at BCS (mean SI_c = -0.16, range -0.54 to 0.14) was supersaturated periodically, but particularly in the fall and winter months. Maximum SI_c was 0.14 on September 26, and on October 10 and 24, 1999, but did not bring about precipitation of carbonate in the form of tufa.

Ca, Mg and total hardness (Tot) at TBS and BCS are inversely related to spring discharge reaching a maximum in fall (TBS: Ca = 48 ppm, Mg = 6 ppm, Tot = 145 ppm; BCS: Ca = 49 ppm, Mg = 6 ppm, Tot = 149 ppm) and a minimum in spring (TBS: Ca =

30 ppm, Mg= 3 ppm, Tot=88 ppm; BCS: Ca= 30 ppm, Mg= 3 ppm, Tot=90 ppm). Although dissolved load at the two sites varies with season, at any given time values at TBS (mean Ca = 39.3 ppm, Mg = 4.7 ppm, Tot = 117.6 ppm) are essentially the same as they are at BCS (mean Ca = 39.2 ppm, Mg = 4.9 ppm, Tot = 118.3 ppm). At most times of the year water at BCS is one to a few ppm harder than at TBS as a small volume of carbonate is dissolved by waters flowing through Buggytop Cave.

Temporal Variations at Pocket Branch

Twenty three water samples were collected from PBS and PFS on 24 sampling dates during the study period (Fig. 3.9). Water temperatures at Pocket Branch Spring vary very little throughout the year (mean = 13.6°C, range = 13.1-14.3°C) (Table 3.4). The mean water temperature is below the average annual air temperature and reflects the higher volume of recharge to the aquifer in the winter and spring seasons when air and water temperatures are relatively low. By contrast, temperature variations at Pocket Falls Spring are greater than at PBS (mean = 13.9°C, range = 12.2-15.7°C) and mirror fluctuations in air temperature at Pocket Branch although the variations are dampened. This is because PFS derives some of its water from PBS, this flow sinking 50 m downstream at ST1, and some from deep ground water, the latter being partly responsible for the dampening effect.

At PBS, pCO_2 was remarkably similar throughout the year averaging $10^{-1.57}$ atm.(range = $10^{-2.1}$ to $10^{-1.3}$ atm.), suggesting that soil CO_2 levels during the main period of recharge in winter and spring were similar and that there was probably some mixing of recharge waters in the aquifer. By contrast, pCO_2 at PFS (mean = $10^{-1.82}$ atm., range = $10^{-2.4}$ to $10^{-1.5}$ atm.) is inversely related to seasonal variations in discharge (Fig. 3.9). We believe that discharge controls pCO_2 at PFS by affecting the amount of CO_2 degassing that occurs between the Pocket Branch Spring outlet and the sinking point of water (ST1) above Pocket Falls. As water sinking at ST1 re-emerges at PFS, what happens between PBS and ST1 influences pCO_2 at PFS. In summer, when the discharge from PBS is modest, there is little turbulence in the flowing water to encourage degassing. By contrast, the higher flows of winter and spring produce turbulent flow that speeds up the degassing process, thus reducing the amount of CO_2 in PFS water. As a result, pCO_2 at PFS was higher in summer ($10^{-1.6}$ atm.) than in winter ($10^{-2.1}$ atm.).

As with pCO_2, pH at PBS remained relatively constant (mean: 6.9, range: 6.6-7.3) throughout the year but the loss of CO_2 between PBS and PFS led to an increase in pH at PFS (mean: 7.1, range: 6.9-7.6). A greater loss of CO_2 during winter and spring, due to more turbulent stream flow, resulted in a higher pH in winter at PFS (7.4) than in summer (7.0). Degassing of CO_2 also increased mean SI_c from -0.44 at PBS to -0.23 at PFS. Water at PBS remained undersaturated w.r.t. calcite throughout the year (-0.7 to -0.2), while the flow from PFS was supersaturated during late fall and winter but undersaturated at other times of the year (March-October).

Mean total hardness (Tot) averages about 220 ppm at both springs but PBS has more Ca (81 vs 77 ppm) and less Mg (4.3 vs.6.5 ppm) than PFS. Ca, Mg and Tot are higher in summer/fall and lower in winter/spring, being inversely related to discharge. Increased values in summer/fall possibly reflect low ground water flow velocities and increased contact time between water and rock during this period of low discharge. Slower flow and more contact time with the limestone almost certainly explains the significantly higher Mg in this period as Mg dissolves more slowly than Ca, and thus requires more time to dissolve. In winter and spring, ground water flow is much more rapid so that contact between water and rock is limited and dissolution is slowed. PFS may contain more Mg than PBS because ground waters feeding this spring may have a different flow path and possibly have more contact with Mg-bearing rock.

Comparison Between Water Chemistry at Lost Cove and Pocket Branch

At Lost Cove, The Big Sink (TBS) and Buggytop Cave Spring (BCS) represent the input and exit points of a dominantly conduit-flow system. At Pocket Branch, Pocket Branch Spring (PBS) is a predominantly diffuse-flow spring while Pocket Falls Spring (PFS) is partly diffuse and partly conduit, as it discharges deep ground water mixed with water from PBS that was pirated underground 50 m from the spring outlet. Because of differences in recharge and flow characteristics, we would expect the waters at the two sites in Lost Cove and two in Pocket Branch to differ in hydrology and in water chemistry. This is certainly the case in regard to discharge, as maximum monthly (March) discharge of Buggytop Cave Spring (2.3 m^3/s), in Lost Cove, is more than ten times the discharge of Pocket Branch Spring (0.22 m^3/s), in Pigeon Mountain (Fig. 3.4).

Aquifer type has also influenced temperature at these four sites (Figs. 3.8, 3.9 and 3.10). At one end of the spectrum is PBS, which discharges ground water that has been in the aquifer for a relatively long time. Water temperature here is greatly influenced by the air temperature at the time of maximum recharge, which is in the winter/spring, and stays much the same throughout the year. PFS is a mixture of diffuse and conduit ground water recharge and so temperature varies seasonally as a result of the input of the conduit recharge whose temperature is influenced by air temperature. However, the influence of the diffuse recharge component dampens temperature fluctuations so these are much less than fluctuations in air temperature. In Lost Cove, TBS and BCS are at the other end of hydrogeologic spectrum to Pocket Branch Spring, and because of the rapid recharge and discharge from the limestone aquifer, water temperatures vary seasonally and are much closer to air temperatures than is the case at Pocket Falls.

Hydrogeology also explains differences in pCO_2 between the two areas. As might be expected, the highest mean value is at PBS, a diffuse flow spring ($10^{-1.6}$ atm.), and the lowest values are at TBS ($10^{-2.5}$ atm.)and BCS ($10^{-2.8}$ atm.), the input and exit points of a conduit system. Pocket Falls Spring has intermediate values ($10^{-1.8}$ atm.) as it is a mix of diffuse and conduit recharge. As with temperature, pCO_2 varies least at PBS (s.d. = 0.16) and most at BCS (s.d. = 0.23). The observed seasonal variations are inversely related to discharge. At times of higher flow at TBS and BCS, there is less time for recharge waters to pick up soil CO_2, and also the CO_2 that is dissolved in the water degasses more rapidly due to more turbulent flow conditions. At PFS, lower CO_2 at high flow is due only to more turbulence in the stream as it flows from PBS to ST1. Because of the conduit flow conditions at Lost Cove, levels of CO_2 in the recharge and spring waters are much lower than at Pocket Branch where the springs have a sizeable component of diffuse recharge. In fact, there is virtually no overlap between pCO_2 in waters at Lost Cove and those at Pocket Branch (Fig. 3.10).

The balance between pCO_2 and hardness determines pH and SI_c of karst waters. This is why mean pH at PBS (6.9) is lower than at PFS (7.1) and significantly lower than at TBS (7.5) and BCS (7.7). In fact, there is little overlap in pH between the conduit waters of Lost Cove and the diffuse and diffuse/conduit spring waters of Pocket Branch (Fig. 3.10). As with pCO_2, pH varies little at PBS but is increasingly influenced by discharge (which controls pCO_2) at PFS, TBS and BCS. Hydrogeology also influences water hardness with mean values at the two springs in Pocket Branch being 220 ppm $CaCO_3$ and comparable values at TBS and BCS in Lost Cove being 118 ppm. Hardnesses are higher at Pocket Branch (1.9 times those at Lost Cove) because of higher pCO_2, lower discharges, and because waters have had more time in the aquifer to dissolve Ca and Mg. They are significantly lower at Lost Cove because of lower CO_2, higher discharge and short residence time in the limestone aquifer.

Although the Pocket Branch springs are in equilibrium with higher CO_2 than the waters of Lost Cove, they also have higher dissolved carbonate which leads to very \

similar saturation states (Fig. 3.10). The conduit waters of Lost Cove, with low CO_2 in the recharge, have relatively low hardness, but remain undersaturated w.r.t. calcite throughout the year. The Pocket Branch springs have high CO_2, high hardness, and because of rapid degassing of $CO_{2,}$ PFS spring water is supersaturate w.r.t. calcite particularly during the winter months (Fig. 3.9), and it does precipitate carbonate at this time. In both areas, Mg is higher during the dry season with values being a little higher in the Pocket Branch springs than at Lost Cove. As a result, mean molar Ca/Mg ratios were higher at PBS (8.3) and PFS (12.9) than at TBS (5.2) and BCS (4.9). Higher Mg at times of low flow may reflect slower groundwater flow velocities and higher residence times in the aquifer.

KARST DENUDATION

Variations in karst denudation at Lost Cove were assessed by examining the discharge and chemistry of the Buggytop Cave Spring in Lost Cove, a predominantly conduit-flow spring. At Pocket Branch denudation was calculated using the combined discharge of Pocket Branch Spring and Pocket Falls Spring, diffuse and diffuse/conduit springs, respectively, but both having a very similar water hardness. The influence of spring discharge on water hardness and denudation will be examined first, and then temporal variations in denudation at Lost Cove and Pocket Branch from June 1999 to May 2000 will be discussed. Finally, we will estimate long-term denudation rates in the Lost Cove conduit aquifer and in the Pocket Branch diffuse-flow aquifer.

Karst denudation was calculated from runoff data using the following equation (Ford and Williams 1989):

$$D = 0.001 \times R \times \frac{H}{p}$$

where D is the karst denudation rate (mm/1000 years), R is annual runoff (mm), H is water hardness (ppm, as $CaCO_3$), and p is the density of carbonate rocks (g/cm^3). In our calculations we assumed p to be 2.71 g/cm^3.

Relationships Between Spring Discharge, Water Hardness and Karst Denudation

Regression relationships between stream discharge and water hardness were developed for Buggytop Cave Spring in Lost Cove (15 measurements) and for Pocket Branch Spring in Pocket Branch(18 measurements) (Fig. 3.11). The Pocket Branch Spring data were compared with discharge data for the combined flow of PBS and PFS to simplify the comparison. In actual fact the discharge of PBS is significantly larger than that of PFS and their chemistries are very similar. The regression relationships clearly show the significantly higher hardness of the diffuse spring (PBS) compared to the conduit spring (BCS) and the decrease in hardness with discharge at both sites. However, the slopes of the regression relationships indicate that the change in hardness with discharge is much more marked at Lost Cove than at Pocket Branch, presumably because an increase in outflow from BCS is also accompanied by a significant increase in the rate of aquifer recharge, and this water will not pick up much CO_2 and so will not be able to dissolve much limestone.

For example, at BCS and PBS water hardness is 186 and 224 ppm, and denudation is 0.02 kg $CaCO_3$/sec, at a discharge of 0.1 m^3/sec (Fig. 3.12). At 1 m^3/sec the hardnesses are 136 and 207 ppm and the denudation rates 0.14 and 0.21 kg $CaCO_3$/sec and at 10 m^3/sec they are 99 and 193 ppm and 0.99 and 1.93 kg $CaCO_3$/sec, respectively. Thus, at Buggytop Cave Spring water hardness at a discharge of 10 m^3/sec is 0.7 times the water hardness at 1 m^3/sec and denudation is 7 times greater. At Pocket Branch comparable figures are 0.9 times the water hardness and a denudation 9 times greater at 10 m^3/sec compared to 1 m^3/sec.

These estimates show that, unlike water hardness, denudation increases with increasing discharge. They also demonstrate that denudation at Pocket Branch (1.93 kg $CaCO_3$/sec) is almost twice (1.95 times) that at Lost Cove (.99 kg $CaCO_3$/sec) at a stream discharge of 10 m^3/sec. This indicates that, at similar discharge, denudation is significantly higher in the diffuse aquifer than in the conduit aquifer.

Seasonal and Annual Variations in Denudation, June 1999 to May 2000

Seasonal variations in karst denudation at Lost Cove and Pocket Branch for June 1999 to May 2000 were calculated using the previously estimated runoff values together with water hardness data for Buggytop Cave Spring and Pocket Branch Spring (Table 3.5). Annual denudation at Lost Cove was 25.1 mm/ka, with 2.4 mm/ka in summer, 3.6 mm/ka in fall, 7.4 mm/ka in winter, and 11.7 mm/ka in spring. About 76% of karst denudation occurred in the cool/wet season (winter and spring) and 24% in the warm/dry season (summer and fall). Annual denudation at Pocket Branch was 34.1 mm/ka with 2.2 mm/ka in summer, 3.5 mm/ka in fall, 12.7 mm/ka in winter, and 15.7 mm/ka in spring. Approximately 83% of denudation was in the cool/wet season and 17% in the warm/dry season.

These estimates indicate that karst denudation at Pocket Branch was 1.4 times that at Lost Cove during the study year. The implication is that denudation in a diffuse aquifer system is significantly higher than in a conduit aquifer system.

Long-term Denudation Rates

As discussed earlier, June 1999-May 2000 precipitation at Lost Cove was 1308 mm, much less than the estimated long-term precipitation of 1515 mm. Comparable figures at Pocket Branch are 965 mm and 1146 mm. Therefore, at Lost Cove, long-term precipitation was 1.16 times the June1999-May 2000 value and at Pocket Branch it was

1.19 times. Assuming that long-term runoff in these two areas will vary in a similar way to precipitation, this suggests that long-term runoff at Lost Cove is 763 mm and at Pocket Branch 480 mm. Using these runoff estimates, and water hardness data for the study year, long-term denudation at Lost Cove is calculated to be 29.9 mm/ka and at Pocket Branch 38.8 mm/ka (Table 3.5).

THEORETICAL ESTIMATES OF WATER HARDNESS AND DENUDATION IN TROPICAL, TEMPERATE AND COLD ENVIRONMENTS

In order to estimate the effect of karst aquifer type (conduit vs. diffuse) on water hardness and denudation rate in karst areas around the world, for comparison with the effects of temperature and soil CO_2, theoretical models were constructed for tropical, temperate and cold regions. Estimates were made for "equilibrium" (E), "disequilibrium" (D), "open" or diffuse (O), and "closed" or conduit (C) conditions for each climate region. Annual temperatures in tropical, temperate, and cold regions were assumed to be 25°C, 15°C, and 5°C (Christopherson, 1997) and dissolved CO_2 $10^{-1.0}$, $10^{-1.5}$, and $10^{-2.0}$ atm. (White, 1988). SI_c was assumed to be 0.0 for equilibrium and -0.5 for disequilibrium conditions. The geochemical computer program, PHREEQC (Parkhurst 1995), was used to calculate water hardness values.

Our theoretical calculations suggest that water hardness should vary from 188 (C/D) to 384 ppm (O/E) in tropical karst, 114 to 297 ppm in temperate karst, and 61 to 231 ppm in cold karst (Fig. 3.13). Figure 13 demonstrates how water hardness in cold and temperate areas may be higher than in tropical environments. For example, under O/E conditions, water hardness (297 ppm) in a temperate area is greater than water hardness in a tropical area under O/D (250 ppm), C/E (245 ppm), and C/D (188 ppm) conditions.

Under O/E, O/D, C/E and C/D conditions, water hardness varies from tropical regions to cold regions by 153 ppm (384-231 ppm), 98 ppm (250-152 ppm), 180 ppm

(245-65 ppm), and 127 ppm (188-61 ppm). These data show that temperature and soil CO_2 influence water hardness in tropical, temperate and cold regions by 100-180 ppm, depending on the aquifer type (i.e. whether solution is open/diffuse or closed/conduit).

Depending on conditions, the range in hardness within tropical karst is 196 ppm (O/E = 384 ppm, O/D = 250 ppm, C/E = 245 ppm, C/D = 188 ppm). Within temperate karst it is 183 ppm (O/E = 297 ppm, C/D = 114 ppm) and within cold karst it is 170 ppm (O/E = 231 ppm, C/D = 61 ppm). These data indicate that within each climatic region aquifer type (open/diffuse or closed/conduit) can affect water hardness by 170-200 ppm.

Thus, our theoretical calculations indicate that aquifer type can influence water hardness by 170-200 ppm within tropical, temperate and cold areas, while temperature and soil CO_2 can influence water hardness by 100-180 ppm between these regions.

Using the hardness values estimated above, theoretical karst denudation models were produced for tropical, temperate and cold regions for runoff from 0-3,000 mm (Fig. 3.14). These are:

$Y = 0.1417 \times X$ in tropical karst (O/E)

$Y = 0.1096 \times X$ in temperate karst (O/E)

$Y = 0.0852 \times X$ in cold karst (O/E)

$Y = 0.0694 \times X$ in tropical karst (C/D)

$Y = 0.0421 \times X$ in temperate karst (C/D)

$Y = 0.0225 \times X$ in cold karst (C/D)

where Y is karst denudation in mm/ka, and X is annual runoff in mm. These equations suggest that for all runoff values denudation rates in one climate region overlap possible denudation rates in the other two regions. Also, at all runoff values, within-region differences in denudation are higher than between-region differences in average denudation. This will be illustrated by considering the situation for one runoff value, namely 1,000 mm/yr.

According to the above equations, for an annual runoff of 1,000 mm, karst denudation should vary from 69 (C/D) to 142 mm/ka (O/E) in tropical karst, 42-110 mm/ka in temperate karst, and 23-85 mm/ka in cold karst. Under O/E conditions, and 1,000 mm runoff, denudation varies by 57 mm/ka in tropical, temperate and cold karsts (142 mm/ka, 110 mm/ka, 85 mm/ka), while under O/D conditions it varies by 36 mm/ka (tropical = 92 mm/ka, cold = 56 mm/ka). Under C/E conditions, denudation varies by 66 mm/ka from 90 mm/ka (tropical) to 24 mm/ka (cold), and under C/D conditions by 46 mm/ka, from 69 mm/ka (tropical) to 23 mm/ka (cold). Therefore, at an annual runoff of 1,000 mm, temperature and soil CO2 differences between tropical, temperate and cold karsts cause a variation in denudation of 40-70 mm/ka.

Within tropical karst, denudation varies by 73 mm/ka, being 142 mm/ka under O/E conditions, 92 mm/ka under O/D conditions, 90 mm/ka under C/E conditions, and 69 mm/ka under C/D conditions. Within temperate karst, denudation varies by 68 mm/ka from 110 mm/ka (O/E) to 42 mm/ka (C/D), and within cold karst by 62 mm/ka from 85 mm/ka (O/E) to 23 mm/ka (C/D). Aquifer type could affect karst denudation in the range 60 to 70 mm/ka.

Thus, temperature and soil CO_2 differences between tropical, temperate and cold karst can cause denudation to vary by 40-70 mm/ka while aquifer type within these climatic regions can vary denudation by 60-70 mm/ka. Thus the within-region variation due to aquifer type is slightly higher than between-region variation due to temperature and soil CO_2.

The above results indicate that water hardness and karst denudation are as sensitive to aquifer conditions (open/closed, equilibrium/disequilibrium) as they are to variations in temperature and soil CO_2. This suggests that aquifer type must be considered in any evaluation of global variations in karst denudation.

DISCUSSION AND CONCLUSIONS

Hydrogeology explained the observed differences in water chemistry at Lost Cove and Pocket Branch in the period June 1999 to May 2000. pCO_2, hardness and SI_c were all higher at the predominantly diffuse-flow Pocket Branch Spring, with lower values at Pocket Falls Spring where the flow is a mixture of diffuse and conduit recharge. The lowest values of these three variables were at The Big Sink and at Buggytop Cave Spring, which are the recharge and discharge points of a conduit-flow system in Lost Cove. The opposite was the case with pH, which was lowest at PBS and successively higher at PFS, TBS and BCS.

Seasonal variations in chemistry were least at the diffuse spring (PBS), intermediate at the mixed diffuse/conduit spring (PFS), and greatest in the conduit system of Lost Cove (TBS and BCS). Water temperature varied little at the diffuse spring and directly with air temperature, with a reduced range, at PFS, TBS and BCS. pCO2, pH, and SI_c also varied little at PBS, but pCO_2 decreased, and pH and SI_c increased during the winter/spring wet season at the other three sites. Increased recharge and spring flow in winter and spring reduced the CO_2 and hardness of the surface and ground waters and, as a result, caused an increase in pH and SI_c.

Karst denudation at Lost Cove and at Pocket Branch from June 1999 to May 2000 was 25.1 mm/ka and 34.1 mm/ka, and long-term denudation is 29.9 mm/ka and 38.8 mm/ka, respectively. Therefore, even with broadly comparable climatic and geologic conditions, karst denudation in the diffuse Pocket Branch aquifer is 1.3-1.4 times that in the conduit Lost Cove aquifer. From June 1999 to May 2000 76% of the denudation at Lost Cove was in the cool/wet season (winter and spring), when 82% of annual runoff occurred, and 24% in the warm/dry season (summer and fall), when 18% of annual runoff occurred. The situation was very similar at Pocket Branch where 83% of denudation was in the cool/wet season (84% of annual runoff), and 17% in the warm/dry season (16% of annual runoff). Therefore, denudation in both study areas was at times of high runoff and ground water recharge (winter and spring) not at times of high soil CO_2 or high temperature (summer and fall). This supports studies by Smith and Atkinson (1976) who found a strong relationship between denudation and amount of runoff in many karst regions of the world.

Assuming an average temperature of 15°C and a soil CO_2 of $10^{-1.5}$ atm. for temperate karst areas, our theoretical models of water hardness and solutional denudation suggest that water hardness will vary by 114-297 ppm, and denudation by 21-55 mm/ka for an annual runoff of 500 mm (as at Pocket Branch), and by 34-88 mm/ka for an annual runoff of 800 mm (as at Lost Cove), depending on aquifer conditions. The lower parts of these ranges cover conduit (closed), disequilibrium conditions, and the upper parts cover diffuse (open), equilibrium conditions. Water hardnesses and denudation rates at Lost Cove (118 ppm, 25.1 mm/ka) and Pocket Branch (220 ppm, 34.1 mm/ka) from June 1999 to May 2000, and also long-term denudation rates (Lost Cove = 29.9 mm/ka, Pocket Branch = 38.8 mm/ka) fit into the lower and upper parts of these temperate karst ranges, respectively, confirming the conduit and diffuse nature of the Lost Cove and Pocket Branch regions (Fig. 3.14).

Based on 154 measurements, Smith and Atkinson (1976) found that water hardness in temperate karst areas around the world averaged 211 ppm, and ranged from 20 to 440 ppm. The observed range in hardness is thus greater than our theoretical range of 114-297 ppm, presumably because in some temperate areas soil CO_2 is much lower than our assumed value of $10^{-1.5}$ atm., and in other areas it is much more.

Smith and Atkinson (1976) also developed the following solutional denudation equation for temperate karst areas:

$$Y = 0.055 \times X + 7.9$$

where Y is karst denudation (mm/ka), and X is annual runoff (mm). Using this equation, denudation at Lost Cove and Pocket Branch were estimated to be 45 and 31 mm/ka in the 12-month period June 1999 to May 2000 and 50 and 34 mm/ka using estimates of long-term runoff. Our empirical data suggest that denudation at Lost Cove (June 1999-May 2000: 25 mm/ka, and long-term: 30 mm/ka) was much lower than denudation estimated using the Smith and Atkinson (1976) equation, while denudation at Pocket Branch (June 1999-May 2000: 34 mm/ka and long-term: 39 mm/ka) was similar to values predicted using this equation. We believe that the poor estimate of denudation at Lost Cove, by the Smith and Atkinson equation, is because of the low water hardness of ground waters in this predominantly conduit-flow karst. In our view Lost Cove is a classic example of an aquifer dominated by conduit flow and because of this denudation is going to be at the very low end of the spectrum for temperate regions and so difficult to predict using a generalized equation.

According to Smith and Atkinson, the average denudation rate in the 87 temperate karst areas they examined was 57 mm/ka. Clearly, our estimates of denudation at Lost Cove and Pocket Branch are below the average for temperate areas around the world. This may be because of relatively low hardness at Lost Cove and relatively low runoff in our two study areas.

Our empirical findings at Lost Cove and Pocket Branch clearly demonstrate the importance of aquifer type in determining water hardness and denudation in karst areas with similar climate and geology. Seasonal variations in denudation in these two areas also demonstrate the importance of runoff over most other variables in determining the timing and amount of solutional denudation. Our theoretical estimates of variations in water hardness and denudation in tropical, temperate and cold karst regions also indicate the importance of aquifer type. According to our calculations, aquifer conditions can produce a "within-region" change in water hardness of 170-200 ppm in tropical, temperate and cold regions, and can change denudation by 60-70 mm/ka (at a runoff of 1,000 mm). The "between-region" effect of temperature, and soil CO_2, on tropical, temperate and cold karsts is somewhat less, these variables causing a change of 100-180 ppm in hardness and 40-70 mm/ka in denudation.

In summary, our empirical and theoretical data support the notion that aquifer type cannot be ignored in studies of global denudation patterns. This is because in-region variations in hardness and denudation due to aquifer type are at least as great as between-region variations in these variables due to the effects of differences in temperature and soil CO_2. If we want to understand the processes that lead to differences in karst landform development and morphology, denudation rates are obviously important. However, our study suggests, as Sweeting tried to point out in 1972, that denudation rates may actually be heavily dependent on aquifer type – and perhaps it is aquifer type and not denudation, per se, that is determining the nature of landform development in a karst area.

ACKNOWLEDGEMENTS

This research was supported by an NSF Doctoral Dissertation Improvement Grant. We thank David S. Leigh and John F. Dowd for the loan of equipment that was used in this study. We also thank Allen Padgett for permission to work in the Crockford Pigeon Mountain Wildlife Management Area and John Christof for permission to work in the Lost Cove area.

REFERENCES

Adams, CS and Swinnerton, AC. 1937. The solubility of limestone. *Transactions of the American Geophysical Union* **18**: 504-508.

Brook, GA and Ford, DC. 1978. The origin of labyrinth nd tower karst and the climatic conditions necessary for their development. *Nature* **275**: 493-496.

Christopherson, RW. 1997. *Geosystems: An Introduction to Physical Geography*. 3rd ed. Upper Saddle River, NJ: Prentice Hall.

Corbel, J. 1959. Erosion en terrain calcaire. *Ann. Geog.* **68**: 97-120.

Crawford, NC. 1992. The Karst Hydrogeology of the Cumberland Plateau Escarpment of Tennessee, Part III: Karst Valley Development in the Lost Cove Area, Franklin County, Tennessee, Center for Cave and Karst Studies, Department of Geography and Geology, Western Kentucky University.

Cressler, CW. 1981. Geology and Ground-Water Resources of Walker County, Georgia. Department of Natural Resources, State of Georgia, Atlanta. Georgia.

Davis, JD and Brook, GA. 1993. Geomorphology and hydrology of Upper Sinking Cove, Cumberland Plateau, Tennessee. *Earth Surface Processes and Landforms* **18**: 339-362.

Dyer, JM and Brook, GA. 1991 Spatial and temporal variations in temperature forest soil carbon dioxide during the non-growing season. *Earth Surface Processes and Landforms* **16**: 411-426.

Ford, DC, Palmer, AN and White, WB. 1988. Landform development: karst. In *Hydrogeology*, eds. Back, W, Rosenshein, JS, and Seaber, PR. 401-12. Boulder, Colo: Geological Society of America, The Geology of North America Vol. O-2.

Ford, DC and Williams, PW. 1989. *Karst Geomorphology and Hydrology*. London: Chapman & Hall

Jakucs, L. 1977. *Morphogenetics of Karst Regions*. New York: John Wiley & Sons.

Kiefer, RH. 1990. Soil carbon dioxide concentrations and climate in a humid subtropical environment. *Professional Geographer* **42**: 182-194.

Moore, JL. 1983. Geologic Map and Mineral Resources Summary of the Sewanee Quadrangle, Tennessee. Division of Geology, State of Tennessee, Nashville, Tennessee.

Palmer, AN. 1990. Groundwater processes in karst terranes. In *Groundwater geomorphology: The role of subsurface water in earth-surface processes and landforms*, eds. Higgins, CG and Coates, DR. 177-209. Boulder, Colo: Geological Society of America, Geological Society of America Special Paper 252.

Parkurst, DL. 1995. User's Guide to PHREEQC- A Computer Program for Speciation, Reaction-Path, Advective-Transport, and Inverse geochemical Calculations. Water-Resources Investigations Report 95-4227. U.S. Geological Survey, Lakewood, Colorado.

Sheen, SW. 2000. A world model of chemical denudation in karst terrains. *Professional Geographer* **52**: 397-406.

Smith, DI and Atkinson, TC. 1976. Process, landforms and climate in limestone regions. In *Geomorphology and climate,* ed. Derbyshire E. 367-409. New York: John Wiley.

Sweeting, MM. 1972. *Karst Landforms*. London: Macmillan.

White,WB. 1988. *Geomorphology and Hydrology of Karst Terrains*. New York: Oxford University Press.

Table 3.1. Summary of climate at Lost Cove and Pocket Branch (1999.6 - 2000.5 and long-term estimates) and at Bridgeport and LaFayette (1999.6 -2000.5 and 1961 - 1990).

	Lost Cove		**Pocket Branch**		**Bridgeport**		**LaFayette**	
	99.6-00.5	**long-term**	**99.6-00.5**	**long-term**	**99.6-00.5**	**1961-1990**	**99.6-00.5**	**1961-1990**
Air Temperature (°C)								
Annual Mean	16.0	15.0	15.8	14.8	15.8	14.5	15.3	14.4
Highest Monthly Mean	24.8 (Aug.)	23.3 (Jul.)	26.1 (Aug.)	25.8 (Jul.)	26.4 (Jul.)	25.0 (Jul.)	25.6 (Aug.)	25.0 (Jul.)
Lowest Monthly Mean	6.3 (Dec.)	5.5 (Jan.)	4.5 (Jan.)	2.8 (Jan.)	4.4 (Jan.)	2.5 (Jan.)	4.3 (Jan.)	2.7 (Jan.)
Summer (Jun.-Aug.)	23.5	22.7	24.6	25.0	25.4	24.3	24.3	24.3
Fall (Sep.-Nov.)	16.5	15.6	16.5	15.6	16.4	15.3	16.1	15.1
Winter (Dec.-Feb.)	8.7	6.7	5.9	4.1	5.9	4.1	6.0	4.0
Spring (Mar.-May)	15.5	15.0	16.1	14.6	15.9	14.4	14.9	14.1
Precipitation (mm)								
Annual Mean	1308	1515	965	1146	1229	1509	1205	1465
Highest Monthly Mean	240 (Apr.)	159 (Mar.)	184 (Apr.)	124 (Mar.)	273 (Apr.)	169 (Mar.)	236 (Apr.)	163 (Mar.)
Lowest Monthly Mean	25 (Dec.)	101 (Oct.)	20 (Dec.)	72 (Aug.)	4 (Aug.)	92 (Oct.)	6 (Aug.)	88 (Aug.)
Summer (Jun.-Aug.)	336	345	183	257	281	333	244	324
Fall (Sep.-Nov.)	184	337	193	268	174	321	201	340
Winter (Dec.-Feb.)	272	414	232	313	309	424	341	404
Spring (Mar.-May)	516	419	357	308	465	431	419	397

Table 3.2. Annual and seasonal runoff at Lost Cove, Pocket Branch, Crow Creek and Lookout Creek.

[*]**Discharge (m^3/s) 1999.6 - 2000.5**	**Buggytop Cave Spring**	**Pocket Branch and Pocket Falls Springs**
Annual Mean	1.01	.09
Summer	.52	.03
Fall	.39	.04
Winter	1.50	.14
Spring	1.65	.16
[$]**Runoff (mm) 1975.10-1996.9**	**Crow Creek at Bass**	**Lookout Creek near New England**
Annual Mean	768	618
Summer	53	50
Fall	114	74
Winter	310	262
Spring	291	232
[#]**Est. Runoff (mm) 1999.6-2000.5**	**Lost Cove**	**Pocket Branch**
Annual	670	427
Summer	54	27
Fall	66	42
Winter	199	151
Spring	351	207
[#]**Est. Runoff (mm) long-term**	**Lost Cove**	**Pocket Branch**
Annual	763	480
Summer	55	39
Fall	121	59
Winter	302	203
Spring	285	179

[*] measured values [$] published data

[#] estimated runoff using rainfall/runoff relationships for Crow Creek (Lost Cove) and Lookout Creek (Pocket Branch)

Table 3.3. Seasonal mean water chemistry at The Big Sink (TBS), Buggytop Cave Spring (BCS), Pocket Branch Spring (PBS) and Pocket Falls Spring (PFS).

Season	Temperature (°C)	pH	Ca (ppm)	Mg (ppm)	Hardness (ppm,$CaCO_3$)	Molar Ca/Mg	Alkalinity (ppm,HCO_3)	log pCO_2	SI_c
TBS, Lost Cove									
Summer	14.9	7.3	42.1	5.4	127	4.7	149	-2.21	-.48
Fall	13.4	7.4	48.2	6.0	145	4.9	157	-2.26	-.33
Winter	11.2	7.6	34.4	4.0	102	5.3	97	-2.64	-.55
Spring	13.1	7.7	29.9	3.3	88	5.6	88	-2.82	-.44
BCS, Lost Cove									
Summer	14.2	7.6	39.2	5.5	120	4.4	140	-2.55	-.22
Fall	12.6	7.8	49.2	6.2	149	5.6	161	-2.69	.11
Winter	10.3	7.9	34.2	3.9	101	5.4	94	-3.03	-.23
Spring	12.1	7.8	30.3	3.4	90	5.4	90	-2.90	-.37
PBS, Pocket Branch									
Summer	13.6	6.9	77.7	5.4	216	8.9	254	-1.57	-.42
Fall	14.0	6.9	82.6	5.3	228	10.6	253	-1.55	-.42
Winter	13.4	6.9	85.8	3.3	228	16.2	241	-1.60	-.40
Spring	13.3	6.8	77. 9	3.0	206	16.5	225	-1.56	-.54
PFS, Pocket Branch									
Summer	15.2	7.0	75.1	7.9	220	6.1	248	-1.61	-.38
Fall	14.5	7.1	78.7	8.4	231	7.1	243	-1.77	-.25
Winter	12.5	7.4	80.4	4.6	220	10.9	232	-2.09	-.01
Spring	13.6	7.1	74.4	4.9	206	9.3	216	-1.83	-.31

Table 3.4. Summary of water chemistry at The Big Sink (TBS), Buggytop Cave Spring (BCS), Pocket Branch Spring (PBS) and Pocket Falls Spring (PFS).

	Temperature (°C)	pH	Ca (ppm)	Mg (ppm)	Hardness (ppm,$CaCO_3$)	Molar Ca/Mg	Alkalinity (ppm,HCO_3)	log pCO_2	SI_c
TBS, Lost Cove (n = 17)									
Mean	13.2	7.5	39.3	4.7	118	5.2	125	-2.48	-.43
S.D.	1.77	.19	9.18	1.37	28.52	.55	37.05	.30	.13
Maximum	15.6	7.9	53.2	6.5	159	6.4	174	-2.06	-.22
Minimum	10.1	7.2	27.5	2.7	80	4.5	79	-2.98	-.64
BCS, Lost Cove (n = 20)									
Mean	12.6	7.8	39.2	4.9	118	4.9	127	-2.75	-.16
S.D.	1.67	.16	8.48	1.37	26.44	.59	35.46	.23	.24
Maximum	15.3	8.1	56.6	7.5	170	6.1	180	-2.44	.14
Minimum	10.0	7.5	28.6	2.9	83	3.6	69	-3.22	-.54
PBS, Pocket Branch (n = 23)									
Mean	13.6	6.9	81.1	4.3	220	12.9	244	-1.57	-.44
S.D.	.35	.14	6.44	1.59	18.56	4.22	26.10	.16	.11
Maximum	14.3	7.3	94.3	7.8	250	21.7	287	-1.32	-.19
Minimum	13.1	6.6	69.0	1.9	180	6.6	189	-2.07	-.68
PFS, Pocket Branch (n = 23)									
Mean	13.9	7.1	77.3	6.5	220	8.3	235	-1.82	-.23
S.D.	1.11	.20	6.43	2.80	19.04	2.90	24.07	.23	.19
Maximum	15.7	7.6	89.8	13.1	245	13.2	262	-1.53	.12
Minimum	12.2	6.9	61.9	3.4	173	3.5	178	-2.41	-.48

Table 3.5. Seasonal and annual karst denudation from June 1999 to May 2000 and long-term values.

	Lost Cove			**Pocket Branch**		
	Runoff (mm)	Water Hardness (ppm, $CaCO_3$)	Denudation* (mm/1000 years)	Runoff (mm)	Water Hardness (ppm, $CaCO_3$)	Denudation* (mm/1000 years)
1999.6 - 2000.5						
Season						
Summer	54	120	2.4	27	216	2.2
Fall	66	149	3.6	42	228	3.5
Winter	199	101	7.4	151	228	12.7
Spring	351	90	11.7	207	206	15.7
Annual			25.1			34.1
Long-term						
Season						
Summer	55	120	2.4	39	216	3.1
Fall	121	149	6.7	59	228	5.0
Winter	302	101	11.3	203	228	17.1
Spring	285	90	9.5	179	206	13.6
Annual			29.9			38.8

* seasonal denudation = .001 × seasonal runoff × hardness / 2.71
annual denudation = ∑ seasonal denudation

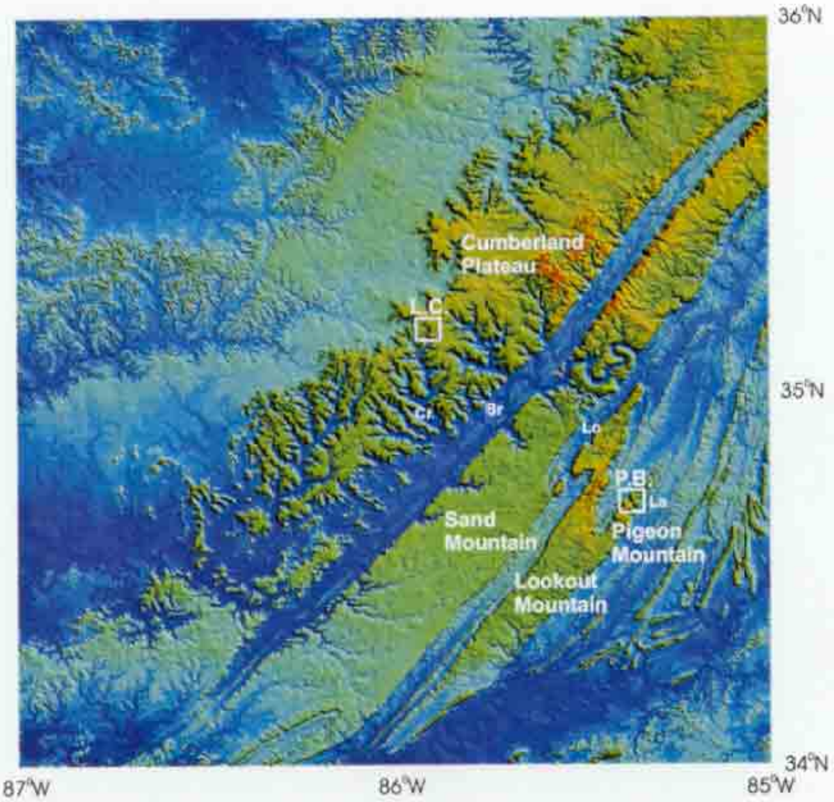

L.C. = Lost Cove P.B. = Pocket Branch
Br = Bridgeport La = LaFayette Cr = Crow Creek at Bass
Lo = Lookout Creek near New England
In the center of this map : 1° long. = 92 km 1° lat. = 111 km

Figure 3.1. Location Map showing Lost Cove, Pocket Branch and other sites mentioned in the text.

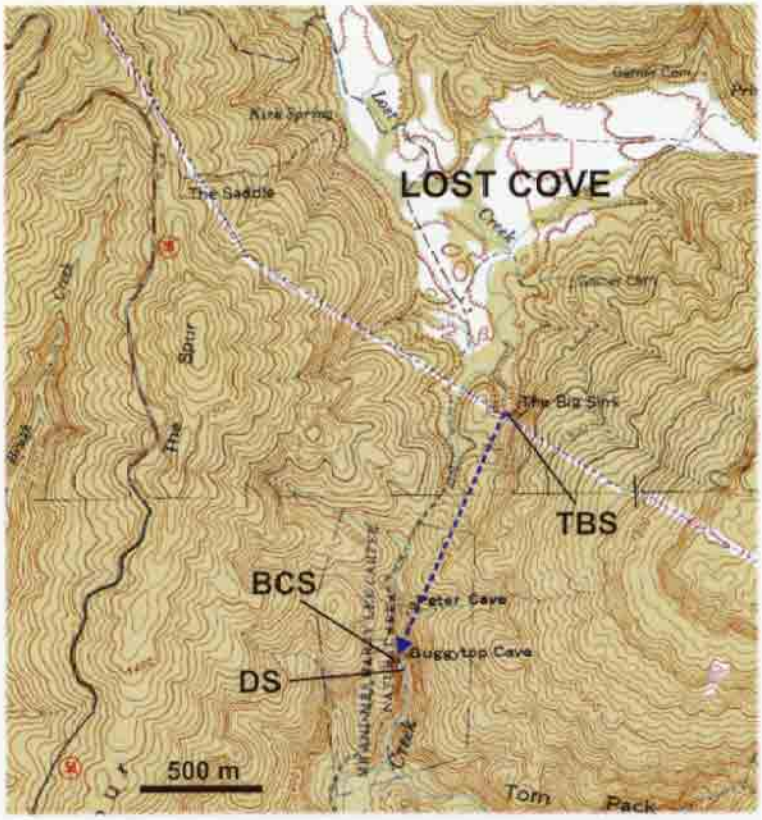

contour interval = 20 ft (6.1 m)
underground flow: from The Big Sink (TBS) to Buggytop Cave Spring (BCS)
DS: Buggytop Cave Spring discharge measurement site 50 m downstream of Buggytop Cave Spring

Figure 3.2. Topography and hydrology of Lost Cove showing water chemistry and discharge measurement sites.

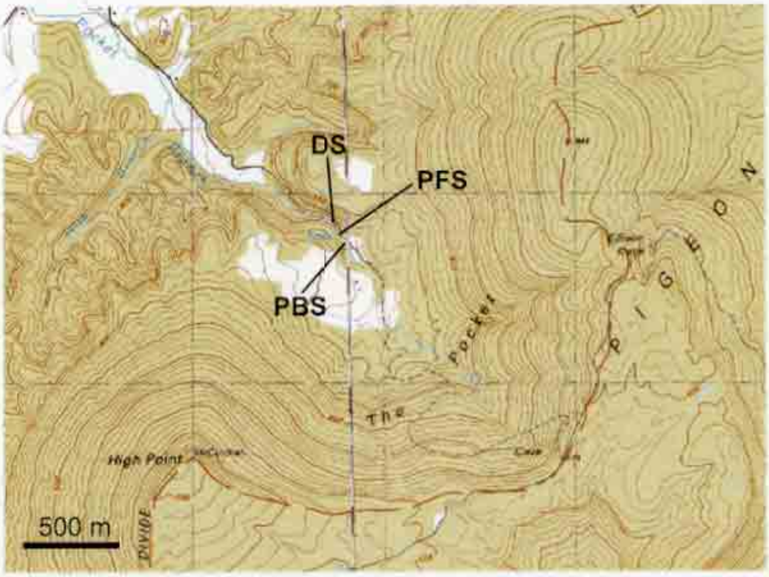

contour interval = 10 m
PBS: Pocket Branch Spring PFS: Pocket Falls Spring
DS: Pocket Branch discharge measurement site 120 m
downstream of Pocket Falls Spring

Figure 3.3. Topography and hydrology of Pocket Branch showing water chemistry and discharge measurement sites.

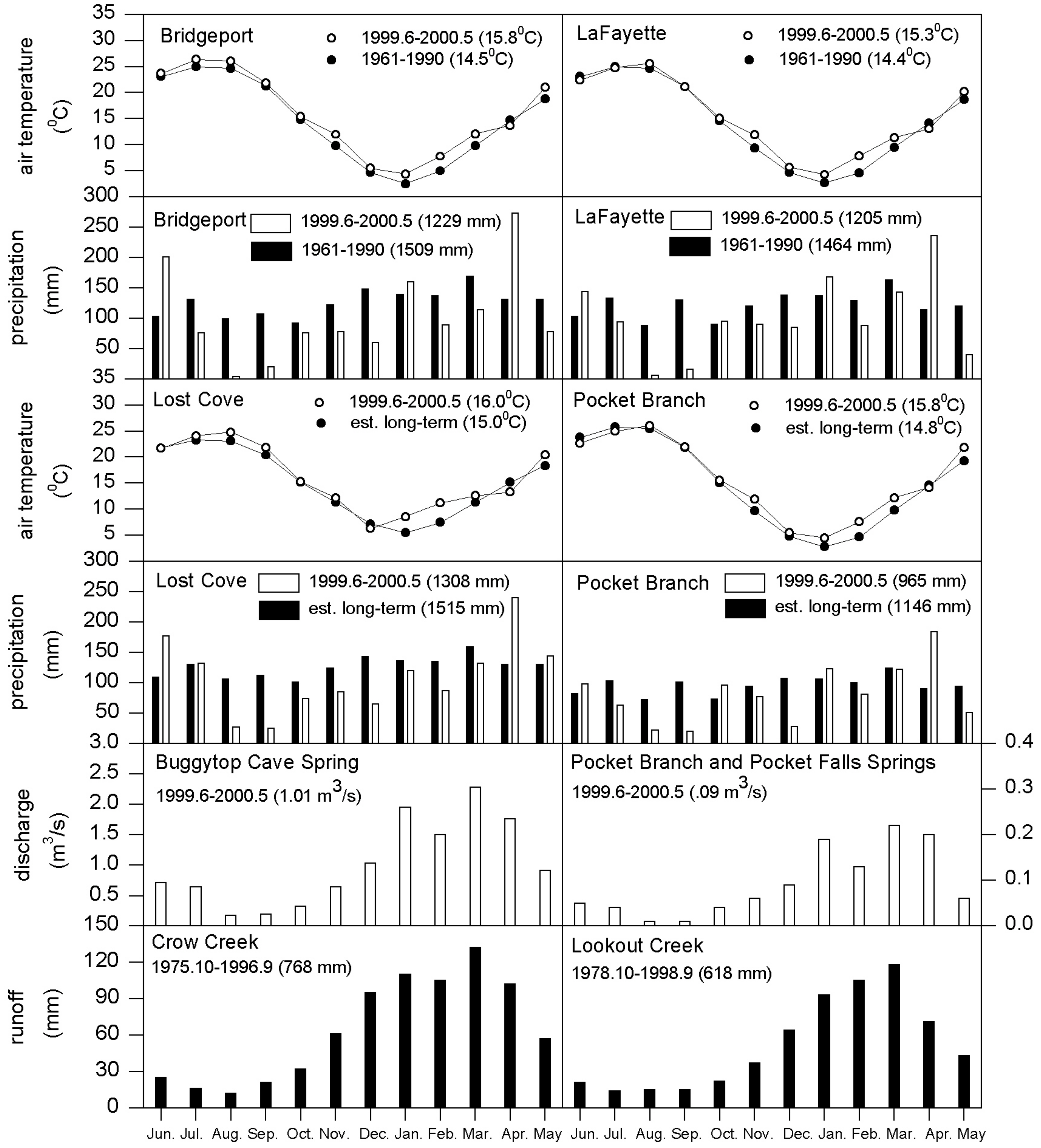

Figure 3.4. Climate (long-term and June 1999-May 2000) at Bridgeport and LaFayette, climate (estimated long-term and June 1999-May 2000) and discharge (June 1999-May 2000) at Lost Cove and Pocket Branch, and runoff (long-term) at Crow Creek at Bass and Lookout Creek near New England gaging stations.

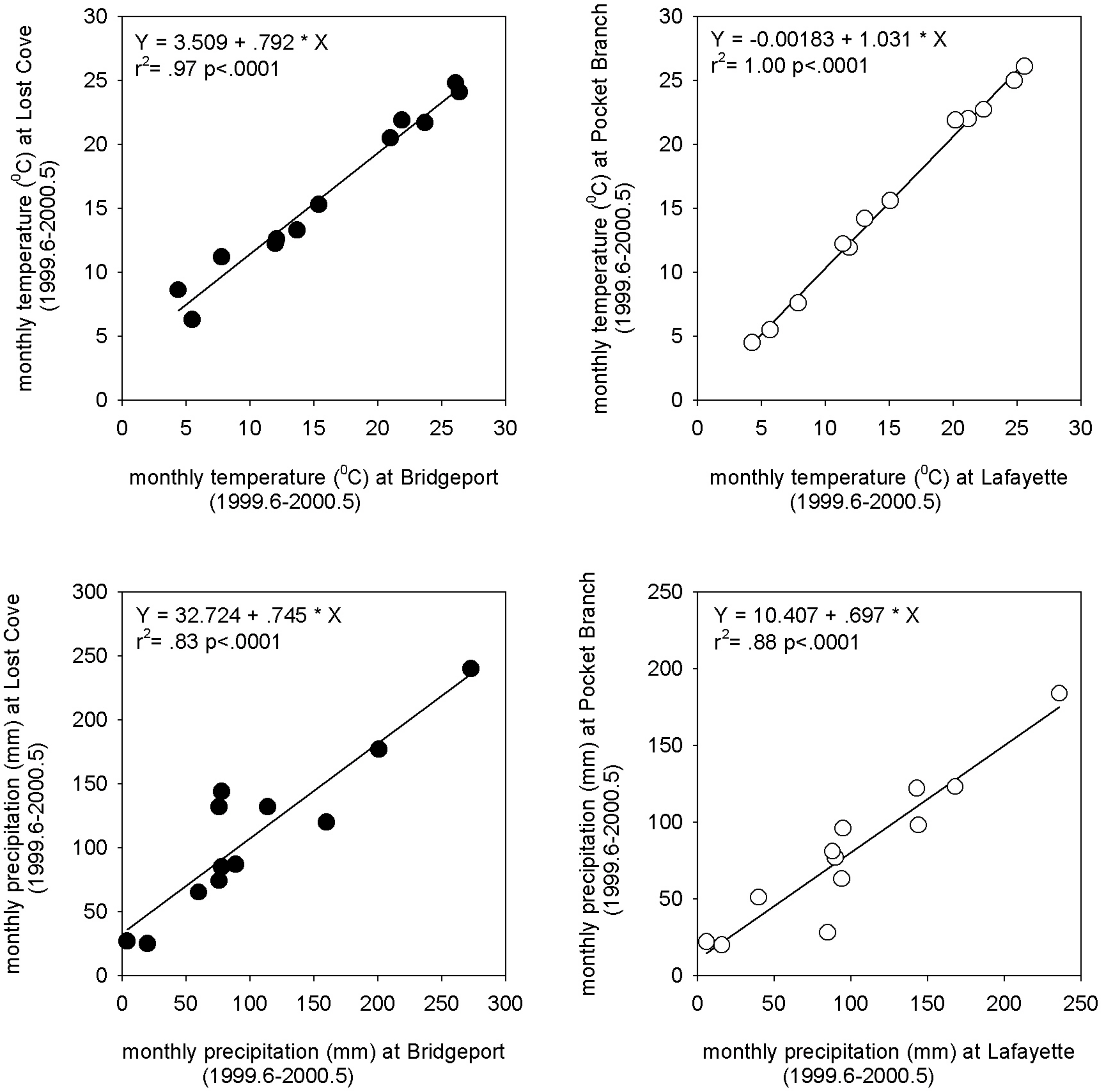

Figure 3.5. Regression relationships between monthly temperature and precipitation at Bridgeport and Lost Cove, and between Lafayette and Pocket Branch from June 1999 to May 2000.

Figure 3.6. Water chemistry measurement sites at Lost Cove:
(1) The Big Sink (TBS) and (2) Buggytop Cave Spring (BCS).

Figure 3.7. Water chemistry measurement sites at Pocket Branch: (1) Pocket Branch Spring (PBS) and (2) Pocket Falls Spring (PFS).

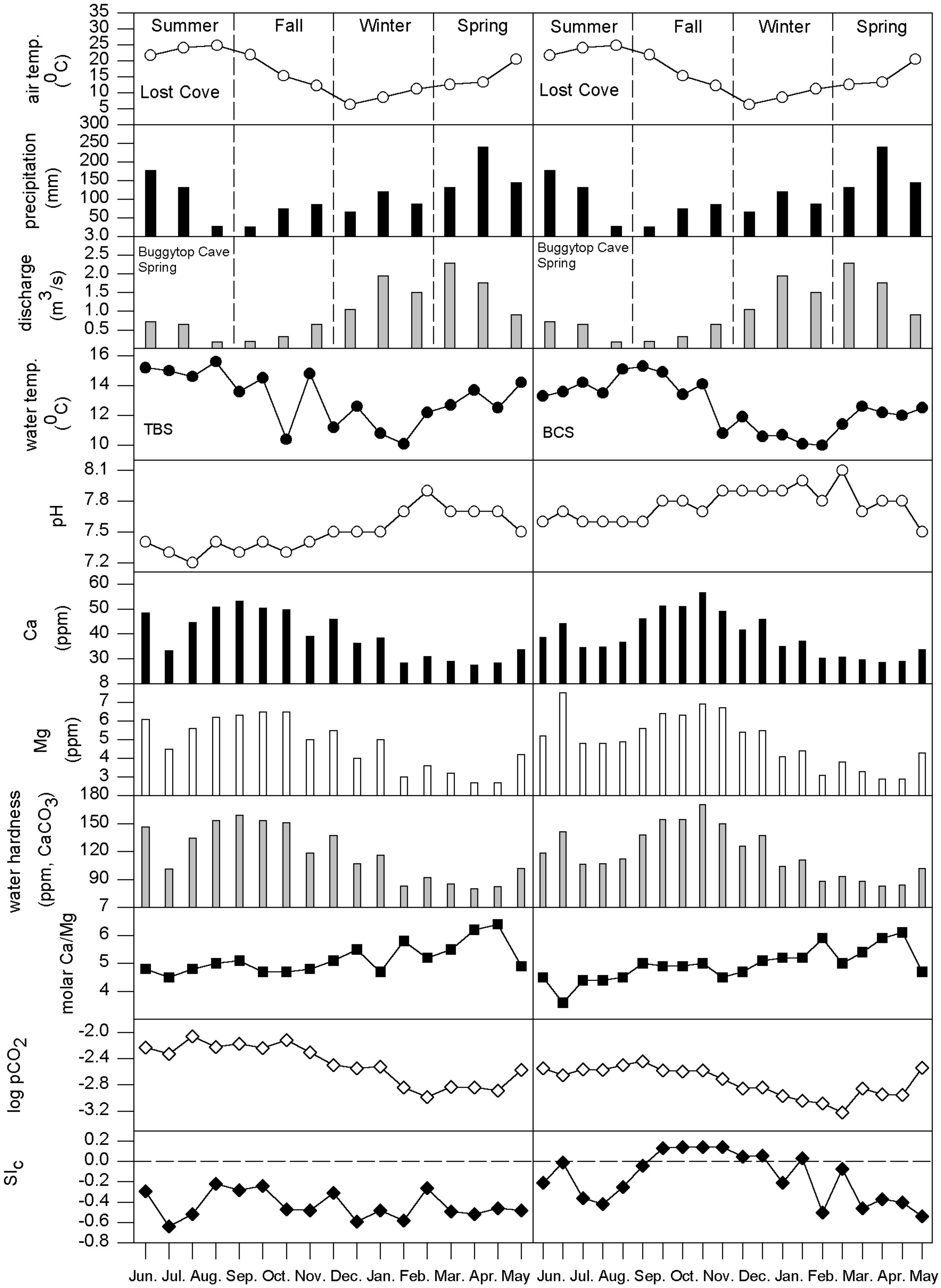

Figure 3.8. Climate (June 1999-May 2000) at Lost Cove and water chemistry at The Big Sink (TBS) and Buggytop Cave Spring (BCS), June 1999-May 2000.

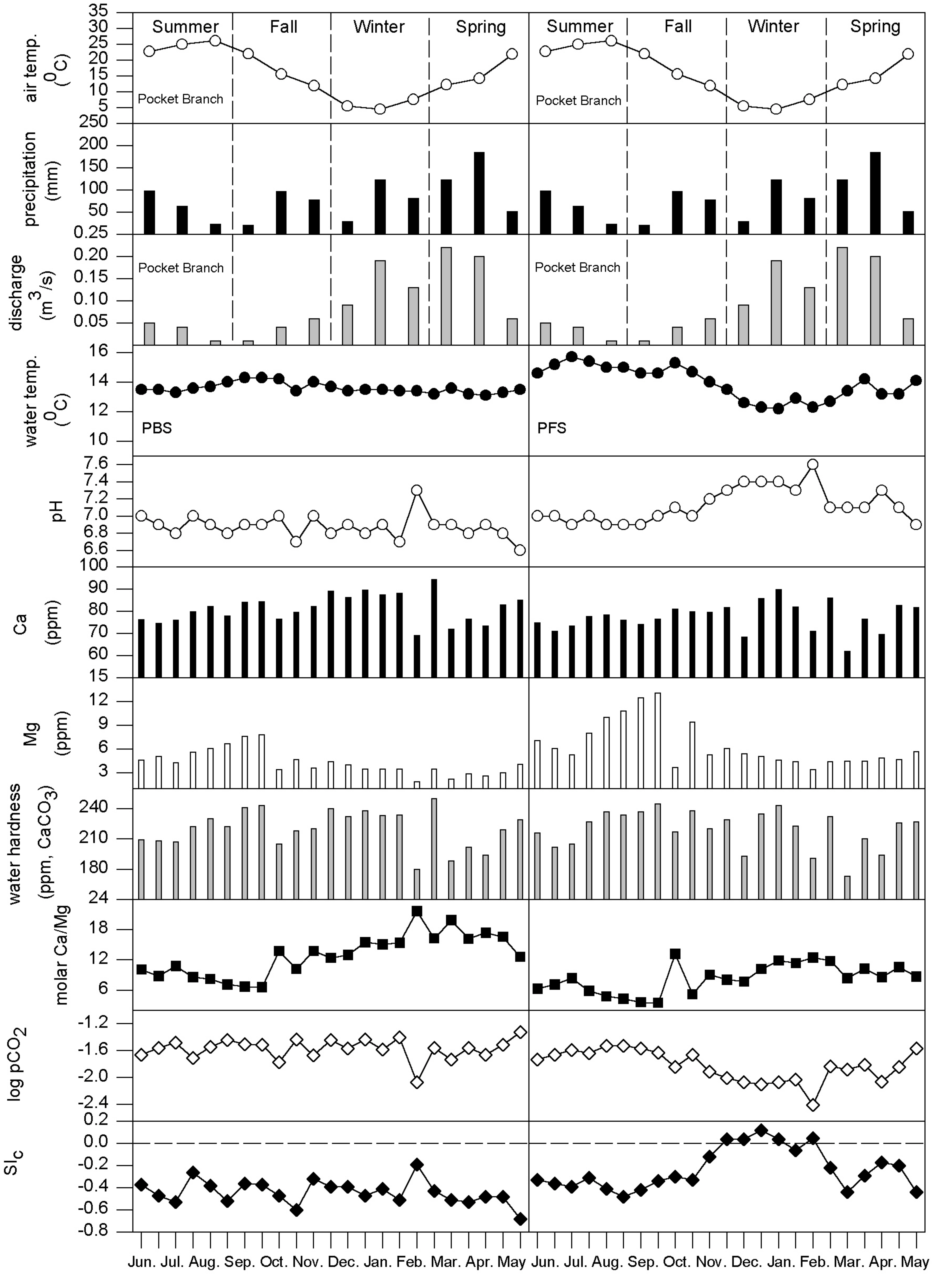

Figure 3.9. Climate (June 1999-May 2000) at Pocket Branch and water chemistry at Pocket Branch Spring (PBS) and Pocket Falls Spring (PFS), June 1999-May 2000.

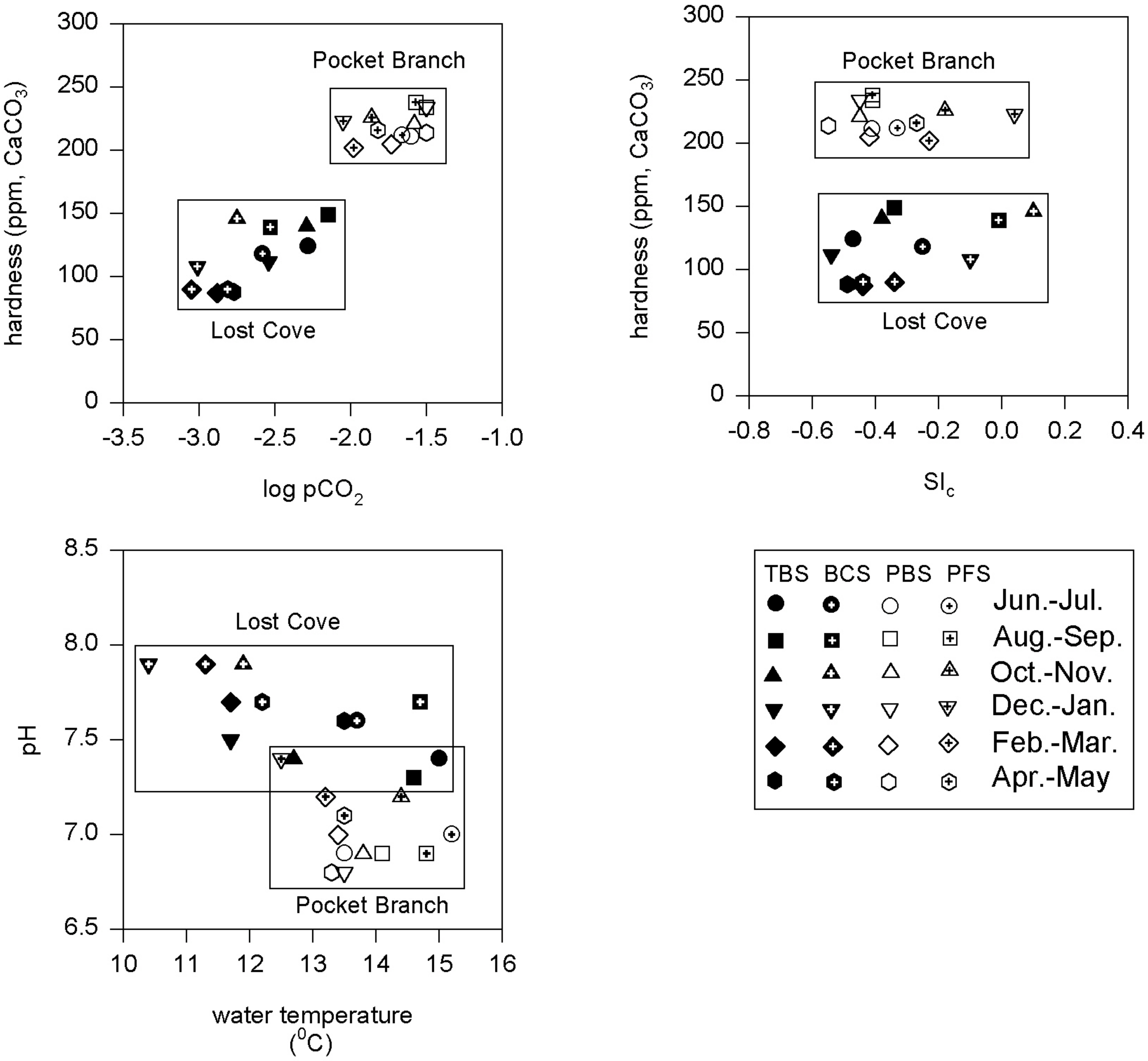

Figure 3.10. Bimonthly mean water temperature, pH, water hardness, log pCO_2, and SI_c at The Big Sink (TBS) and Buggytop Cave Spring (BCS), Lost Cove, and at Pocket Branch Spring (PBS) and Pocket Falls Spring (PFS), Pocket Branch, June 1999-May 2000.

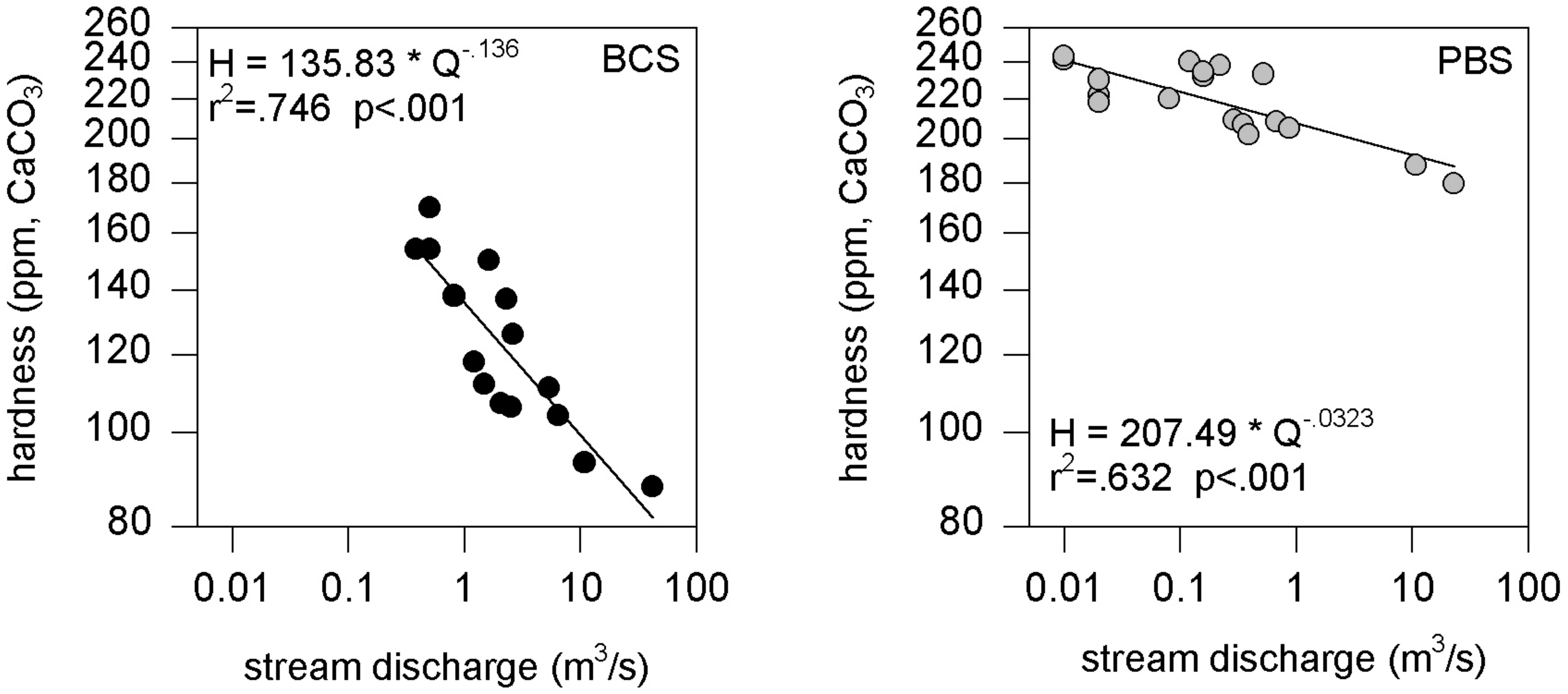

Figure 3.11. Water hardness stream discharge curves for
Buggytop Cave Spring (BCS), Lost Cove, and
Pocket Branch Spring (PBS), Pocket Branch.

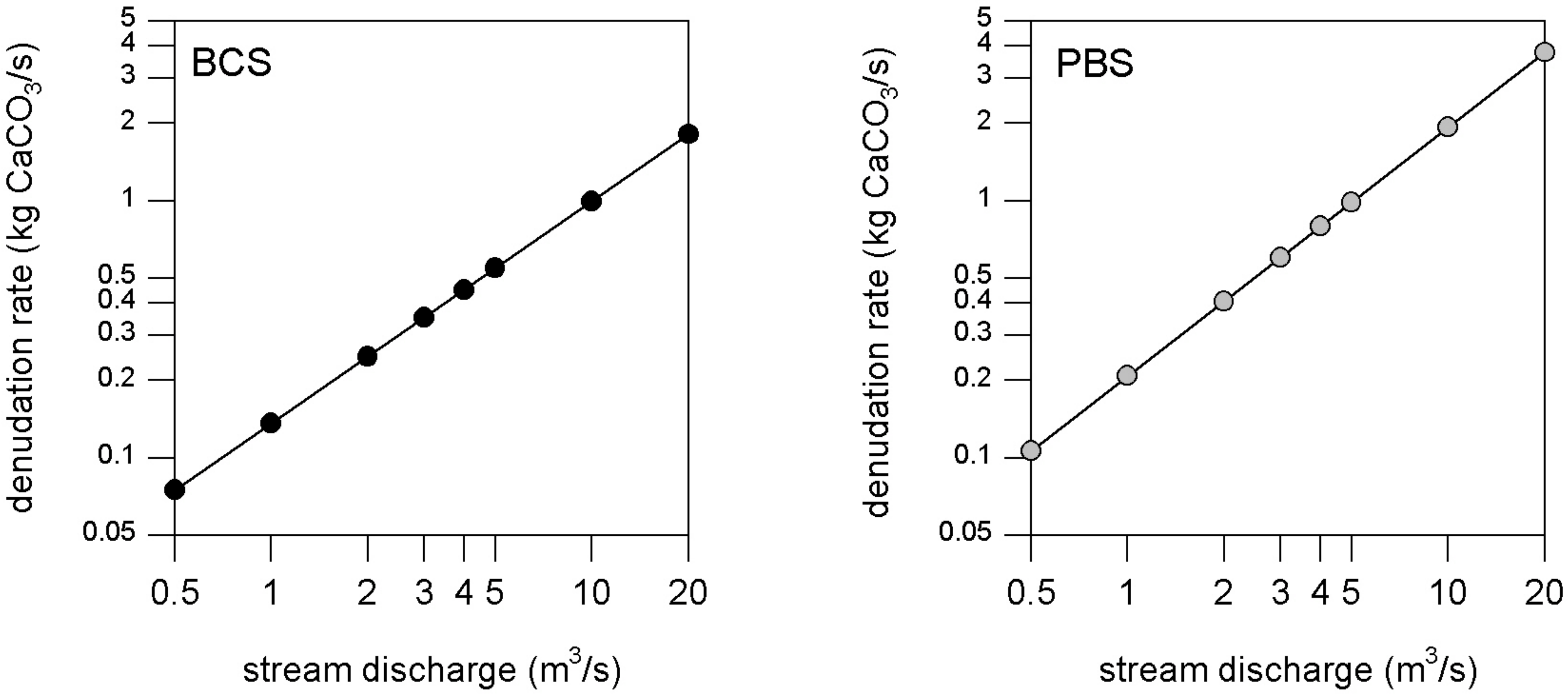

Figure 3.12. Estimated denudation rates at Buggytop Cave Spring (BCS), Lost Cove, and at Pocket Branch Spring (PBS), Pocket Branch.

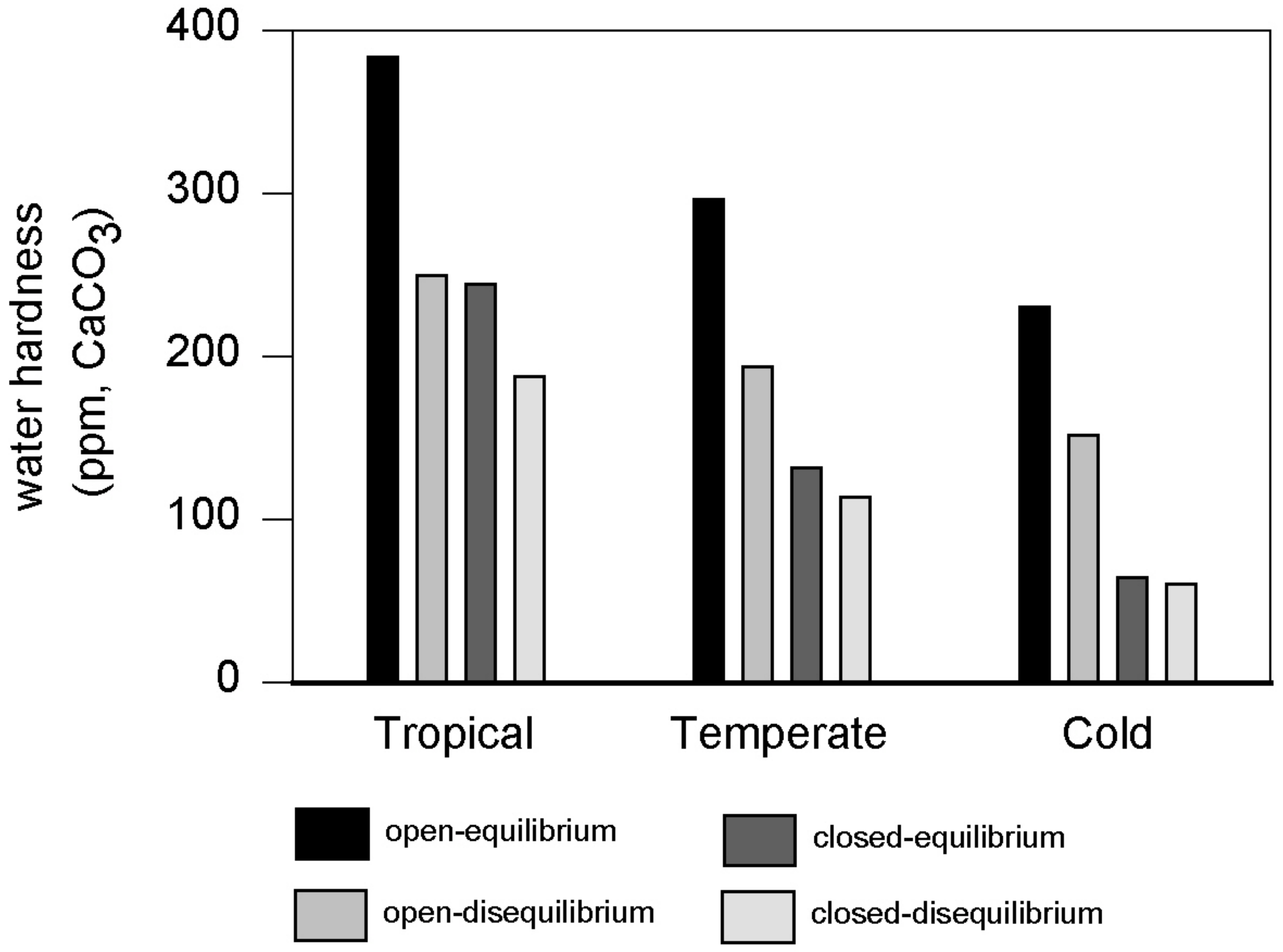

Figure 3.13. Estimated water hardness in tropical, temperate and cold karst.

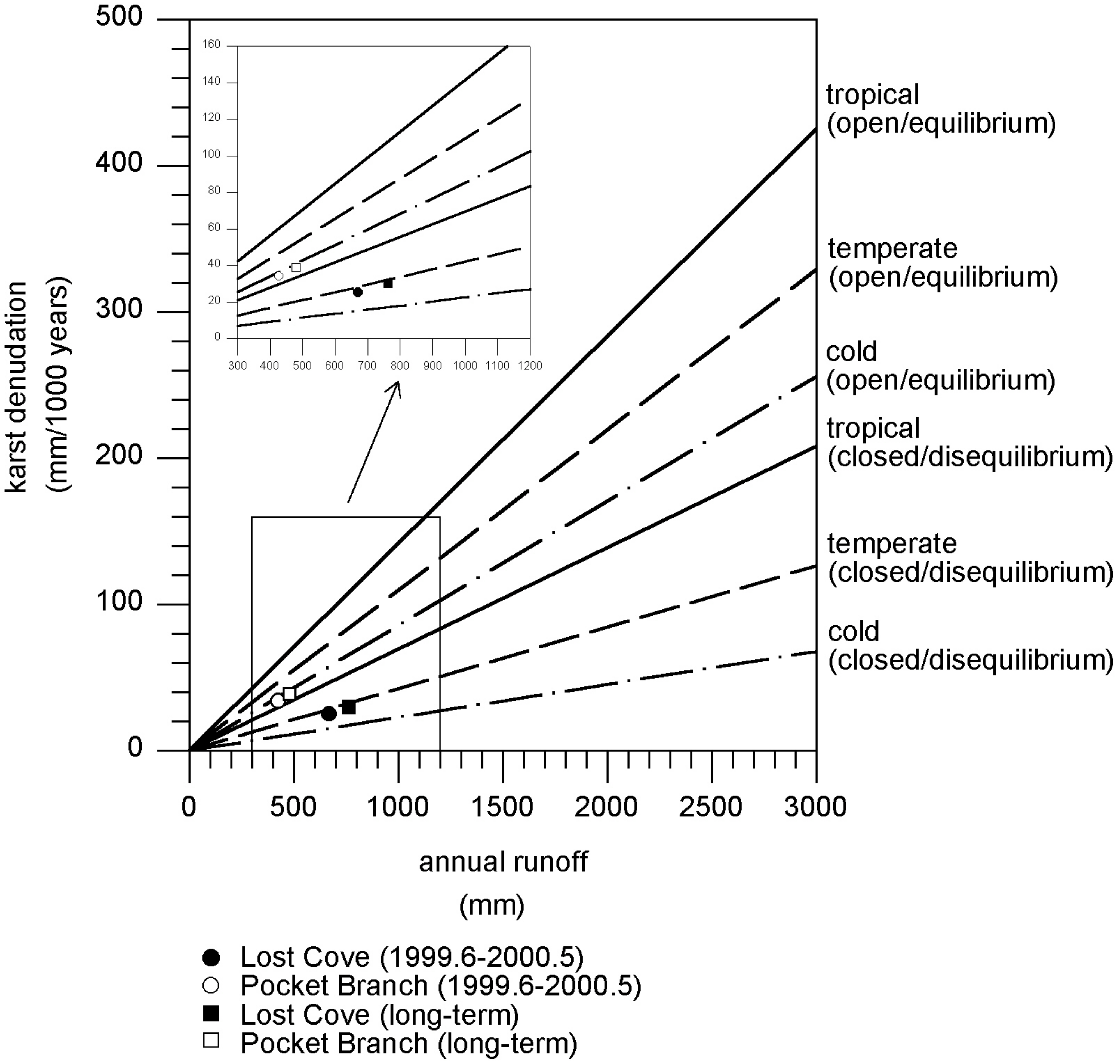

Figure 3.14. Theoretical estimates of karst denudation in tropical, temperate and cold karst terrains compared with denudation at Lost Cove and Pocket Branch.

CHAPTER 4

ENVIRONMENTAL CONTROLS ON PRESENT AND PAST TUFA DEPOSITION ALONG POCKET BRANCH, NORTHWEST GEORGIA, U.S.A.[*]

---

[*] Sheen, S.-W. and G.A. Brook 2001. To be submitted to *Geomorphology*

ABSTRACT

There are both relict and recent tufa deposits along Pocket Branch, Georgia. Present deposition is influenced by algae with calcite tubes forming around each algal cell. Tufa is deposited at most times of the year except during high streamflow conditions when some erosion occurs. This suggests that in other parts of the world tufa deposition may also be determined by streamflow conditions not by climate alone. During the 12-month study period deposition of $CaCO_3$ along Pocket Branch was 0.5 mg per liter of stream water, per meter of stream channel, in August and September, and 0.1 mg per liter in February and March. About 65% of tufa deposition occurred during the winter and spring wet season, with 35% being deposited in the summer and fall dry season. Relict tufas in Pocket Branch are of early-Holocene age. The large size of the relict tufa at Pocket Falls suggests that in the early to middle Holocene rainfall and ground water was more substantial than today. It is possible that increased summer (monsoonal) rainfall in this region caused massive tufa deposition at Pocket Falls in the past. Climate warming at the end of the Little Ice Age (ca. AD 1850) may explain whey there is tufa deposition at Pocket Branch today. Key Words: tufa, karst, water chemistry, Holocene.

INTRODUCTION

Tufas are freshwater calcareous deposits that are chemically or biologically precipitated from supersaturated karst waters. Active and relict tufas are found in most of the major karst areas of the world (e.g. Ford and Pedley, 1996; Lu *et al.*, 2000; Pedley *et al.*, 1996; Wright, 2000). Relict deposits are often an indication of different climatic conditions at the site in the past. In dry areas they frequently record past periods of increased rainfall and ground water flow (Brook *et al.*, 1997; Kronfeld *et al.*, 1988) ; in cold areas they may record past periods of warmer climate (Horvatinčić *et al.*, 2000; Frank *et al.*, 2000)

In early studies, tufa was regarded as a wholly physico-chemical precipitate induced by degassing of CO_2, which leads to supersaturation of spring waters (Lorah and Herman, 1988), but later research has shown that biogenic processes are also important (Emeis *et al.*, 1987; Freytet and Verrecchia, 1999; Janssen *et al.*, 1999; Merz-Preiβ and Riding, 1999; Wright, 2000). Freytet and Verrecchia (1999) argue that when the physico-chemical conditions necessary for carbonate precipitation exist, organisms provide a framework upon which the crystals precipitate (direct role) and determine the mineralogy, nucleation rate, crystal growth and habit (indirect role, biological mediation). Based on studies of two tufa-depositing streams in Germany, Merz-Preiβ and Riding (1999) argue that although degassing is the principal cause of precipitation, organic substrates, particularly cyanobacteria-dominated microbial mats and biofilms, favor calcium carbonate precipitation by providing suitable sites for calcite nucleation. Biological activity also appears to play an important role in determining both the rate of deposition and the internal structure of tufa, in ephemeral streams in the Kimberley region of northwest Australia (Wright, 2000).

The principal aim of this paper is to examine controls on present-day tufa deposition along Pocket Branch, Georgia, U.S.A., and to apply this knowledge to an interpretation of older tufa deposits at the site. Pocket Branch has the only tufas known in the State of Georgia.

STUDY AREA

Geology and Hydrology

Pocket Branch, with a drainage area less than 10 km^2, is located in Pigeon Mountain, a southwestern plunging synclinal mountain in northwestern Georgia (Fig. 4.1). Pigeon Mountain forms the eastern front of the Cumberland Plateau and is the western boundary of the Valley and Ridge Province. It is characterized by rolling hills and shallow valleys except where downcutting streams have formed canyons (Cressler, 1981). The mountain rises about 400 m above the adjacent valleys; it is underlain by essentially horizontally bedded Pennsylvanian and Mississippian clastics and carbonates. The mountain slopes are almost entirely in Mississippian-age limestones and cherts, except for the Pennington Shale near the top of the sequence. At about 600 m elevation the sequence is capped by sandstones and shales of Pennsylvanian age.

Headward sections of Pocket Branch are characterized by a series of dry valleys which rarely produce enough surface flow to reach the middle sections of the drainage basin. However, in the middle part of the basin is Pocket Branch Spring (PBS), which flows year round and which, at times, reaches Pocket Falls, a 20m high waterfall perched on Fort Payne Chert. Pocket Falls is about 100 m down valley from PBS (Figs. 4.2 and 4.3). During the summer, the spring flow is often insufficient to reach Pocket Falls and all of the water sinks at a streamsink (ST1) 50 m downstream, and about 50 m from Pocket Falls. At times of higher flow some water sinks at ST1 and the rest flows over the falls. Water sinking at ST1 resurges a short distance down valley at the base of Pocket Falls, forming part of the flow of a second perennial spring, Pocket Falls Spring (PFS), which also discharges deep ground water. Therefore, downstream of Pocket Falls, flow during the summer/fall dry season is predominantly from PFS, and in the winter/spring wet season it is a combination of water from PFS and water flowing over Pocket Falls. There are both active and relict freshwater calcareous tufa deposits at and immediately below Pocket Falls (Fig. 4.4). One further aspect of the region's hydrology that is important to this study is that after heavy rains water may flow from the usually-dry valleys (PBV in Figs. 4.2 and 4.3) upstream of Pocket Branch Spring. During these rare events, water from these valleys may join the discharge from PBS a short distance downvalley of the spring site, before it reaches the streamsink at ST1.

Climate and Runoff

The climate of the study area is humid subtropical (Köppen Cfa). Air temperature and precipitation were monitored at Pocket Branch during the 12-month period from June 1999 to May 2000 (Fig. 4.5). Air temperature was measured using a HOBO temperature datalogger (Onset Computer Corp.), and precipitation with a tipping bucket rain gauge, Rain Collector II, connected to a HOBO event rainfall logger. Annual mean air temperature during the study year was 15.8°C and precipitation 965 mm (Table 4.1). About 61% of precipitation occurred in winter and spring and 39% in summer and fall.

In order to determine if the study year was wetter/drier or warmer/colder than long-term conditions, and to estimate long-term precipitation and temperature for Pocket Branch, we compared our results with data for the nearest climate station, LaFayette (244 m a.s.l.), 5 km away. Air temperature and precipitation at LaFayette during the study year were compared with long-term climate data (Fig. 4.5). The June 1999-May 2000 annual temperature at LaFayette was 15.3°C, 0.9°C higher than the long-term average, while precipitation (1205 mm) was 260 mm lower than the 1465 mm long-term average.

Also, during the study year, at Pocket Branch 61% (589 mm) of precipitation was in winter and spring and 39% (376 mm) in summer and fall, compared to 63% (760 mm) and 37% (445 mm) at LaFayette, with long-term values at LaFayette being 55% (801 mm) and 45% (664 mm) (Table 4.1). These data suggest that LaFayette were 220 mm drier than normal in summer and fall, and 40 mm drier in winter and spring, respectively.

These comparisons clearly indicate that our study year was somewhat warmer and quite a bit drier than the long-term averages. In order to estimate long-term temperature and precipitation at Pocket Branch, regression relationships were developed between long-term monthly temperature and precipitation, and monthly temperature and precipitation in the period June 1999-May 2000, for LaFayette. The regression equations were used to estimate long-term temperature (14.8°C) and precipitation (1146 mm) at Pocket Branch. The estimated long-term annual mean temperature value at Pocket Branch are 1°C cooler than the annual mean temperature during the study year. The estimated long-term annual precipitation value for Pocket Branch is 1.2 times the annual precipitation during the study year. These data indicate that Pocket Branch was 150 mm drier than long-term estimates in summer and fall, and 30 mm in winter and spring, respectively.

We also monitored combined Pocket Branch and Pocket Falls Springs discharge during the study year. Stream width was measured by tape and velocity using a flow meter (Global Water) at DS 120 m downstream of Pocket Falls (Figs. 4.2 and 4.3). A Enmos pressure transducer (Environmental Monitoring Systems), installed in a stilling well, recorded stream depths from June to October 1999 and a PDCR 1830 pressure transducer (Druck) linked to a CR10X datalogger (Campbell Scientific) recorded depths from November 1999 to May 2000. A rating curve was developed to estimate discharge from the stream depth data. Monthly mean stream discharge was highest in March (0.22 m^3/sec) and lowest in September (0.01 m^3/sec). Average annual discharge was 0.09 m^3/sec (Table 4.2).

It is difficult to calculate the area drained by the two springs at Pocket Branch, we uses precipitation/runoff ratios to estimate runoff in our study area. Topographic map analysis indicates that drainage area is small, less than 10 km^2. Also, in the period June 1999-May 2000, there was no significant lag between precipitation and streamflow, indicating rapid ground water flow-through times. Based on this finding, June 1999-May 2000 and long-term runoff for Pocket Branch, was estimated using long-term precipitation/runoff ratios derived from LaFayette climate data and runoff at nearby U.S. Geological Survey stream gaging stations

The closest stream gaging station to LaFayette is Lookout Creek, near New England, Georgia (202 m a.s.l.) (Fig. 4.1). Long-term annual runoff at Lookout Creek is 618 mm, 80% occurring in the wet season, and 20% in the dry season (Table 4.2).

Comparison of long-term annual rainfall (1465 mm) at LaFayette and annual runoff (618 mm) at Lookout Creek indicates that 42% of annual rainfall becomes runoff. In summer, fall, winter, and spring, runoff is 15%, 22%, 65%, and 58% of precipitation. If these rainfall/runoff percentages hold for our June 1999 - May 2000 and long-term estimates of annual and seasonal rainfall at Pocket Branch, this means that in the period June 1999 to May 2000 annual runoff was 427 mm. Summer, fall, winter, and spring runoff were 27 mm, 42 mm, 151 mm, and 207 mm, respectively (Table 4.2). Long-term annual runoff at Pocket Branch is 480 mm, 80% occurring in the wet season and 20% in the dry season. The estimated long-term annual runoff value for Pocket Branch is 1.1 times the annual runoff during the study year

THE TUFA DEPOSITS

Pocket Falls is dominated by a massive, relict tufa, about 15 m high, 6 m wide, and 1.5 m thick. The deposit has a volume of about 135 m^3. There are several potholes in the tufa at the top of the waterfall, indicating solutional/mechanical stream erosion since its deposition, presumably under high-flow conditions. Part of the tufa mass has collapsed and some of the collapsed blocks now rest a short distance from the waterfall. In addition, near the base of the waterfall and downstream of it, there is clear evidence of present-day deposition of tufa often associated with aquatic vegetation including algae and mosses.

In order to determine when the relict tufas formed, ^{14}C ages were obtained for five tufa samples, one of them a modern deposit. The uncorrected age of the modern sample allowed us to estimate the percent of old carbon (10%) in the tufa at the time of deposition (Jan. - Jun.,1999), taking into account the presence of excess bomb ^{14}C (Genty and Massault, 1997). Assuming that the relict tufas also contained 10% old carbon at the time of their deposition, the massive Pocket Falls carapace dates to 8,580, 7,950 and 7,525 BP, and the relict mass of tufa downstream of the falls, and apparently deposited in place, dated to 6,030 BP (Table 4.3).

Samples of recently precipitated tufa, for microscopic and SEM analysis, were obtained by placing limestone rock tablets (diameter: 2.5 cm), 6 × 6 cm squares of nylon mesh, 2 × 2 cm iron metal squares, and 3 × 4 cm glass slides in the Pocket Branch stream at TU2 and TU3. These were removed after 6 months (Jan. - Jun., 1999); all had tufa deposits on them, with thickness ranging from 0.1 to 0.5 mm.

Tufa deposited on the limestone, mesh, metal and glass substrates inserted into the stream had one of two general morphologies: a ‘cluster’ type with more regular and clean mineral arrangements and a ‘bundle’ type with more random mineral arrangements (Figs. 4.7 and 4.8). X-ray diffraction indicates that calcite is the major component of both precipitates. Field observations and light microscopy show that green-colored ball-like clusters of calcium carbonate were more common in flowing water, while the brown-colored random bundles were typically found beneath dripping water inside small tufa cavities. Both morphologies consist of calcite crystals around algal filaments which appear to be oriented differently in the two water flow regimes.

SEM studies indicate that algae are almost always associated with modern tufa deposits with calcite tubes forming around each algal cell (Fig. 4.9). In time, the algal cells become dislodged from their calcite tubes, giving the tufa a honeycomb structure. The flat tube ends are of a single crystal face which can extend across hundreds of cells. Diatom frustules were also found in the tufas. This indicates that aquatic organisms (principally algal cells at Pocket Branch) are important sites for tufa precipitation. This supports the findings of Freytet and Verrecchia (1999) who found that, in tufa deposition, organisms provide a framework upon which the crystals precipitate and determine crystal growth and habit.

Biological processes by aquatic plants (e.g., cyanobacteria (blue-green algae), algae, and mosses) appear to be important in tufa precipitation (Emeis *et al.*, 1987; Merz-Preiβ and Riding, 1999). Chafetz *et al.* (1991) found calcite crystals growing symmetrically around a thread or stalk of algae suggesting a biotic influence on precipitation. Merz-Preiβ and Riding (1999) also found that calcification around algal stalk creates calcareous tubes enclosing cyanobacterial filaments. Heimann and Sass (1989) considered that photosynthetic uptake of CO_2 by aquatic vegetation causes carbonate precipitation from thin layer of slow-flowing water near plant tissue. Fast-flowing spring water, and hence low residence time with plant material, will therefore reduce the importance of photosynthesis as a driving force for tufa deposition. CO_2 degassing by photosynthetic uptake may be important on the microenvironment scale and not on the ‘average’ stream water (Chafetz *et al.*, 1991). Chafetz *et al.* (1991) indicate that carbonate deposition occurs from the layer of water molecules immediately adjacent to the substrate, but in their study of German tufas Merz-Preiβ and Riding (1999) found that photosynthesis by aquatic plants was not important in tufa precipitation.

The mineralogy, isotope chemistry and morphology of active and relict tufa deposits were examined to investigate present conditions of deposition and any diagenetic changes that may have occurred in the older deposits. Powders were dissolved in hydrochloric acid and analyzed using inductively coupled plasma spectroscopy (Chemical Analysis Laboratory, University of Georgia). All of the deposits were very pure calcium carbonate. Average magnesium concentration in 5 modern deposits was 0.15 mole % (0.11 - 0.20 mole %) and in 7 relict samples it was 0.48 mole % (0.34 - 0.68 mole %). Higher magnesium levels in the older deposits might be due to deposition of secondary sparry calcite cement that fills many primary voids in these deposits (Fig. 4.6). Increased ionic concentration of precipitating waters might explain the higher Mg, and might suggest a reduction in flow over the tufa after its initial deposition.

$\delta^{13}C$ values of tufa also provide information on the vegetation in the drainage basin (Jassen *et al.*, 1999). During tufa deposition, a first source of carbon is atmospheric CO_2 with a mean carbon value of -6‰ (PDB) (Brook, 1999). Carbon is also derived from the dissolution of limestone, with a value about 1‰. The third source is biological coming from CO_2 liberated by respiration and decay of organic matter. For example, C_3 plants respire CO_2 with a $\delta^{13}C$ of -27‰. Soil CO_2 is isotopically heavier than soil organic matter and respired CO_2 because of more rapid diffusion of the lighter isotope ^{12}C. Therefore, beneath pure C_3 plants soil CO_2 is about -22‰. Under a C_3 biomass, calcite deposited in isotopic equilibrium from waters is likely to have a $\delta^{13}C$ value -12‰ under open system conditions (Brook, 1999).

$\delta^{18}O$ and $\delta^{13}C$ (PDB) of one modern and six relict tufas, and $\delta^{18}O$ of four present-day stream waters were measured on a Finnigan Delta mass spectrometer (Stable Isotope Laboratory, Department of Geology, University of Georgia). Gaseous CO_2 was liberated from the tufa by treatment with 100% H_3PO_4 at 50°C. Stream water was first equilibrated with CO_2 at 25°C in order to let gaseous CO_2 have the same $\delta^{18}O$ as the stream water. Oxygen isotopes in the CO_2 was then measured by the mass spectrometer. $\delta^{13}C$ (PDB) of the total dissolved carbon in the stream water was determined by the liberation of CO_2 in H_3PO_4 at room temperature on a Finnigan Mat 252 mass spectrometer (Center for Applied Isotope Studies, University of Georgia).

The recent tufa had a $\delta^{13}C$ of -11.3 and a $\delta^{18}O$ of -5.5‰ (Table 4.4). $\delta^{13}C$ of the relict tufas averaged -9.8‰ (-10.7 to -8.8‰), and $\delta^{18}O$ averaged -5.4‰ per mil.(-6.2 to -4.5‰). $\delta^{13}C$ of the recent and relict tufas are generally very similar suggesting that conditions in the early Holocene were comparable to those of today, and the vegetation was probably dominated by C_3 plants as it is today. The average $\delta^{13}C$ of the stream water samples (mean = -12.3‰, range = -13.2 to -11.6‰) is almost identical to that predicted for open-system conditions with a C_3 vegetation (-12‰), and is similar to that of the recent tufa (-11.3‰). This suggests isotopic equilibrium between carbon in the water and carbon in the precipitated tufa. Average stream water $\delta^{18}O$ was -35.6‰ (PDB). with values ranging from -35.7 to -35.5‰.

The most commonly used relationship for determining temperature from carbonate oxygen isotope data is (O'Neil *et al.*, 1969):

$$T = 16.9 - 4.38 \times (\delta^{18}O_c - \delta^{18}O_w) + 0.10 \times (\delta^{18}O_c - \delta^{18}O_w)^2$$

where T is temperature in °C, and $\delta^{18}O_c$ (PDB) and $\delta^{18}O_w$ (SMOW) are the oxygen isotopic characteristics of the carbonate and the water. This equation applies only under conditions of isotopic equilibrium. Tufa is not precipitated in isotopic equilibrium because rapid CO_2 degassing and evaporation occur in the spring waters. However, we used the equation to determine if $\delta^{18}O$ values of recent tufa and water still record present temperatures. The estimated water temperature during precipitation of recent tufa is 15.6°C and that for relict tufa is 15.2°C. The actual water temperature during deposition of the active tufa (January - June, 1999) was 12 - 14°C which is 1.6 - 3.6°C less than the estimated temperature. If $\delta^{18}O$ of spring water was the same in the early Holocene as it is now, the similarity in tufa $\delta^{18}O$ values suggest deposition at similar water temperatures - basically 12 - 14°C.

The stable isotope results from the Pocket Branch tufas suggest that $\delta^{13}C$ and $\delta^{18}O$ at the time of deposition are preserved in ancient deposits, if sampling is done carefully so as to avoid younger void fillings usually of sparry calcite. Therefore, stable isotope data from older tufas may provide information on vegetation type at the time of deposition ($\delta^{13}C$ values indicating the percent of C_3 vegetation), water temperature, and possibly moisture (air mass) source ($\delta^{18}O$ values will be higher for colder temperatures, and generally lower for a more distant moisture source). These conclusions agree with those of Pedley *et al.* (1996) and Andrews *et al.* (2000) who have also argued that tufas preserve evidence of paleoenvironmental conditions during their formation.

WATER CHEMISTRY

In order to determine when tufa is being deposited and the factors responsible for deposition, temporal and spatial variations in water chemistry were investigated every 2-3 weeks over a 12- month period from June 1999 to May 2000 at 8 monitoring sites (PBS, ST1, ST2, WF, PFS, TU1, TU2 and TU3) along Pocket Branch (Figs. 4.3 and 4.10). ST1 is the point at which waters from PBS sink underground. In the dry season water rarely goes beyond ST1 but in the wet season only a portion of the flow is lost underground at this point. ST2 is the stream before it goes over Pocket Falls, while WF is water going over the falls. TU1, TU2 and TU3 are 20 m, 40 m and 62 m downstream of Pocket Falls, respectively. Stream discharge was measured at DS, 120 m downstream of Pocket Falls. The discharge at this location includes flow from both PBS and PFS.

In the field water pH, and temperature were measured using a Cole-Parmer Digi-Sense pH and temperature meter; pH buffers 7 and 10 were used for calibration. Alkalinity was measured in the laboratory by titration with 0.02 N hydrochloric acid to an end point pH 4.5, immediately after returning from the field. Major cation concentrations (e.g., Ca^{2+}, Mg^{2+}, K^+, and Na^+) were determined by ICP analysis (Chemical Analysis Laboratory, University of Georgia). Total water hardness was calculated from calcium and magnesium concentrations. The program PHREEQC (Parkhurst, 1995) was used to analyze the water chemistry data and to estimate the partial pressure of dissolved carbon dioxide and the saturation index with respect to calcite (SI_c).

A total of 151 water samples were collected at 8 sites on 24 sampling dates during the study year. The results show that CO_2 degassing occurs both above and below the Pocket Falls waterfall, but that tufa is deposited only by water below the waterfall. The flow in the stream beyond the waterfall was generally below 1 m/s throughout the year.

Broad Temporal and Spatial Variations in Water Chemistry

In order to examine broad variations in water chemistry along Pocket Branch, 23 samples were analyzed from four major sites during the 12-month study period: PBS, PFS, TU1 and TU3. To simplify analysis, the data were also converted into 3-month averages for summer (June- August), fall, (September - November), winter (December - February), and spring (March-May) (Table 4.5).

As Figs. 4.11 and 4.12 show, water temperatures at the four sites reflect site hydrogeology and time of year. The temperature at PBS remained fairly constant (13.1°C to 14.3°C) through the year reflecting the temperature of recharge to the diffuse aquifer (mainly in winter and spring), and the temperature of the aquifer bedrock, the latter being close to the mean annual temperature for the region. The very small variations in temperature suggest some mixing of waters in the aquifer and a standardization of water temperatures. Water emerging from PFS flowed 50 m from PBS before sinking back underground. As a result, this water was influenced by the air temperature during its passage from PBS to PFS and, because of this, it is colder in winter and warmer in summer than PBS waters (12.2-15.7°C). The influence of ambient air temperature is even more marked at TU1, where temperatures range from 11.4°C to 17.8°C, and at TU3, where the range is 10.6°C to 20.1°C. These results show that after water emerges from PBS it is more and more influenced by air temperatures which lower water temperatures in winter and raise them in summer. This effect is illustrated by the standard deviation of water temperature at the four sites, standard deviation increasing gradually from PBS to TU3 (0.4 at PBS, 1.1 at PFS, 1.9 at TU1, and 3.0 at TU3) (Table 4.6).

In karst areas water pH, log pCO_2, and SI_c are frequently related with pH and SI_c generally increasing as CO_2 partial pressure decreases. This is certainly the case at Pocket Branch (Figs. 4.11 and 4.12). At PBS all three variables remain fairly constant throughout the year (pH = 6.6 to 7.3, log pCO_2 = -2.07 to -1.32, and SI_c = -0.68 to -0.19), presumably because recharge waters have a fairly uniform carbon dioxide level, and a similar aquifer residence time. pH, log pCO_2 and SI_c at PFS, TU1 and TU3 reflect the increasing loss of carbon dioxide from the original spring water emerging from PBS. However, this difference is much more marked in the winter/spring wet season than in the summer/fall dry season. For example, in the dry season degassing of CO_2 was modest, log pCO_2 falling to -2.01 to -1.53 at PFS, -2.58 to -2.10 at TU1, and -2.74 to - 2.34 at TU3. This gradual loss of CO_2 along the stream was accompanied by gradual increases in pH (6.9 to 7.3 at PFS, 7.4 to 7.8 at TU1 and 7.7 to 8.0 at TU3) and in SI_c (-0.48 to - 0.04 at SP2, 0.12 to 0.48 at TU1 and 0.32 to 0.52 at TU3). In the wet season the loss of CO_2 was much more marked (-2.41 to -1.57 at PFS, -2.92 to - 2.09 at TU1 and -3.03 to -2.39 at TU3) so that increases in pH (6.9 to 7.6 at PFS, 7.4 to 8.1 at TU1 and 7.6 to 8.2 at TU3) and SI_c (-0.44 to 0.12 at PFS, 0.00 to 0.53 at TU1 and 0.13 to 0.65 at TU3) were equally marked.

As log pCO_2 at PBS was no higher in the wet season than in the dry season, we believe that the marked increase in CO_2 degassing in the wet season was due to the higher discharge of the spring in this period. Degassing was probably enhanced by more turbulent flow and by flow of some water over Pocket Falls. During the dry season flow was modest and not sufficient to induce rapid mixing of air with the water, so that degassing was slow.

Water at PBS (mean $SI_c = -0.44$) was undersaturated w.r.t. calcite through the year, while water at PFS (mean $SI_c = -0.23$) was slightly supersaturated in winter and undersaturated in other seasons. Water at TU1 (mean $SI_c = 0.29$) and TU3 (mean $SI_c = 0.39$) was supersaturated throughout the year.

Dissolved Ca varied in two ways. First, it was inversely related to spring/stream discharge. Lower values in the wet season were probably due to the reduced contact time between the water and the host bedrock because of the increased volume of recharge. Secondly, there is a gradual drop in Ca concentrations from PBS to TU3 as Ca is precipitated from solution. For example, average values are 81 ppm at PBS, 77 at PFS, 73 at TU1, and 69 at TU3 (Table 4.6).

Mg concentrations also vary with season/discharge and along the stream spring/stream system. Mean Mg increased from PBS to TU3 (4.3 ppm at PBS, 6.5 ppm at PFS, 6.3 ppm at TU1 and 6.4 ppm at TU3) probably because of a higher Mg content in the bedrock below Pocket Falls. Mg was also higher at all sites in the warm/dry season (summer and fall) possibly because under conditions of reduced discharge the water had more time to dissolve Mg than in the wet season when flow was more rapid and contact time between water and rock more limited. Changes in Ca and Mg along the drainage system are also reflected in molar Ca/Mg ratios, which are lower in the dry season when Mg concentrations are high, and higher in the wet season when they are low. Because of the increase in Mg downstream, mean molar Ca/Mg ratios were 12.9 at PBS, 8.3 at PFS, 8.8 at TU1 and 8.2 at TU3.

Differences in water temperature, pH, hardness, log pCO_2 and SI_c between PBS, PFS, TU1, TU2 and TU3 are clearly apparent in Fig. 4.13 which illustrates that throughout the study year there was a gradual decrease in pCO_2 and hardness, and an increase in pH and SI_c from PBS through PFS, TU1, TU2 to TU3. As mentioned previously, this reflects the gradual loss of CO_2, with increasing supersaturation of the spring water and eventually the precipitation of carbonate at high levels of supersaturation.

Spatial Variations on Specific Days During Different Seasons

To better understand the spatial variations in water chemistry that affect tufa deposition, we also examined conditions at all 8 measurement sites on particular days during the dry and wet seasons. An important implication of the data presented in Fig. 4.14 is that Pocket Falls Spring discharges deep groundwater, like spring PBS, and also water from PBS that sinks at ST1 before reaching Pocket Falls. The evidence for this is particularly clear in the pH, log pCO_2 and SI_c records. On the days discussed below, pH and SI_c rise from PBS to ST1 (and, if there is flow over Pocket Falls it also increases to ST2 and WF), while at the same time log pCO_2 falls due to degassing of CO_2 (Fig. 4.14). However, at PFS these trends are reversed but not to the extent that they return to PBS values. This indicates that PFS is discharging deep groundwater as well as water from PBS that sinks above Pocket Falls.

The Summer/Fall Dry Season

Fig. 4.14 presents chemical data for three different days during the dry season, namely June 27, August 29, and October 23, 1999. There was no flow of PBS springwater beyond the ST1 sink on any of these days. On June 27 and August 29 there was a clear increase in temperature from PBS to ST1, and then a return to cooler temperatures at PFS because of the addition of deeper, colder groundwaters. Downstream of PFS temperatures increased gradually as the ambient air temperature was higher than the water temperature. October 23 was a much colder day, with air temperatures cooler than spring water temperatures. As a result, water temperature decreases from PBS to ST1 but then increases again at PFS, before decreasing gradually along the stream below Pocket Falls.

On all days log pCO_2 decreases gradually from PBS to TU3 except for an increase at PFS because this spring adds deep groundwater to the flow below Pocket Falls. The decrease is due to degassing of CO_2 from the springwaters and it is accompanied by an increase in pH and SIc, with the values at PFS briefly reversing the trends. On all days waters beyond Pocket Falls are supersaturated w.r.t. calcite and this resulted in the deposition of calcite along the stream channel from TU1 to TU3, the magnitude being 14.5 ppm (as $CaCO_3$) on June 27, 20.7 ppm on August 29, and 24.5 ppm on October 23. Although Ca decreased on these days, Mg increased at PFS suggesting that PFS waters have higher Mg than those of PBS. A slight increase in Mg downstream of PFS may suggest that the bedrock beyond Pocket Falls contains more Mg than the bedrock of the aquifer above Pocket Falls.

The Winter/Spring Wet Season

Fig. 4.15 presents chemical data for three different days during the winter/spring wet season, namely December 17, 1999, February 26, and April 22, 2000. On December 17 there was no flow beyond ST1 but on the other two days water flowed over Pocket Falls joining the flow from PFS below this point. In December, flow from PBS and PFS was warmer than the ambient air temperature and so there was a general increase in water temperature downstream. On the other two days the air was warmer than the groundwater and so water temperatures increased downstream.

As in the dry season, degassing of CO_2 led to a decrease in pCO_2 downstream to ST1 or WF depending on flow characteristics, and then a slight increase at PFS due to input of deeper groundwater with a higher CO_2 content. Degassing continued below Pocket Falls to TU3. Accompanying the degassing was an increase in pH and in SI_c with waters beyond Pocket Falls being supersaturated w.r.t. calcite. Again, PFS waters lowered pH and SI_c temporarily due to addition of undersaturated, lower-pH water. Ca/Mg ratios dropped steadily along the stream from PBS except for a slight rise at PFS due to mixing of water with a higher Ca/Mg ratio. This trend in Ca/Mg was partly due to the precipitation of Ca below Pocket Falls due to saturation of the water (removal of Ca raised the Ca/Mg ratio), and partly due to addition of Mg from Mg-rich PFS water and dissolution of Mg from the rocks below the falls. The magnitude of Ca deposition was 8.7 ppm (as $CaCO_3$) on December 17, 3.2 ppm on February 26, and 18.2 ppm on April 22.

Comparing chemistry on the three dry-season and three wet-season days, it is clear that deposition of Ca in ppm was greater on the dry-season days although log pCO_2, pH and SI_c values appear little different between the two seasons. However, Mg was noticeably higher on the dry-season days August 29 and October 23 due mainly to higher Mg in PFS waters. It may be that reduced flow allows more time for dissolution of $CaMg(CO_3)_2$, which takes much longer to dissolve than $CaCO_3$.

TUFA DEPOSITION AND EROSION

Temporal Variations in Water Chemistry Below Pocket Falls in the Area of Tufa Deposition

Based on field observations, the main area of tufa deposition along Pocket Branch is presently below Pocket Falls, between monitoring sites TU1 and TU3. Chemistry was monitored on 23 sampling dates during the study year. Measurements of the decrease in Ca from TU1 to TU3 indicate that tufa was being deposited on 20 of the 23 sampling dates, with deposition occurring in every month of the year. Only on October 10 and December 12, 1999, and March 11, 2000, was there no precipitation of carbonate between these sites. On 20 sampling dates the Ca concentration at TU3 was on average 4.9 ppm less than at TU1 (range from 0.5 ppm on January 9, 2000 to 10 ppm on August 7, 1999). These numbers indicate that during the study year 12.2 mg of calcite is precipitated per liter of streamflow, or 6.7% of the dissolved calcium at TU1, the range being 0.7-13.8%.

On three of the 23 sampling dates we observed a mean increase in Ca of 2.4 ppm between TU1 and TU3 with values being 1.8 ppm on March 11, 2000, to 2.7 ppm on both October 10 and December 12, 1999. This translates into 6.0 mg calcite erosion per liter of stream water, or 3.3% of the dissolved calcium at TU1 (range 2.7-3.4%). Mg concentration increased, on average, only 0.2 ppm (20 of the 23 sampling dates) between TU1 and TU3, but pH and SI_c increased by 0.17 (20 of the 23 sampling dates) and 0.11 (22 of the 23 sampling dates), respectively, and log pCO_2 and molar Ca/Mg ratio decreased by 0.20 (22 of the 23 sampling dates) and 0.60 (22 of the 23 sampling dates), respectively.

The highest bimonthly tufa deposition rate was in August and September when7.9 ppm, or 11.0% of the dissolved Ca at TU1, was deposited between TU1 and TU3 (Table 4.7). This is 19.7 mg of calcite deposition per liter of stream water. The highest bimonthly tufa deposition rate was 6.6 times the lowest rate in February and March.

Between TU1 and TU3 an average 6.8 ppm Ca was deposited in summer, 6.7 ppm in fall, 2.2 ppm in winter, and 3.5 ppm in spring. The annual mean Ca deposition rate was 4.8 ppm, which is 12 mg of calcite per liter of stream water.

Fig. 4.16 shows details of the chemistry between TU1 and TU3 during the study year. Water temperature increases during the summer and drops slightly during the fall, when discharge along Pocket Branch is low. During winter and spring, when discharge increases substantially there is little change in water temperature probably because the colder air temperatures can not influence water temperature significantly because of the large volume of flow. Log pCO_2 drops much more in summer, possibly in part due to the increase in water temperature during this season, which would encourage degassing of CO_2 as this gas is less soluble in warmer water. Accompanying the change in pCO_2, pH and SI_c increase more in the dry season than in the wet season, while Ca and total hardness decrease more in summer and fall than in winter and spring. Mg concentrations increase very slightly throughout the year probably due to contact with rocks of higher Mg content along the stream channel. Ca and total hardness increase on only three measurement dates during the study year emphasizing the dominance of carbonate deposition over carbonate solution.

Temporal Variations in Chemistry on August 3, 1999

On August 3, 1999 there was no flow over Pocket Falls, and stream discharge was only about 0.01 m^3/s below Pocket Falls. Water samples were collected at TU1 and TU3 at noon, 3 pm and 6 pm to examine possible variations in tufa deposition during the day (Table 4.8).

At noon, the water temperature increased from 17.1°C at TU1 to 18.6°C at TU3 and log pCO_2 decreased from -2.29 to -2.52. Accompanying the decrease in pCO_2 due to degassing of CO_2, pH increased from 7.6 to 7.8, and SI_c increased from 0.27 to 0.41. This increase in supersaturation led to a decrease in dissolved Ca from 70 to 65 ppm indicating 5 ppm of Ca deposition or 8% of the dissolved Ca at TU1.

At 3 pm, the water temperature at TU1 had increased by 0.7 deg. C to 17.8°C and by 2.0 deg. C to 20.6°C at TU3. Degassing of CO_2 had increased slightly with log pCO_2 dropping from -2.25 to -2.57 between TU1 and TU3. As a result of the increased degassing, pH increased from 7.6 to 7.9, and SI_c from 0.23 to 0.45, leaving water at TU3 more supersaturated than earlier in the day. As a result, Ca decreased from 69 to 60 ppm between TU1 and TU3, indicating about 9 ppm of Ca deposition or 13% of the dissolved Ca at TU1.

By 6 pm, the water temperature at TU1 had returned to its noon value (17.1°C) and had dropped by 0.4 deg. C to 20.2°C at TU3. Degassing of CO_2 was less marked than at 3 pm with log pCO_2 dropping from -2.19 to -2.47. This reduced degassing may have been due to the slightly lower water temperatures. The degassing resulted in an increase in pH from 7.5 to 7.8, and an increase in SI_c from 0.17 to 0.40. Increasing supersaturation of the water led to precipitation of 6 ppm Ca or 8% of the dissolved Ca at TU1 with Ca concentration dropping from 69 to 63 ppm between TU1 and TU3.

The above measurements indicate that on August 3, 1999 tufa deposition was slightly more rapid at 3 pm in the afternoon, than at noon, or at 6 pm in the evening. Therefore, deposition was greater during the warmest part of the day when CO_2 was at its lowest level ($10^{-2.57}$ atm.). The low CO_2 levels were almost certainly due in part to increased degassing due to the highest water temperatures of the day (as pointed out earlier, CO_2 is less soluble at higher temperature). However, we believe that deposition at 3 pm was also greater because of the increased absorption of CO_2 from the stream water by aquatic plants at a time of increased photosynthesis (highest temperatures and highest solar radiation during the 3 pm measurement period). As aquatic plants absorb dissolved CO_2 from the water during photosynthesis, we believe that they create a thin layer of highly supersaturated water near their foliage, and that this encourages precipitation of Ca. In addition to this, the plants provide an extensive surface area for deposition to occur. This might help to explain our earlier observation that tufa precipitation along Pocket Branch is intimately associated with aquatic plants, particularly algae.

Water Chemistry at Times of Tufa Erosion

Our data indicate that there were only three measurement days when tufa was being eroded from the stream channel below Pocket Falls rather than being deposited. Here we discuss conditions on two of those dates, October 10, during fall, 1999, and February 12, during winter, 2000. On both dates water flowed over Pocket Falls in part because there was also flow of water from upvalley of PBS (PBV in Figs. 4.3 and 4.17), this water joining the flow from PBS between PBS and ST1. Such flow only occurs after particularly heavy rains as runoff produced by lesser rains simply sinks along the normally-dry valleys of this area. Below Pocket Falls stream discharge on both dates was about 26 m^3/s; the width of the stream was about 8 m, the depth 0.4 m and stream velocity about 8 m/sec.

On Oct. 10 1999, water temperature increased gradually downvalley from PBS because air temperature was higher than the temperature of the spring water (Fig. 4.17). On February 12 there was a slight decrease in water temperature downstream because the spring water was warmer than the air. Log pCO_2 decreased from -1.77 to -2.62 from PBS to TU3 on October 10 and from -2.07 to -3.03 on February 12, partly due to the addition of CO_2-poor valley water from PBV. On both dates pCO_2 increased slightly due to addition of CO_2-rich spring water from PFS. The loss of CO_2 resulted in downstream increases in pH (7.0 to 7.8 on Oct. 10 and 7.3 to 8.2 on Feb. 12) and SI_c (-0.47 to 0.45 on Oct. 10 and -0.19 to 0.65 on Feb. 12). On both dates low pH and low SI_c water added by PFS raised the acidity of the stream waters at the base of Pocket Falls. Importantly, even though the stream water was supersaturated on both measurement dates ($SI_c = 0.40$ at TU1 on Oct. 10 and 0.53 on Feb. 12), to a level comparable with periods when there was deposition of tufa, there was no deposition of Ca. In fact, Ca and total hardness increased from 80 to 83 and 213 to 220 on Oct. 10 and from 71 to 74 and 186 to194 on Feb. 12. Thus, there was slight erosion of carbonate below Pocket Falls on these two days rather than the usual deposition.

Water chemistry data indicate that tufa is eroded below Pocket Falls during high discharge conditions (stream velocity ≥8 m/s) after large storm events. Erosion occurred despite supersaturation levels similar to periods of deposition. We believe that the reason for erosion rather than deposition may be reduced photosynthesis of aquatic vegetation during cloudy, rainy conditions, and the greater depth of water, both of which would reduce solar inputs to the submerged algae. Also, it may be that more turbulence in the flowing water may break or prevent the development of a highly supersaturated layer near to vegetation surfaces due to removal of dissolved CO_2 by photosynthesizing aquatic plants. During periods of lesser flow, and less turbulent conditions, this thin supersaturated layer may not be disrupted by the flow.

Tufa Deposition Rates

Bimonthly and seasonal tufa deposition rates were calculated using stream discharge data and the loss of dissolved $CaCO_3$ in stream waters from TU1 to TU3 (Table 4.9). An average 20 ppm of $CaCO_3$ was deposited in August and September and 3 ppm in February and March.

Stream discharge was derived from measurement site DS 120 m dowstream of Pocket Falls (Fig. 4.3). The area of stream channel between TU1 and TU3 where tufa is being deposited is about 210 m^2 in area (5 m wide by 42 m long). The highest bimonthly mean tufa deposition rate was 572 g of $CaCO_3$ per m^2 per day (April and May) and the lowest 81 g of $CaCO_3$ per m^2 per day (August and September). The deposition rate during April and May was 7.1 times that in August and September.

Between TU1 and TU3 tufa deposition was 210 g/m^2 day in summer, 275 g/m^2 day in fall, 317 g/m^2 day in winter, and 573 g/m^2 day in spring. These estimates show that 65% of tufa is deposited in the wet season (winter and spring) and 35% in the dry season (summer and fall). Annual mean tufa deposition was 344 g/m^2 day. Our findings indicate that tufa is eroded during brief periods of increased streamflow, when flow from higher up in the Pocket Branch system joins flow from PBS. Because of these brief periods of erosion, which are difficult to fully evaluate without detailed discharge and chemical data, tufa deposition below Pocket Falls is probably slightly less than the 344 g/m^2 day.

The estimated long-term runoff at Pocket Branch is about 1.1 times the annual runoff during the study year. Therefore, long-term tufa deposition may be 378 g/m^2 day rather the 344 g/m^2 day for the period June 1999 - May 2000.

DISCUSSION AND CONCLUSIONS

SEM photos of recent tufa deposits indicate the importance of aquatic plants, particularly algae, in the precipitation process, with calcite tubes commonly forming around individual algal cells. Our finding that precipitation of tufa occurs more rapidly at the hottest time of the day, when pCO_2 is at its lowest, and when aquatic plant photosynthesis is also at a maximum, suggests that organisms such as algae may remove CO_2 from a thin layer of water near the plant thus significantly increasing the level of supersaturation in that layer. The aquatic vegetation also provides ideal surfaces for precipitation to occur, and so tufa deposition is enhanced by biological activity and occurs preferentially on aquatic plant surfaces.

Along Pocket Branch there was almost continuous deposition of tufa throughout our year of study although, for short periods after heavy rains, flow from upvalley, which joined the flow from PBS before ST1, caused some slight erosion of tufa rather than precipitation. Erosion was not caused by lower saturation of the water as SI_c values were similar at these times to values when tufa was precipitated. We suggest that the increased depth and velocity of the water (erosion occurred only at flow velocities $\geq$ 8m/s) may prevent deposition by reducing plant photosynthesis (reduced light penetration) and by disrupting the layer of supersaturated water generated close to the plant tissue by removal of CO_2 from the stream water during photosynthesis.

Below Pocket Falls the deposition of $CaCO_3$ was a maximum of about 0.5 mg per liter of water per meter of stream channel in August and September, and a minimum of 0.1 mg/liter in February and March (Table 4.10). Annual mean deposition was 0.3 mg/liter/m of channel. Approximately 65% of deposition occurred in the winter/spring wet season and 35% in the summer/fall dry season. Other researchers have also reported a higher per liter rate of deposition in the dry season. For instance, Lorah and Herman (1988) report that along Falling Spring Creek, a thermal spring-fed creek in Virginia, calcite precipitation reached a peak in July (118 mg/l) and was lowest in February (56 mg/l). Dandurand et al. (1982) investigated Ca in waters going over a 20 m high waterfall in the Pyrenees of France. They found that during high-flow conditions Ca decreased from 82 to 76 ppm from the top to the bottom of the falls. During low-flow conditions the decrease was from 77 to 43 ppm. Dandurand et al. (1982) proposed that at low discharge the small amount of water is spread over the surface of the waterfall and this causes a high rate of CO_2 escape which leads to rapid and marked supersaturation and deposition of Ca. Despite the frequently greater loss of Ca per liter at times of low flow, the greatest deposition rates are most often during the wet season when the increased volume of flow offsets the reduced loss of Ca per liter of flow.

At other cold spring tufa sites around the world carbonate is being precipitated from waters with initial Ca concentrations of 72-213 ppm (Table 4.10). Water hardnesses at Pocket Branch (62-85 ppm) are at the lower end of this range. Loss of Ca ranges from 6 ppm (82 to 43 ppm, January, 1979) in Foix, France (Dandurand *et al.*, 1982) to145 ppm (213 to 68 ppm, July, 1993) in Sichuan, China (Liu *et al.*, 1995). In addition, $CaCO_3$ deposition rates ranged from 0.08 mg/l/m of channel in the Nahanni Karst, Canada (Brook and Ford, 1982) to 2.1 mg/l/m of channel in Foix, France (Dandurand *et al.*, 1992). The rate of tufa deposition at Pocket Branch (0.3 mg/l/m of channel) lies in the middle of this range.

The active tufa deposits at Pocket Falls appear to be in equilibrium with $\delta^{18}O$ and $\delta^{13}C$ in the spring waters, and similar values in relict deposits suggest conditions generally similar to those of today during deposition of these masses. This indicates deposition under a predominantly C_3 vegetation such as exists at the site today. The relict tufa carapace at the falls was deposited in the time range 8.6-7.5 ka B.P. (8,600 - 7,500 ^{14}C years before present (1950)) while another relict deposit below Pocket Falls dates to 6.0 ka B.P. No sample from the massive waterfall tufa has been dated to younger than 7.5 ka B.P. suggesting that the deposits downstream of the base were laid down by flow from PFS and perhaps also by limited flow down the waterfall, with little or no precipitation on the waterfall itself.

Based on tufa deposition on substrates inserted into the stream as part of this study, current tufa accumulation is about 0.5 mm/yr. At a similar rate of accumulation, the large tufa at Pocket Falls would have taken about 3 ka to form. As radiocarbon ages for this deposit indicate deposition over a period of only 1 ka, a more rapid rate of tufa deposition is required to form this massive accumulation. Currently, most tufa deposition along Pocket Branch occurs during the cool, wet season, when water pCO_2 and Ca precipitation rates are at their lowest. Deposition during the warm, dry season is much more rapid per liter of water, but, because of reduced spring discharge in this season, maximum deposition occurs during the wet season, which is the season of maximum spring discharge.

To deposit the massive tufa at Pocket Falls, spring flow during the early Holocene must have been more than it is today either on an annual or seasonal basis. Even when there is flow over Pocket Falls today, there is no deposition on the ancient waterfall tufa, suggesting that CO_2 in the spring water during the early Holocene may also have been a little higher than now.

Therefore, it appears that spring flow in the early Holocene (8.6-7.5 ka) was greater than it is today. Either there was more runoff in all seasons of the year or runoff was much higher seasonally. Leigh and Feeney (1995), Brook F. (1996), Leigh and Brook F. (1996), and Lamoreaux (1999) have all found evidence of increased summer monsoonal rainfall during the early to middle Holocene and this could explain the ages we have obtained for the large relict tufa deposits in Pigeon Mountain.

Based on the occurrence of several large paleomeanders in the Middle Ogeechee River of the Georgia Coastal Plain, Leigh and Feeney (1995) suggest that the discharge of floods during paleomeander formation, from about 8.5-4.5 ka B.P., was at least double that of modern river floods, and that there was a much wetter climate, at least seasonally, during paleomeander development. Also, according to paleoclimatic simulations by Kutzbach (1987), the climate of the Southeast was wetter 9.0-3.0 ka B.P. because of higher summer solar radiation caused by intensified summer monsoon conditions. Kutzbach estimates an increase of 180-360 mm/yr in rainfall in the Georgia Coastal Plain, which Leigh and Feeney suggest is insufficient to explain the formation of the paleomeanders if it is distributed evenly through the year. So, they propose that there was, instead, a pronounced shift in the seasonal pattern of precipitation during paleomeander formation, with summers much wetter than now and winters much drier. In fact, Brook F. (1996) suggests that in the early/mid Holocene almost all of the precipitation may have been in summer.

At Pocket Falls the evidence seems to suggest that during the early Holocene, from about 8.6-7.5 ka B.P., springflow along Pocket Branch was greater than it is today and water flowed over Pocket Falls for a considerable portion of the year. It was during this period that the large tufa carapace was deposited. In the period 7.5-6.0 ka B.P. there was a reduction in the flow of water over the waterfall and after 6.0 ka B.P. the flow was further reduced. This change may have been partly caused by the pirating of PBS waters underground at ST1 but, in our view, it was more likely caused by a significant reduction in springflow possibly during the summer and fall which may have been substantially wetter than now. Today, the summer and fall are the seasons of highest pCO_2 and Ca concentration in the spring water and so an increase in spring flow would significantly increase the rate of tufa formation over present levels.

Assuming that the early Holocene rate of tufa deposition was at least double that of today and that winter/spring deposition was the same, this implies that stream discharge and rainfall in summer/fall in the early Holocene was 3.8 times that of today and annual precipitation about twice that of today (2018 mm/yr). Theses calculations assume a similar rate of tufa deposition (ppm/liter) during the early Holocene summer as during the present summer. Based on present long-term estimates of rainfall at Pocket Branch (1146 mm) this implies an increase in annual rain in early Holocene of 1.8 times and an increase in summer/fall long-term rainfall of 2.7 times.

As the winter/spring rate of tufa precipitation at Pocket Branch is less than the summer rate, if the increase in rainfall during the early Holocene was during these seasons rather than during summer/fall the projected increase in annual rainfall would be even greater.

Some time after about 6.0 ka B.P. spring flow dropped so much that there was no longer significant flow beyond the ST1 sink and so the Pocket Falls tufa became inactive. Deposition clearly continues below the falls today but the volume of tufa in this area, given that it has had at least 6.0 ka to form is very modest.

The period of deposition of the Pocket Falls tufa was clearly one of high discharge, for the top of the tufa carapace is pockmarked by solutionally and/or mechanically eroded potholes that are typical of fluvial situations, but which require considerable flow for their formation. Even today, major storm events generate sufficient flow from the usually-dry valleys upstream of PBS. At these times there is modest erosion below Pocket Falls. After about 6.0 ka B.P. it is possible that high flows in winter and spring were more common than now and may have been responsible for the potholes so evident on the upper surface of the Pocket Falls tufa.

It is evident that after about 6.0 ka B.P. tufa deposition slowed, probably to rates lower than those of today. Flow over Pocket Falls diminished substantially although it did not cease altogether. This water percolated through the voids of the early/mid Holocene deposit, filling them with sparry calcite richer in Mg, probably because of higher ionic concentrations in the water. We argue for a reduction in tufa accumulation after 6.0 ka B.P. with a later increase to present levels because at present rates of accumulation a sizeable tufa mass could have been deposited over as long a period as 6 ka. We would estimate that given the very modest volume of recent tufa material downstream of Pocket Falls that the present period of higher deposition has not been a lengthy one possibly beginning only in the last few hundred years. One possible explanation for the recent increase in tufa deposition may be warming of global climates since about A.D. 1850 at the end of the Little Ice Age, accompanied by global warming due to the increase in greenhouse gases in the Earth's atmosphere. Higher temperatures may have increased rates of vegetation growth, this increasing soil CO_2 levels, and thus the ability of ground waters to dissolve limestone. Higher temperatures may also have increased the rate of CO_2 degassing from spring waters because CO_2 is less soluble in warmer water, and they may also have increased rates of photosynthesis of aquatic vegetation which might also increase CO_2 degassing and water saturation levels.

Goudie *et al.* (1993) have argued that in the late Holocene there was a marked decline in the deposition of tufa in cool temperate areas. There has been considerable debate about the causes of this possible decline, with some authors postulating the importance of natural climatic changes, and others asserting that human influences have been crucial. Baker and Simms (1998) suggest that the apparent decline may be more related to the under-reporting of contemporary tufa deposition than to a real decline in tufa activity.

The evidence from northwest Georgia appears to support the notion of an early to mid Holocene period of increased tufa deposition in this area, and of a reduction in tufa deposition rates subsequently. At Pocket Branch we suggest that the period of increased tufa deposition was at a time in the past when rainfall and ground water recharge was more substantial because of a more monsoonal climate that brought a very substantial increase in summer and fall rainfall to the region. It is possible that rainfall regime and annual amount may also explain increased tufa deposition during the early/mid Holocene in other temperate areas of the world, but it is also possible that temperature conditions played a role. Baker and Simms (1998) have argued that to assess whether there was a period of increased tufa deposition in the early/mid Holocene we need to know more about presently active sites. In the case of Pocket Branch there is deposition today but the evidence at the site still suggests more rapid deposition of tufa in the past.

ACKNOWLEDGEMENTS

This research was funded by a NSF Doctoral Dissertation Improvement Award. We thank David S. Leigh and John F. Dowd who provided some of the equipment used in this study. We thank John Christof of the South Cumberland Recreation Area for permission to work at Lost Cove, and Allen Padgett of the Crockford Pigeon Mountain Wildlife Management Area for permission to work at Pocket Branch.

REFERENCES

Andrews, JE, Pedley, M and Dennis, P. 2000. Palaeoenvironmental records in Holocene Spanish tufas: a stable isotope approach in search of reliable climatic archives. *Sedimentology* **47**: 961-978.

Baker, A and Simms, MJ. 1998. Active deposition of calcareous tufa in Wessex, UK, and its implications for the 'late-Holocene tufa decline'. *The Holocene* **8**: 359-365.

Brook, FZ. 1996. A Late-Quaternary pollen record from the Middle Ogeechee River valley, southeastern Coastal Plain, Georgia. M.A. Thesis, Department of Geography, University of Georgia, 110 p.

Brook, GA and Ford, DC. 1982. Hydrologic and geologic control of carbonate water chemistry in the subarctic Nahanni karst, Canada. *Earth Surface Processes and Landforms* **7**: 1-16.

Brook, GA, Cowart, JB, Brandt, SA and Scott, L. 1997. Quaternary climatic change in southern and eastern Africa during the last 300 ka: The evidence from caves in Somalia and the Transvaal region of South Africa. *Zeitschrift für Geomorphologie* N.F. Suppl.-Bd. **10**:15-48.

Brook, GA. 1999. Arid zone palaeoenvironmental records from cave speleothems. In eds. Singhvi AK, Derbyshire E. *Paleoenvironmental Reconstruction in Arid Lands*. 217-262. Oxford & IBH. New Delhi.

Chafetz, HS, Ruch, PF and Utech, NM. 1991. Microenvironmental controls on mineralogy and habit of $CaCO_3$ precipitates: an example from an active travertine system. *Sedimentology* **38**: 107-126.

Cressler, CW. 1981. Geology and Ground-Water Resources of Walker County, Georgia. Department of Natural Resources, State of Georgia, Atlanta. Georgia.

Dandurand, JL, Schott, J, Usdowski, E, Gout, R, Hoefs, J and Menschel, G. 1982. Kinetically controlled variations of major components and carbon and oxygen isotopes in a calcite-precipitating spring (Pyrenees, France). *Chemical Geology* **36**: 299-315.

Emeis, KC, Richnow, HH and Kempe, S. 1987. Travertine formation in Plitvice National Park, Yugoslavia: chemical versus biological control. *Sedimentology* **34**: 595-609.

Ford, TD and Pedley, HM. 1996. A review of tufa and travertine deposits of the world. *Earth-Science Reviews* **41**: 117-175.

Frank, N, Braum, M, Hambach, U, Mangini, A and Wagner, G. 2000 Warm period growth of travertine during the last interglaciation in southern Germany. *Quaternary Research* **54**: 38-48.

Freytet, P and Verrecchia, EP. 1999. Calcitic radial palisadic fabric in freshwater stromatolites: diagenetic and recrystallized feature or physicochemical sinter crust? *Sedimentary Geology* **126**: 97-102.

Genty, D and Massault, M. 1997. Bomb ^{14}C recorded in laminated speleothems: calculation of dead carbon proportion. *Radiocarbon* **39**: 33-48.

Goudie, AS, Viles, HA and Pentecost, A. 1993. The late-Holocene tufa decline in Europe. *The Holocene* **3**: 181-186.

Heimann, A and Sass, E. 1989. Travertines in the northern Hula Valley, Israel. *Sedimentology* **36**: 95-108.

Horvatinčić, N, Čalić, R and Geyh, MA. 2000. Interglacial growth of tufa in Croatia. *Quaternary Research* **53**: 185-195.

Janssen, A, Swennen, R, Podoor, N and Keppens, E. 1999. Biological and diagenetic influence in Recent and fossil tufa deposits from Belgium. *Sedimentary Geology* **126**: 75-95.

Kronfeld, J, Vogel, JC, Rosenthal, E and Weinstein-Evron, M. 1988. Age and paleoclimatic implications of the Bet Shean Travertines. *Quaternary Research* **30**: 298-303.

Kutzbach, JE. 1987. Model simulations of the climatic patterns during the deglaciation of North America. *North America and adjacent oceans during the last deglaciation*. The Geology of North America. Vol. K-3. The Geological Society of America. 425-446.

Lamoreaux, HJK. 1999. Human-environmental relationships in the Coastal Plain of Georgia based on high-resolution paleoenvironmental records from three peat deposits. Ph.D. Dissertation, Department of Geography, University of Georgia, 229 p.

Leigh, DS and Feeney, TP 1995. Paleochannels indicating wet climate and lack of response to lower sea level, Southeast Georgia. *Geology* **23** (8): 687-690.

Leigh, DS and Brook, FZ. 1996. Paleochannels and pollen record indicative of enhanced monsoonal circulation and wetness during the early and middle Holocene in southeastern Georgia. *Abstracts with Programs, Geological Society of America* **28** (7): 304.

Liu, Z, Buhmann, D, Svensson, U, Dreybrodt, W and Yuan, D. 1995. Hydrodynamic control of inorganic calcite precipitation in Huanglong Ravine, China: field measurements and theoretical prediction of deposition rates. *Geochimica et Cosmochimica Acta* **59**: 3087-3097.

Lorah, MM and Herman, JS. 1988. The chemical evolution of a travertine-depositing stream: geochemical processes and mass transfer reactions. *Water Resources Research* **24**: 1541-1552.

Lu, G, Zheng, C, Donahoe, RJ and Lyons, WB. 2000. Controlling processes in a $CaCO_3$ precipitating stream in Huanglong Natural Scenic District, Sichuan, China. *Journal of Hydrology* **230**: 34-54.

McNeely, R. 1994. Long-term environmental monitoring of ^{14}C levels in the Ottawa region. *Environment International* **20**: 675-679.

Merz-Preiβ, M and Riding, R. 1999. Cyanobacterial tufa calcification in two fresh streams: ambient environment, chemical thresholds and biological processes. *Sedimentary Geology* **126**: 103-124.

O'Neil, JR, Clayton, RN and Mayeda, T. 1969. Oxygen isotope fractionation in divalent metal carbonates. *Journal of Chemical Physics* **51**:5547-5558.

Parkurst, DL. 1995. User's Guide to PHREEQC- A Computer Program for Speciation, Reaction-Path, Advective-Transport, and Inverse geochemical Calculations. Water-Resources Investigations Report 95-4227. U.S. Geological Survey, Lakewood, Colorado.

Pedley, M, Andrews, J, Ordonez, S, Garcia del Cura, MA, Gonzales Martin, JA and Taylor, D. 1996. Does climate control the morphological fabric of freshwater carbonates? A comparative study of Holocene barrage tufas from Spain and Britain. *Palaeogeography, Palaeoclimatology, Palaeoecology* **12**: 239-257.

Wright, JS. 2000. Tufa accumulations in ephemeral streams: observations from the Kimberley, north-west Australia. *Australian Geographer* **31**: 333-347.

Table 4.1. Summary of climate at Pocket Branch (1999.6-2000.5 and long-term estimates) and at LaFayette (1999.6-2000.5 and 1961-1990).

	Pocket Branch		**LaFayette**	
	99.6-00.5	**long-term**	**99.6-00.5**	**1961-1990**
Air Temperature (°C)				
Annual Mean	15.8	14.8	15.3	14.4
Highest Monthly Mean	26.1 (Aug.)	25.8 (Jul.)	25.6 (Aug.)	25.0 (Jul.)
Lowest Monthly Mean	4.5 (Jan.)	2.8 (Jan.)	4.3 (Jan.)	2.7 (Jan.)
Summer (Jun.-Aug.)	24.6	25.0	24.3	24.3
Fall (Sep.-Nov.)	16.5	15.6	16.1	15.1
Winter (Dec.-Feb.)	5.9	4.1	6.0	4.0
Spring (Mar.-May)	16.1	14.6	14.9	14.1
Precipitation (mm)				
Annual Mean	965	1146	1205	1465
Highest Monthly Mean	184 (Apr.)	124 (Mar.)	236 (Apr.)	163 (Mar.)
Lowest Monthly Mean	20 (Dec.)	72 (Aug.)	6 (Aug.)	88 (Aug.)
Summer (Jun.-Aug.)	183	257	244	324
Fall (Sep.-Nov.)	193	268	201	340
Winter (Dec.-Feb.)	232	313	341	404
Spring (Mar.-May)	357	308	419	397

Table 4.2. Annual and seasonal runoff at Pocket Branch and Lookout Creek.

[*]**Discharge (m^3/s) 1999.6 - 2000.5**	**Pocket Branch and Pocket Falls Springs**
Annual Mean	.09
Summer	.03
Fall	.04
Winter	.14
Spring	.16

[$]**Runoff (mm) 1975.10-1996.9**	**Lookout Creek near New England**
Annual Mean	618
Summer	50
Fall	74
Winter	262
Spring	232

[#]**Est. Runoff (mm) 1999.6-2000.5**	**Pocket Branch**
Annual	427
Summer	27
Fall	42
Winter	151
Spring	207

[#]**Est. Runoff (mm) long-term**	**Pocket Branch**
Annual	480
Summer	39
Fall	59
Winter	203
Spring	179

---

[*] measured values [$] published data

[#] estimated runoff using rainfall/runoff relationships

Table 4.3. Radiocarbon dates of recent and relict tufa from Pocket Branch, Georgia.

Sample ID	Description	Laboratory ID	$\delta^{13}C$ (PDB)	F (pmc)[*]	^{14}C age (yr BP)	Corrected ^{14}C age (yr BP)
PT1[#]	Recent, near TU3	AA36784	-11.9	.9888±.0050	90±40	recent
PT2	Relict, base waterfall formation	AA36781	-8.3	.3527±.0026	8,370±60	7,525±280
PT3	Relict, near TU3	AA36782	-9.5	.4248±.0050	6,875±95	6,030±260
PT4	Relict, top waterfall formation	AA36783	-10.2	.3346±.0027	8,790±65	7,950±280
PT5	Relict, core waterfall formation	UGA7109			9,420±100	8,580±300

[*] pmc: percent modern carbon

[#] estimation of dead carbon in PT1

$$dcp = \left(1 - \frac{a^{14}C_c}{a^{14}C_{atm}}\right) \times 100\% \text{ (Genty and Massault, 1997)}$$

where dcp: dead carbon proportion, $a^{14}Cc$: activity of ^{14}C of calcite, and $a^{14}Catm$: activity of ^{14}C of atmosphere

$a^{14}C_c$ is 98.88 at PT1 and $a^{14}C_{atm}$ is estimated to be 110 at year 1999 (McNeely, 1994)

Table 4.4. δ^{18}O and δ^{13}C at tufa and water, Pocket Branch, Georgia.

Recent tufa sample ID	δ^{13}C (PDB)	δ^{18}O (PDB)	Relict tufa sample ID	δ^{13}C (PDB)	δ^{18}O (PDB)	Water sample ID	δ^{13}C (PDB)	δ^{18}O (SMOW)	δ^{18}O (PDB)	Sampling date	Sampling site
ATU1	-11.3	-5.5	RTU1	-10.0	-5.6	WA1	-13.2	-5.7	-35.5	3/11/00	TU3
			RTU2	-8.8	-6.2	WA2	-11.6	-5.7	-35.5	3/25/00	TU3
			RTU3	-9.3	-5.0	WA3	-12.1	-5.8	-35.6	4/8/00	TU3
			RTU4	-10.7	-5.7	WA4		-5.9	-35.7	4/22/00	TU3
			RTU5	-9.4	-4.5						
			RTU6	-10.4	-5.5						

Table 4.5. Seasonal mean water chemistry at PBS, PFS, TU1 and TU3, Pocket Branch.

Season	Temperature (°C)	pH	Ca (ppm)	Mg (ppm)	Hardness (ppm,$CaCO_3$)	Molar Ca/Mg	Alkalinity (ppm,HCO_3)	log pCO_2	SI_c
PBS									
Summer	13.6	6.9	77.7	5.4	216	8.9	254	-1.57	-.42
Fall	14.0	6.9	82.6	5.3	228	10.6	253	-1.55	-.42
Winter	13.4	6.9	85.8	3.3	228	16.2	241	-1.60	-.40
Spring	13.3	6.8	77. 9	3.0	206	16.5	225	-1.56	-.54
PFS									
Summer	15.2	7.0	75.1	7.9	220	6.1	248	-1.61	-.38
Fall	14.5	7.1	78.7	8.4	231	7.1	243	-1.77	-.25
Winter	12.5	7.4	80.4	4.6	220	10.9	232	-2.09	-.01
Spring	13.6	7.1	74.4	4.9	206	9.3	216	-1.83	-.31
TU1									
Summer	16.5	7.7	71.1	8.0	211	5.8	246	-2.31	.31
Fall	14.4	7.7	75.2	8.5	223	7.2	232	-2.38	.30
Winter	12.3	7.7	73.1	4.2	200	11.4	218	-2.47	.28
Spring	13.3	7.7	73.0	4.1	199	11.4	208	-2.44	.25
TU3									
Summer	18.3	7.9	64.3	8.2	195	5.2	210	-2.58	.44
Fall	14.8	7.8	70.1	8.6	210	6.7	216	-2.59	.42
Winter	12.0	7.9	71.8	4.3	197	10.9	209	-2.61	.38
Spring	13.4	7.8	70.6	4.2	193	10.7	200	-2.55	.31

Table 4.6. Summary of water chemistry at PBS, PFS, TU1 and TU3, Pocket Branch.

	Temperature (°C)	pH	Ca (ppm)	Mg (ppm)	Hardness (ppm,$CaCO_3$)	Molar Ca/Mg	Alkalinity (ppm,HCO_3)	log pCO_2	SI_c
					PBS (n = 23)				
Mean	13.6	6.9	81.1	4.3	220	12.9	244	-1.57	-.44
S.D.	.35	.14	6.44	1.59	18.56	4.22	26.10	.16	.11
Maximum	14.3	7.3	94.3	7.8	250	21.7	287	-1.32	-.19
Minimum	13.1	6.6	69.0	1.9	180	6.6	189	-2.07	-.68
					PFS (n = 23)				
Mean	13.9	7.1	77.3	6.5	220	8.3	235	-1.82	-.23
S.D.	1.11	.20	6.43	2.80	19.04	2.90	24.07	.23	.19
Maximum	15.7	7.6	89.8	13.1	245	13.2	262	-1.53	.12
Minimum	12.2	6.9	61.9	3.4	173	3.5	178	-2.41	-.48
					TU1 (n = 23)				
Mean	14.2	7.7	73.1	6.3	209	8.8	227	-2.40	.29
S.D.	1.86	.17	4.88	3.20	17.36	4.09	23.96	.20	.15
Maximum	17.8	8.1	82.0	13.5	236	18.4	253	-2.09	.53
Minimum	11.4	7.4	65.0	2.3	175	3.1	172	-2.92	.00
					TU3 (n = 23)				
Mean	14.7	7.8	69.1	6.4	199	8.2	209	-2.58	.39
S.D.	3.00	.15	5.59	3.20	13.01	4.08	17.81	.15	.13
Maximum	20.1	8.2	82.9	13.6	221	18.0	238	-2.34	.65
Minimum	10.6	7.6	61.3	2.5	176	2.9	171	-3.03	.13

Table 4.7. Bimonthly and seasonal variations in tufa deposition between TU1 and TU3.

Months	Change in Ca from TU1 to TU3		Season	Change in Ca from TU1 to TU3	
	(ppm)	(%)		(ppm)	(%)
Jun./Jul.	-5.5	-7.9	Summer	-6.8	-9.4
Aug./Sep.	-7.9	-11.0	Fall	-6.7	-9.0
Oct./Nov.	-6.7	-8.7	Winter	-2.2	-3.0
Dec./Jan.	-2.4	-3.2	Spring	-3.5	-4.5
Feb./Mar.	-1.2	-1.7			
Apr./May	-4.3	-5.6			

Table 4.8. Water chemistry at TU1 and TU3 on August 3 1999.

Sampling time	**TU1**					**TU3**					Change in Ca from TU1 to TU3	
	Temp. (°C)	pH	Ca (ppm)	log pCO_2	SI_c	Temp. (°C)	pH	Ca (ppm)	log pCO_2	SI_c	(ppm)	(%)
Noon	17.1	7.6	69.8	-2.29	.27	18.6	7.8	64.6	-2.52	.41	-5.2	-7.5
3 pm	17.8	7.6	68.5	-2.25	.23	20.6	7.9	59.5	-2.57	.45	-9.0	-13.1
6 pm	17.1	7.5	69.1	-2.19	.17	20.2	7.8	63.4	-2.47	.40	-5.7	-8.2

Table 4.9. Bimonthly and seasonal variations in tufa deposition between TU1 and TU3.

Bimonthly				**Seasonal**			
Months	Discharge (m^3/s)	$CaCO_3$ (ppm)	Tufa Deposition (g/m^2 day)	Season	Discharge (m^3/s)	$CaCO_3$ (ppm)	Tufa Deposition (g/m^2 day)
Jun./Jul.	.05	13.7	282	Summer	.03	17.0	210
Aug./Sep.	.01	19.7	81	Fall	.04	16.7	275
Oct./Nov.	.05	16.7	344	Winter	.14	5.5	317
Dec./Jan.	.14	6.0	346	Spring	.16	8.7	573
Feb./Mar.	.18	3.0	222				
Apr./May	.13	10.7	572				

Table 4.10. Selected published tufa deposition rates in cold water springs in temperate and cold areas.

	Date	**Change in Ca (ppm)**	**Deposition rate**[*]	**Channel length (m)**	**Deposition rate per m of channel**[**]		**Source**
Temperate Areas							
Georgia, USA	Aug.-Sep., 1999	72→64	20	42	.48	**.29**	this study
	Feb.-Mar., 2000	69→68	3		.07		
Sichuan, China	Sep., 1991	198→84	285	3500	.08	**.09**	Liu *et al.*, 1995
	Jun., 1992	202→66	340		.10		
	Jul., 1993	213→68	362		.10		
Sichuan, China	Jul., 1996	120→56	160	800	.20	**.20**	Lu et al., 2000
Westerhof, Germany	Aug., 1974	152→134	45	265	.17	**.17**	Jacobson and Usdowski, 1975
Westerhof, Germany	Jun., 1986	186→157	72	256	.28	**.28**	Dreybrodt *et al.*, 1992
Bad Urach, Germany	Sep., 1994	122→76	115	1000	.12	**.11**	Merz-Preiβ and Riding, 1999
	Jan., 1995	176→137	97		.10		
Girona, Spain	Apr.-Oct., 1989	108→78	75	750	.10	**.10**	Mas *et al.*, 1992
Foix, France	Jan., 1979	82→76	15	24	.63	**2.1**	Dandurand *et al.*, 1982
	Mar., 1979	77→43	85		3.54		
Cold Areas							
N.W.T., Canada	Jul., 1972	111→92	48	600	.08	**.08**	Brook and Ford, 1982

[*] deposition rate (mg $CaCO_3$ per liter of water)

[**] deposition rate per m of channel (mg $CaCO_3$ per liter of water per meter of channel); average value in bold

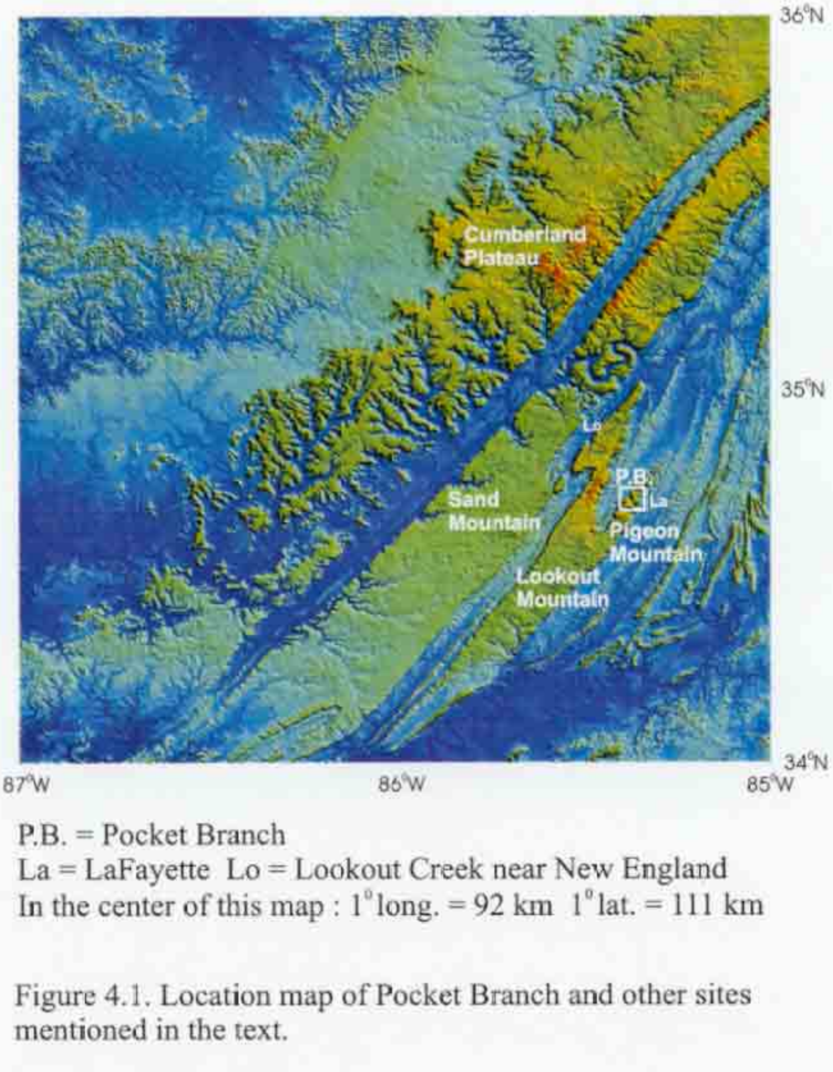

P.B. = Pocket Branch

La = LaFayette Lo = Lookout Creek near New England

In the center of this map : 1° long. = 92 km 1° lat. = 111 km

Figure 4.1. Location map of Pocket Branch and other sites mentioned in the text.

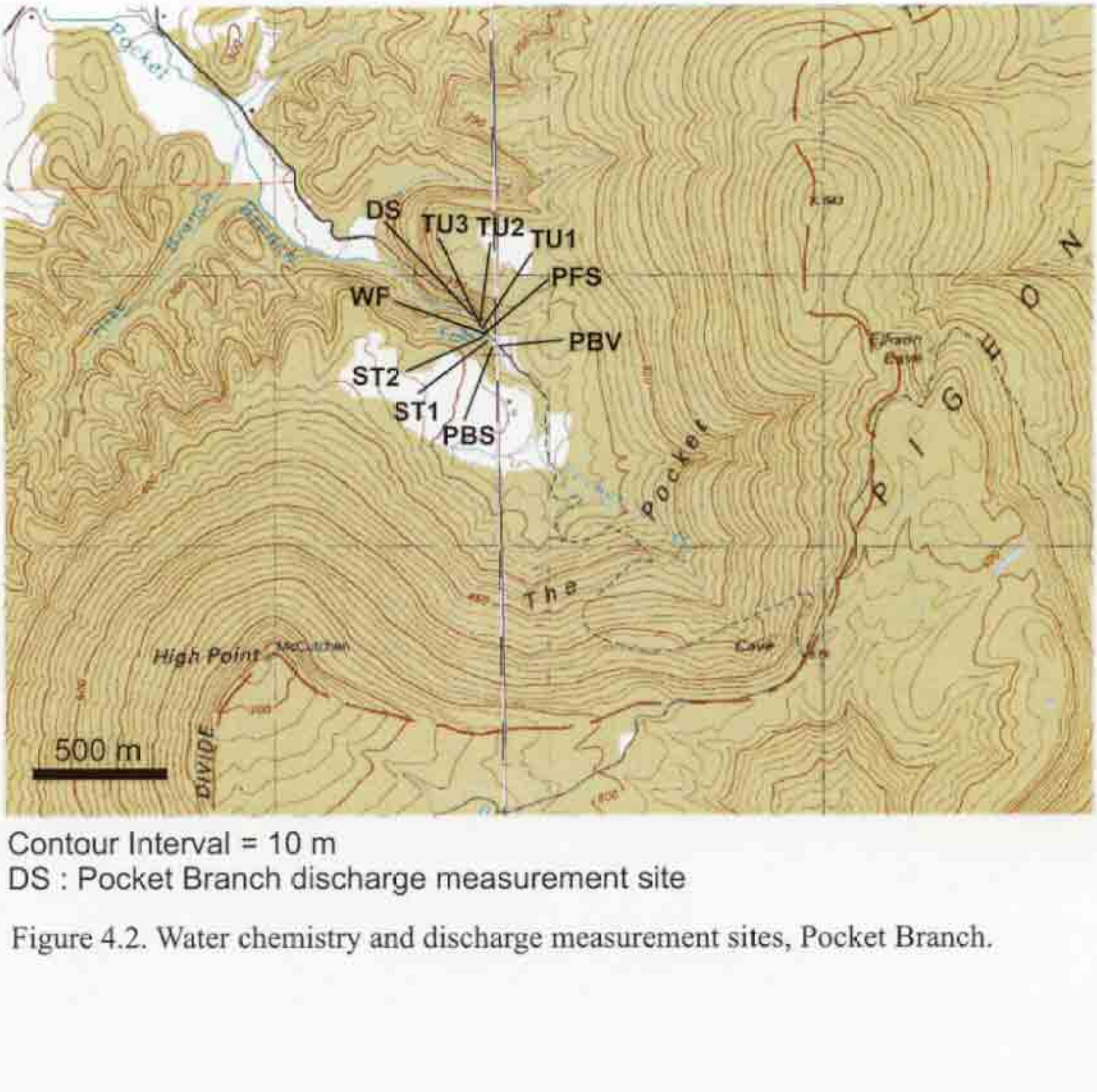

Contour Interval = 10 m
DS : Pocket Branch discharge measurement site

Figure 4.2. Water chemistry and discharge measurement sites, Pocket Branch.

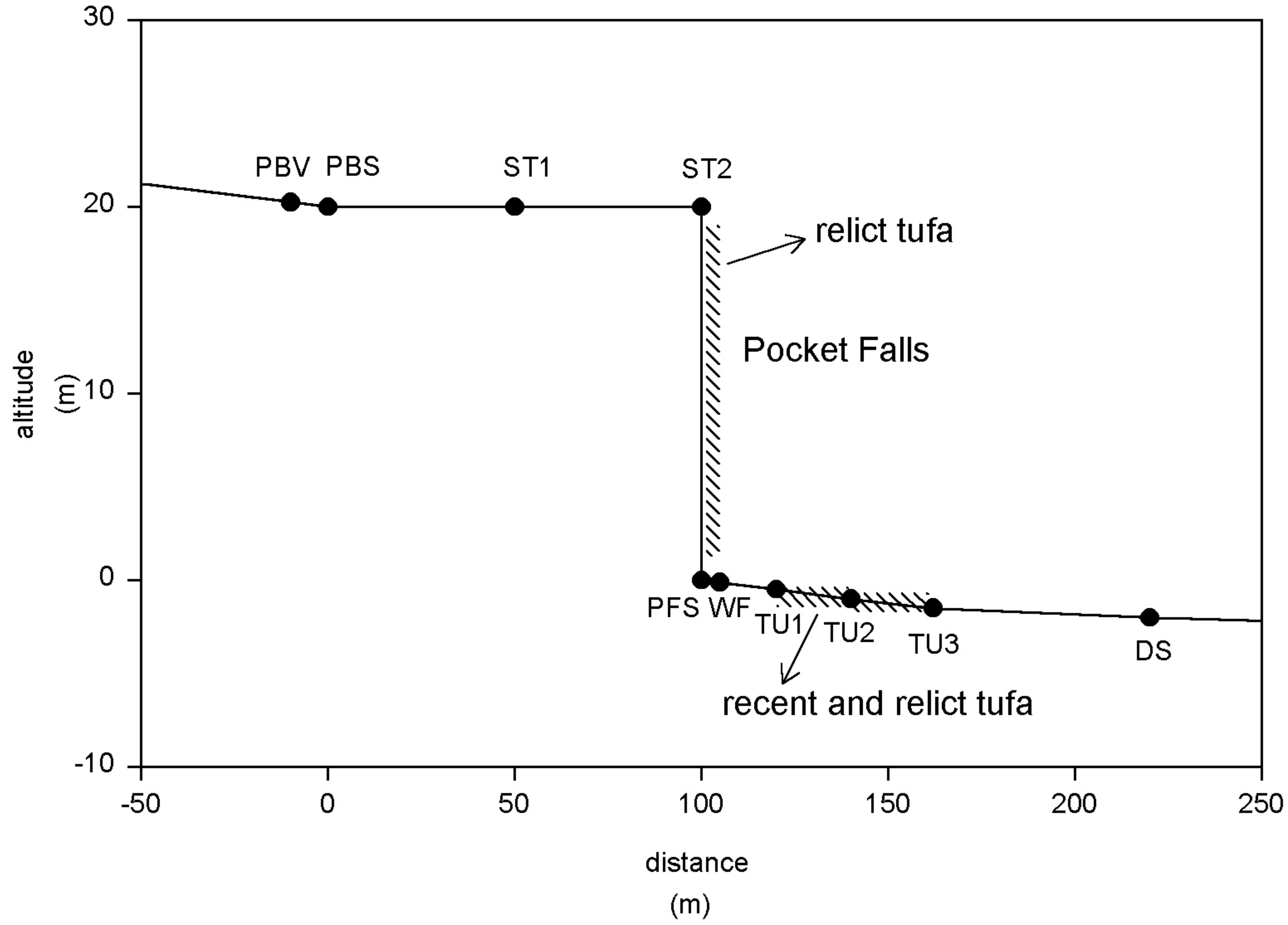

PBV: Pocket Branch valley above Pocket Branch Spring (PBS)
DS: discharge measurement site 120 m dowstream Pocket Falls

Figure. 4.3 Schematic diagram of hydrology in Pocket Branch.

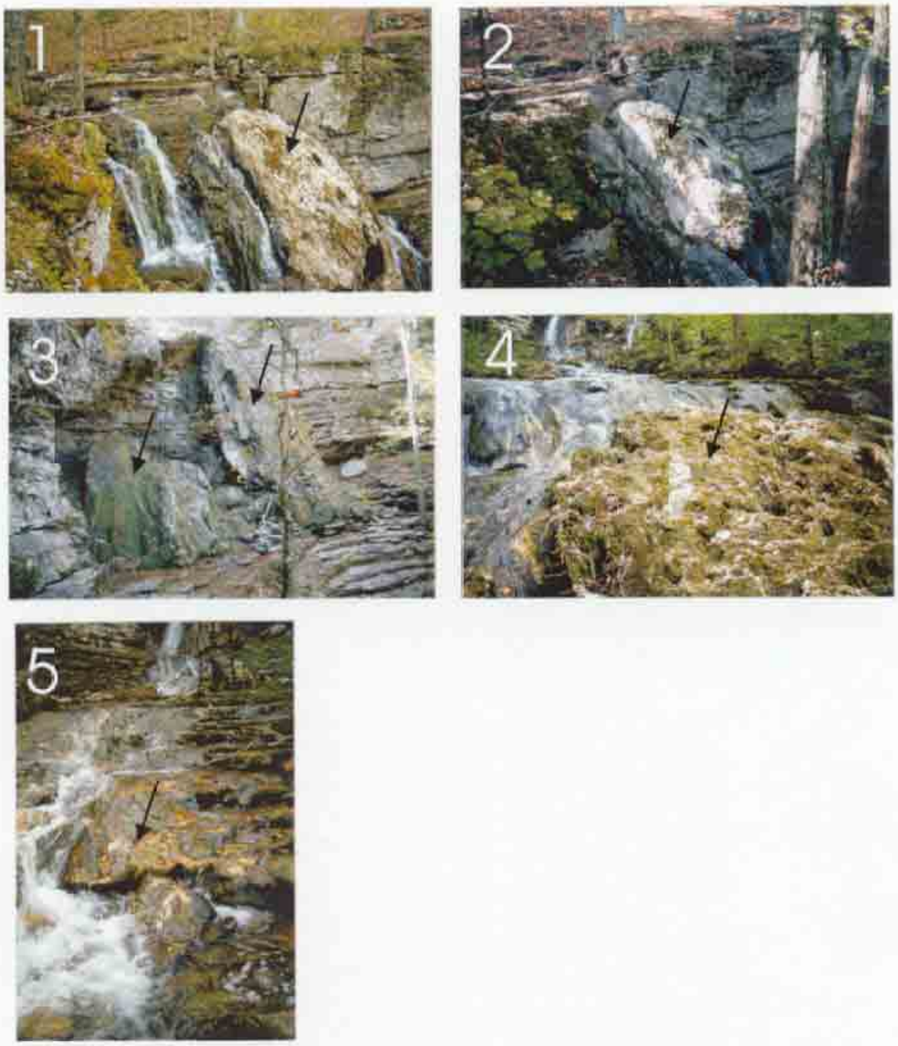

Figure 4.4. Relict and recent tufa deposits at Pocket Branch:
upper part of relict waterfall tufa in wet winter (1) and in dry summer (2),
lower part of relict waterfall tufa in dry summer (3),
relict tufa downstream of Pocket Falls (4) and
recent tufa downstream of Pocket Falls (5).

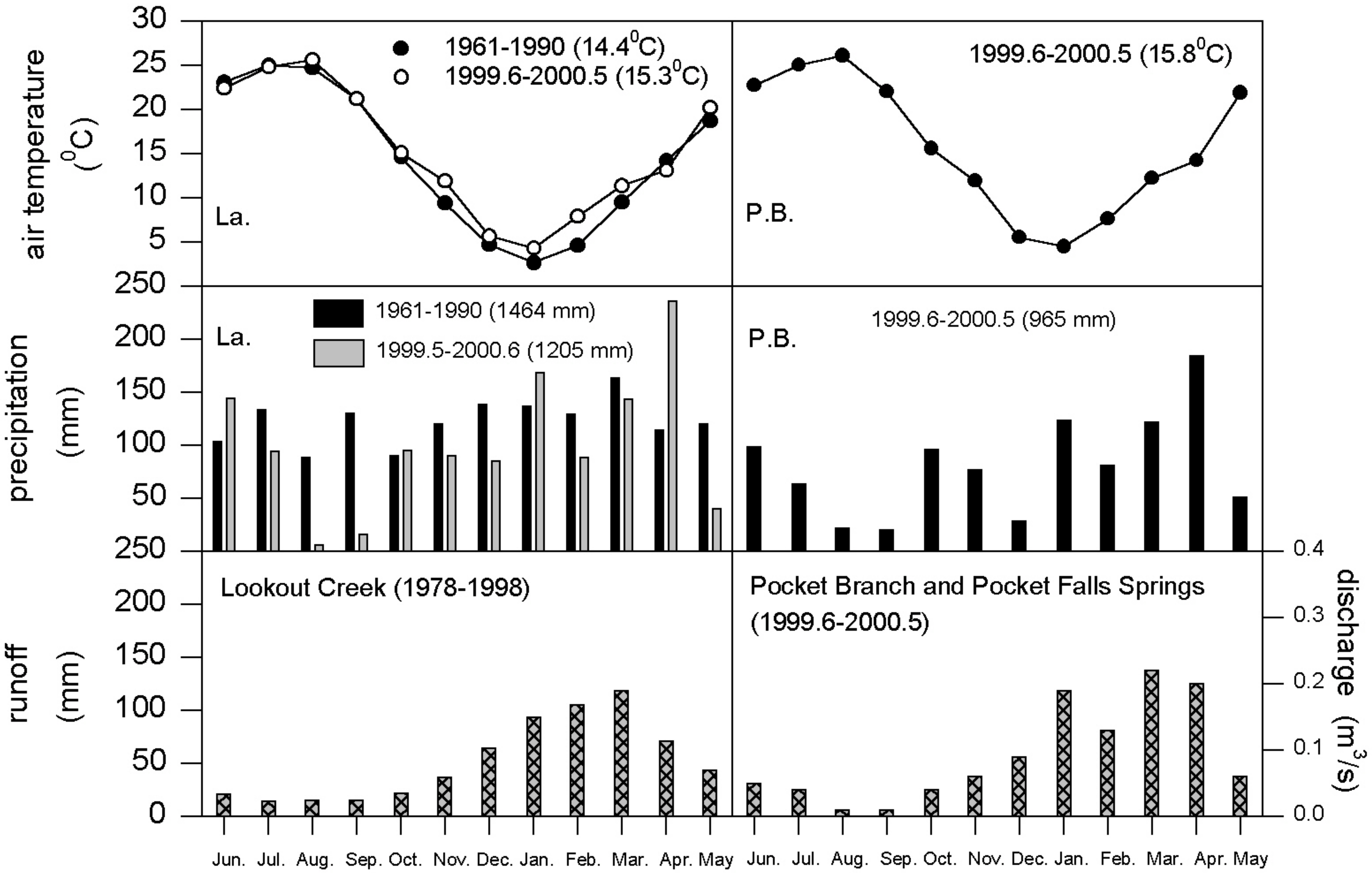

Figure 4.5. Climate at LaFayette (La.) and runoff at Lookout Creek gaging station near New England and climate and discharge at Pocket Branch (P.B.).

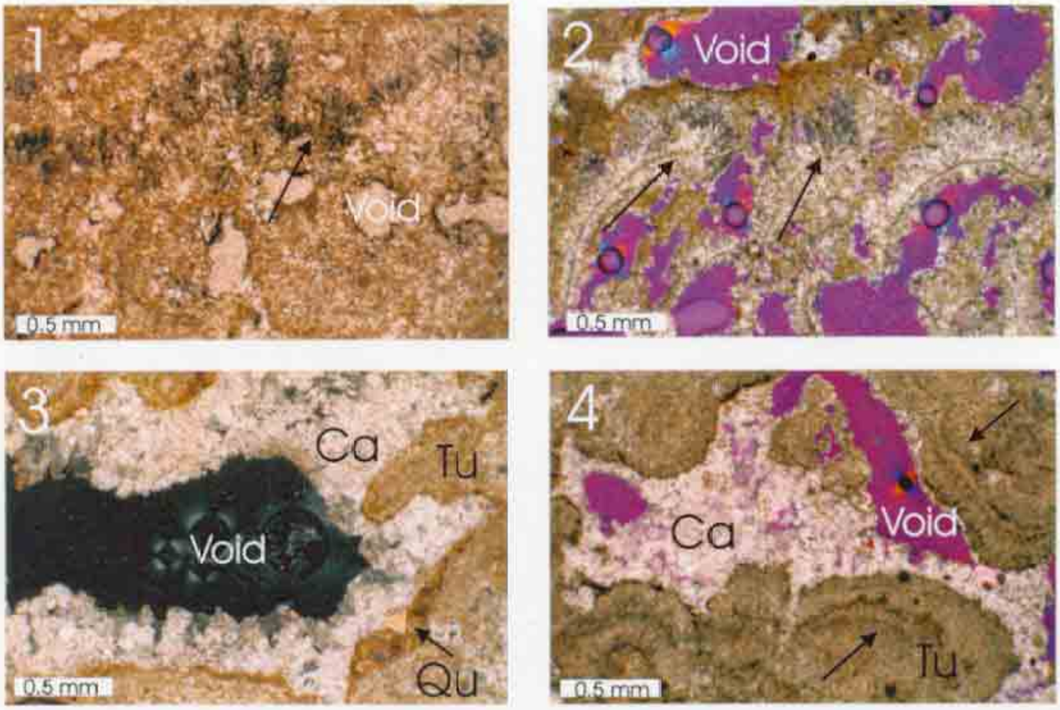

Figure 4.6. Photomicrographs of relict tufa from Pocket Branch:
tufas deposited around aquatic plants (1, 2 & 4), and primary tufa deposits (Tu) and secondary calcite crystals (Ca) (3 & 4), and quartz (Qu) (3).

Figure 4.7. Recent tufa deposition on nylon mesh (6 by 6 cm) and limestone rock tablet (diameter = 2.5 cm):
nylon mesh under flowing water (1),
nylon mesh under dripping water (2),
recent precipitates on tablet under flowing water (3), and
recent precipitates on nylon mesh under dripping water (4).

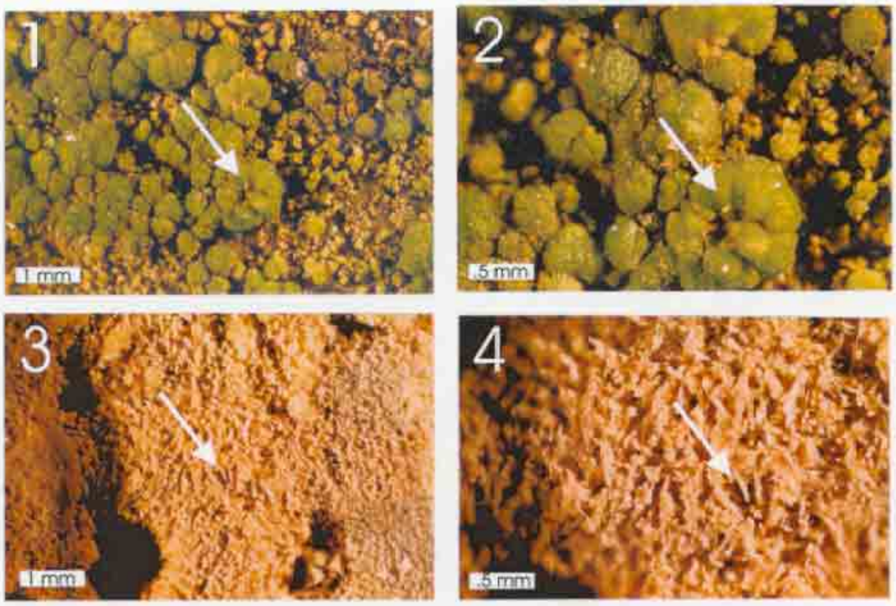

Figure 4.8. Recent tufa deposits:
"cluster" deposits precipitated under flowing water (1 & 2), and
"bundle" deposits precipitated under dripping water (3 & 4).

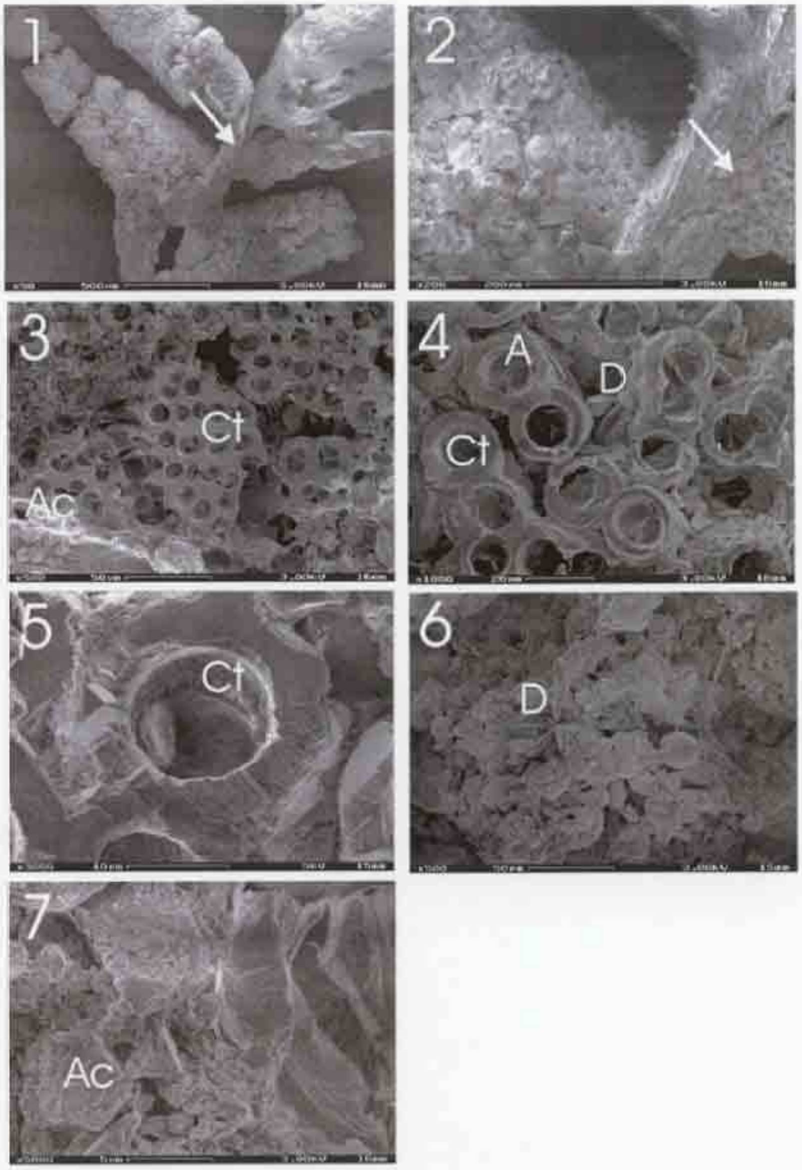

Figure 4.9. SEM photographs of recent tufa deposits:
(1&2) tufa precipitated on the plant material, and
(3-7) calcite tubes (Ct), algal cells (A), abiotic calcite crystals (Ac), and diatoms (D) within tufa deposits.

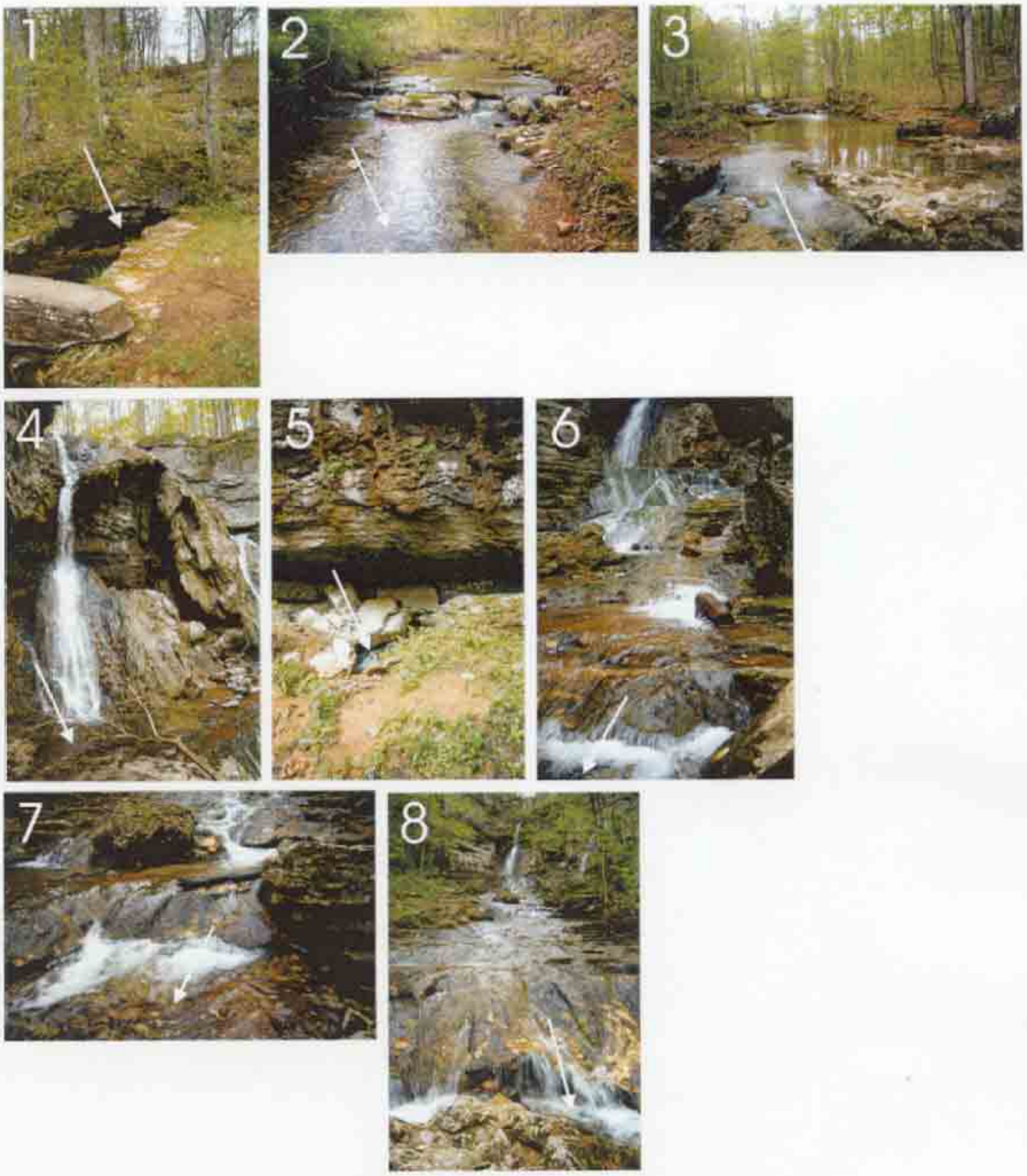

Figure 4.10. Water chemistry measurement sites at Pocket Branch:
(1) PBS, perennial spring above Pocket Falls,
(2) STI, sinking point of PBS water 50 m down valley,
(3) ST2, 100 m downstream of PBS, close to Pocket Falls,
(4) WF, base of Pocket Falls,
(5) PFS, perennial spring below Pocket Falls,
(6) TU1, 20 m downstream of PFS,
(7) TU2, 40 m downstream of PFS, and
(8) TU3, 62 m downstream of PFS.

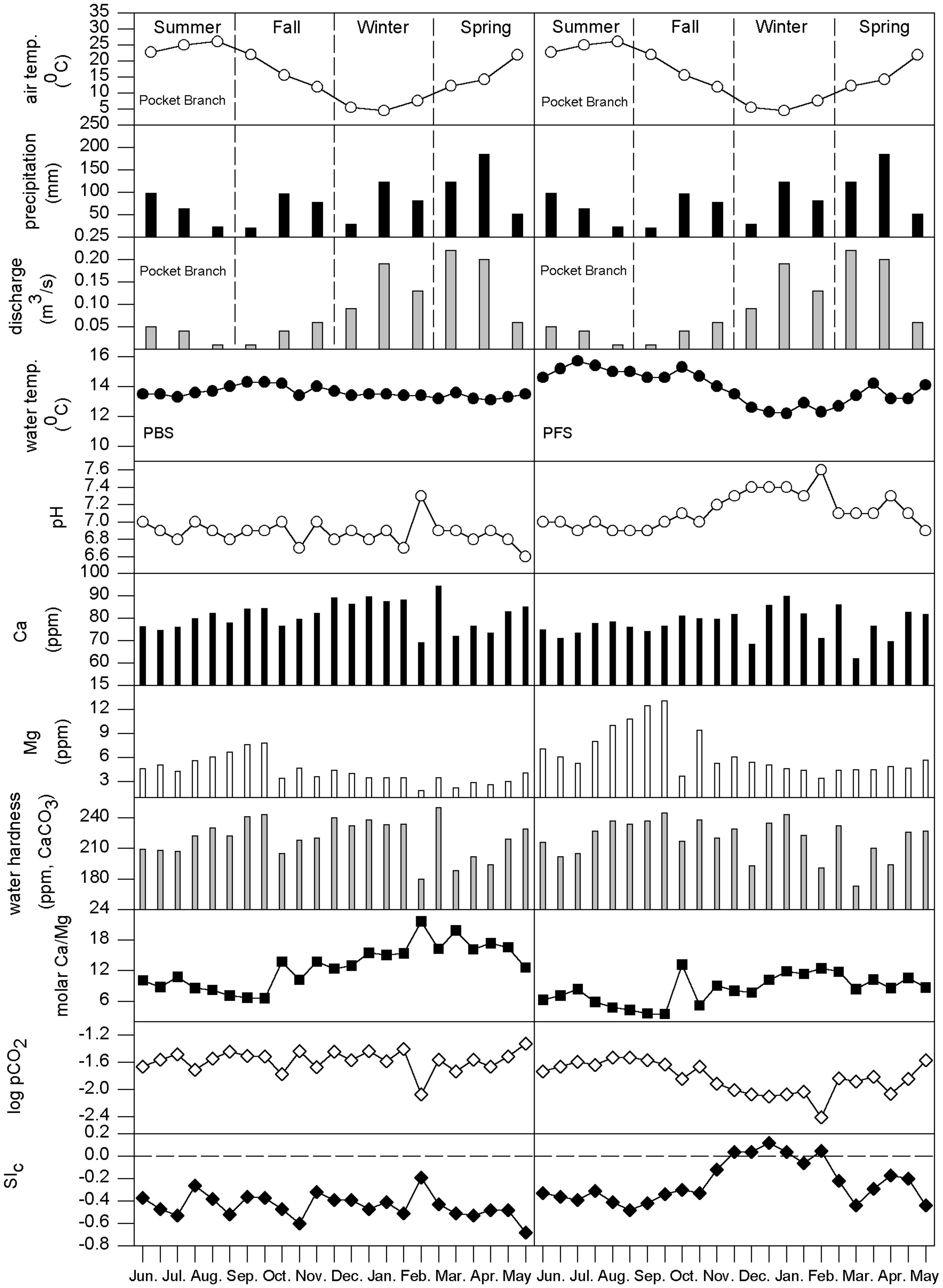

Figure 4.11. Climate and discharge at Pocket Branch and variations in water chemistry at Pocket Branch Spring (PBS) and Pocket Falls Spring (PFS) from June 1999 to May 2000.

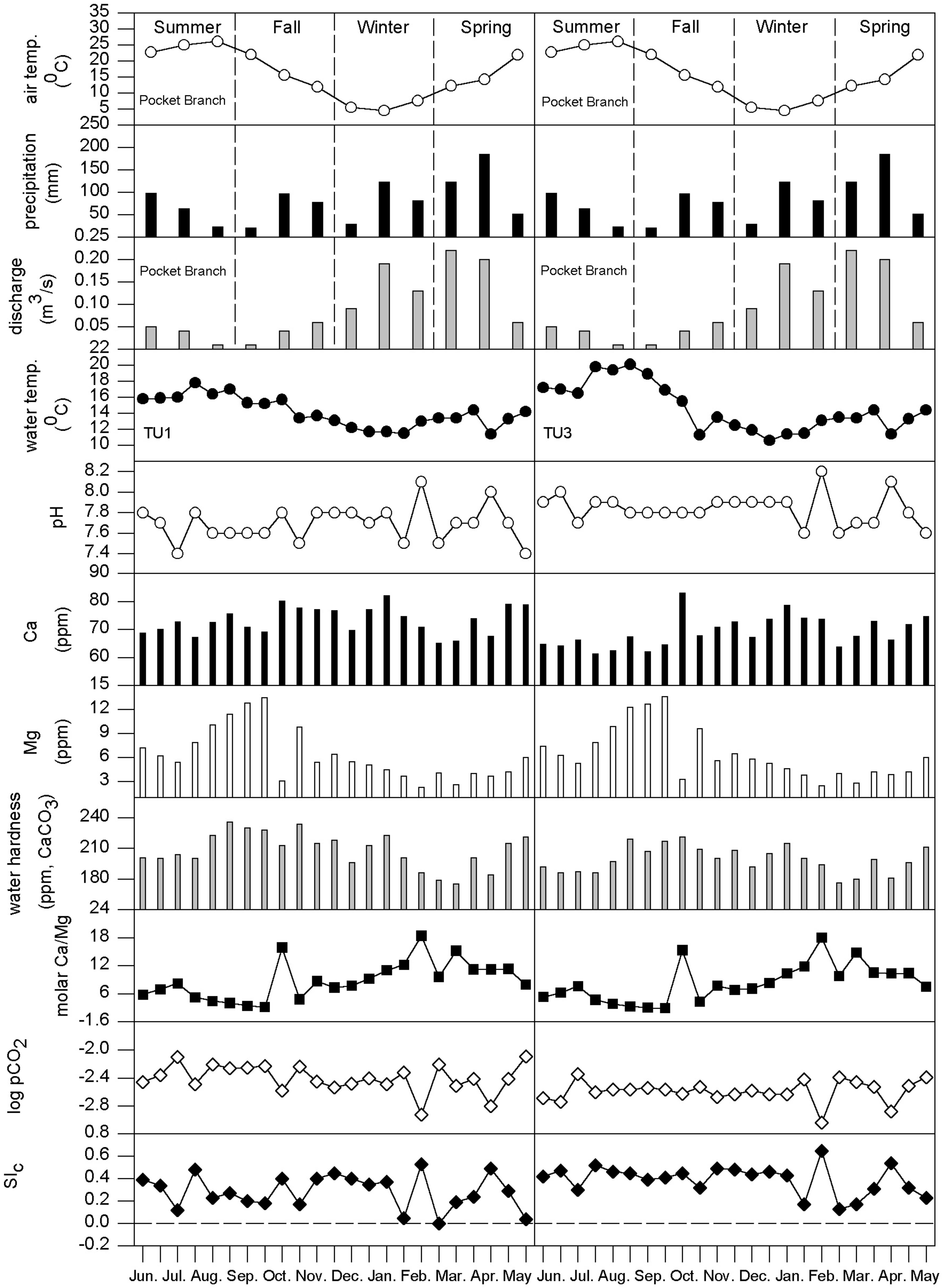

Figure 4.12. Climate and discharge at Pocket Branch and variations in water chemistry at TU1 and TU3 from June 1999 to May 2000.

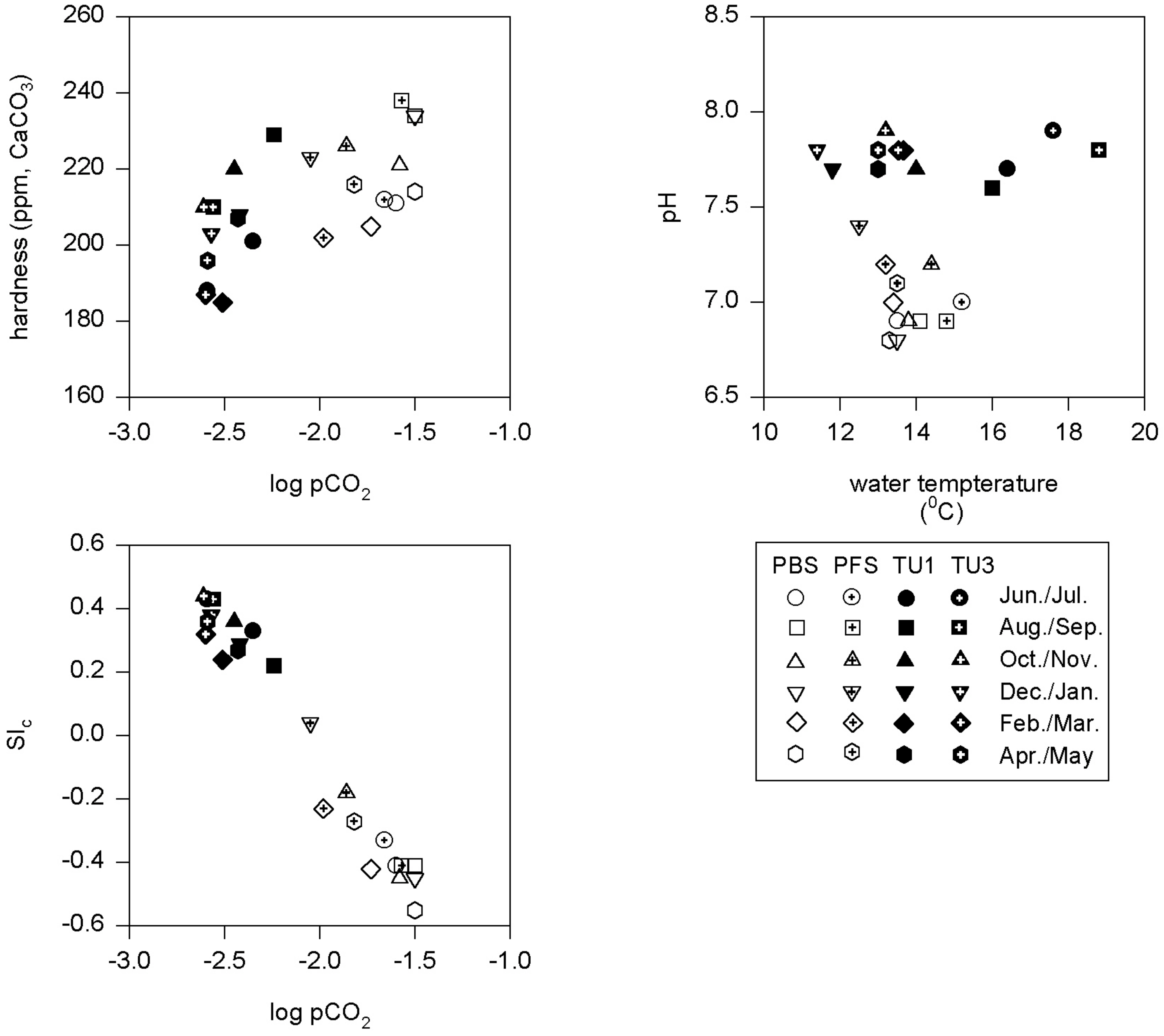

Figure 4.13. Bimonthly mean water temperature, pH, water hardness, log pCO$_2$ and SI$_c$ at PBS, PFS, TU1 and TU3 from June 1999 to May 2000.

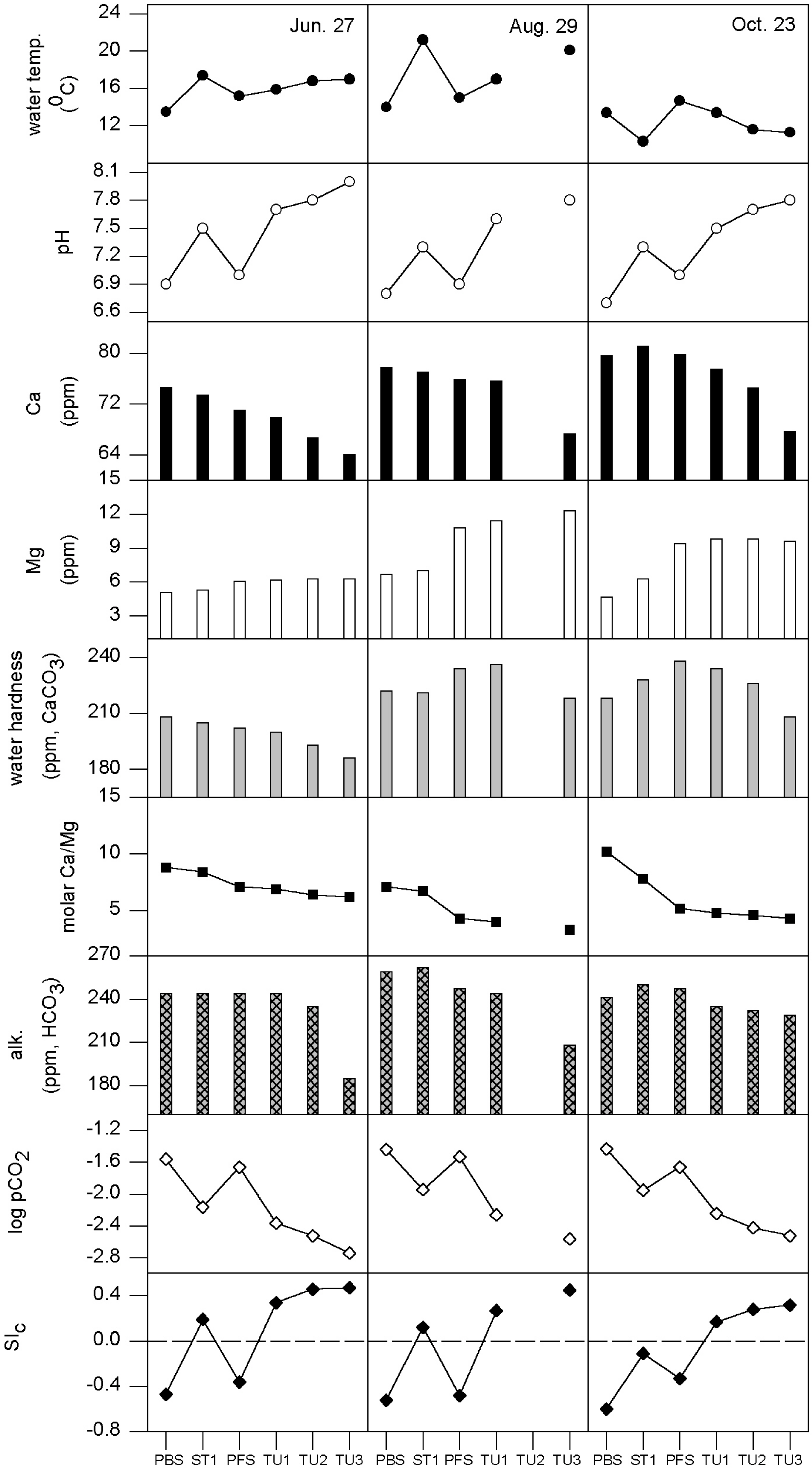

Figure 4.14. Spatial variations of water chemistry at Pocket Branch during the summer/fall dry season.

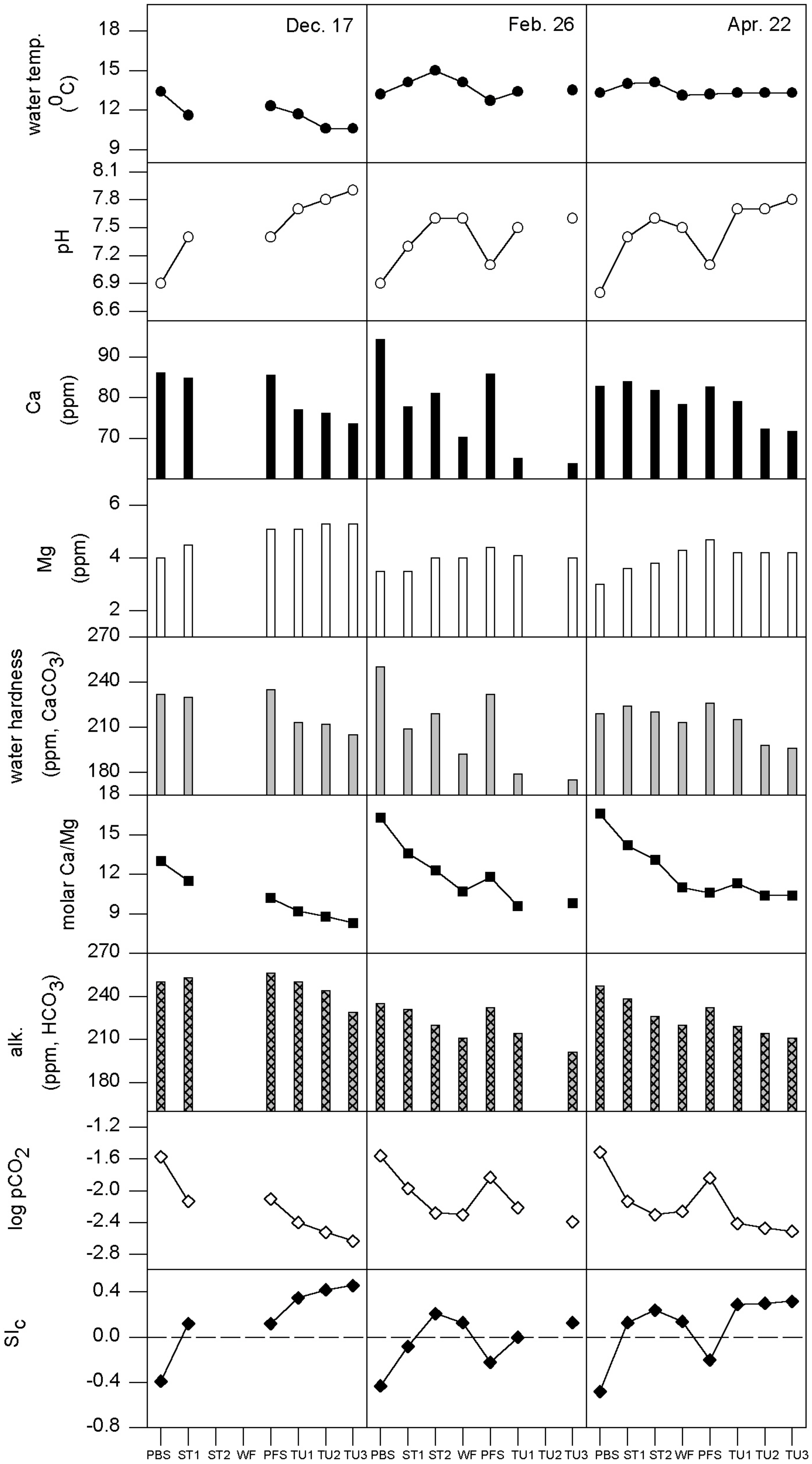

Figure 4.15. Spatial variations of water chemistry at Pocket Branch during the winter/spring wet season.

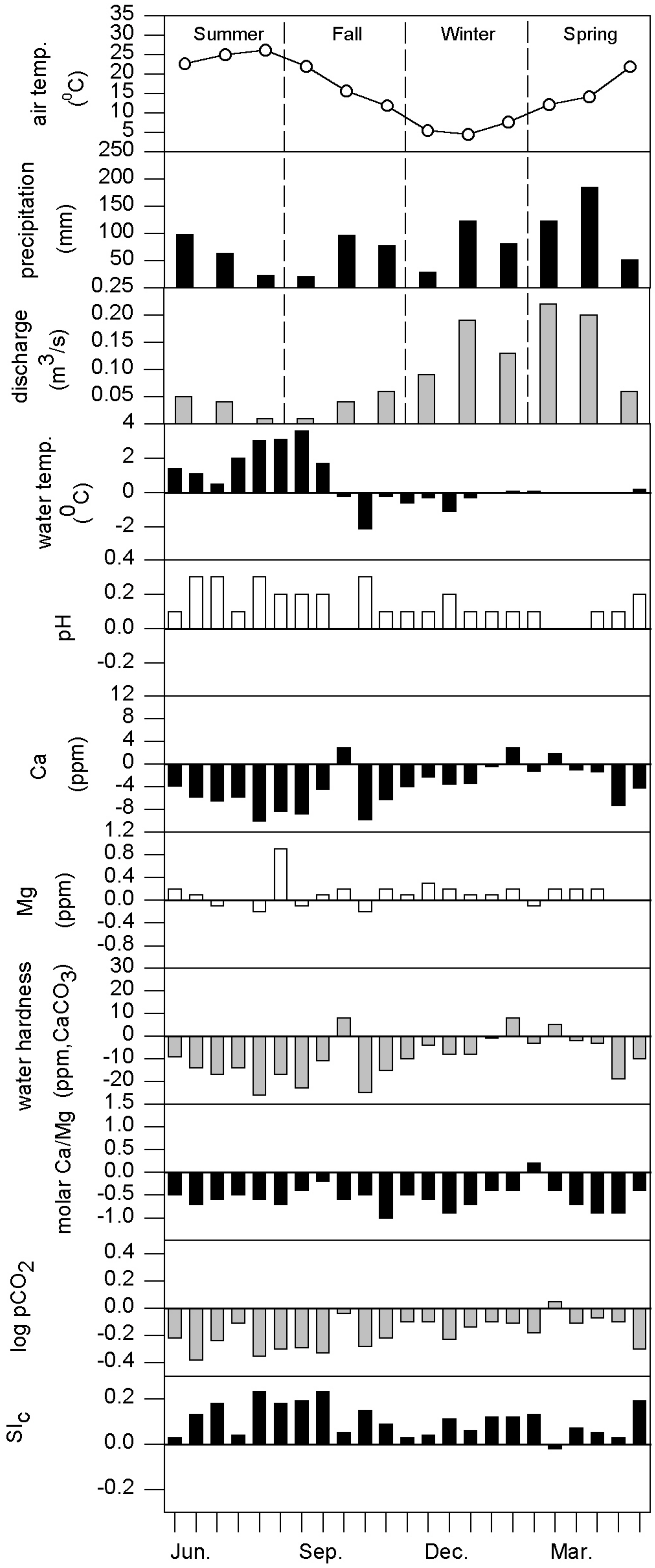

Figure 4.16. Climate and discharge at Pocket Branch and changes of water chemistry between TU1 and TU3 from June 1999 to May 2000.

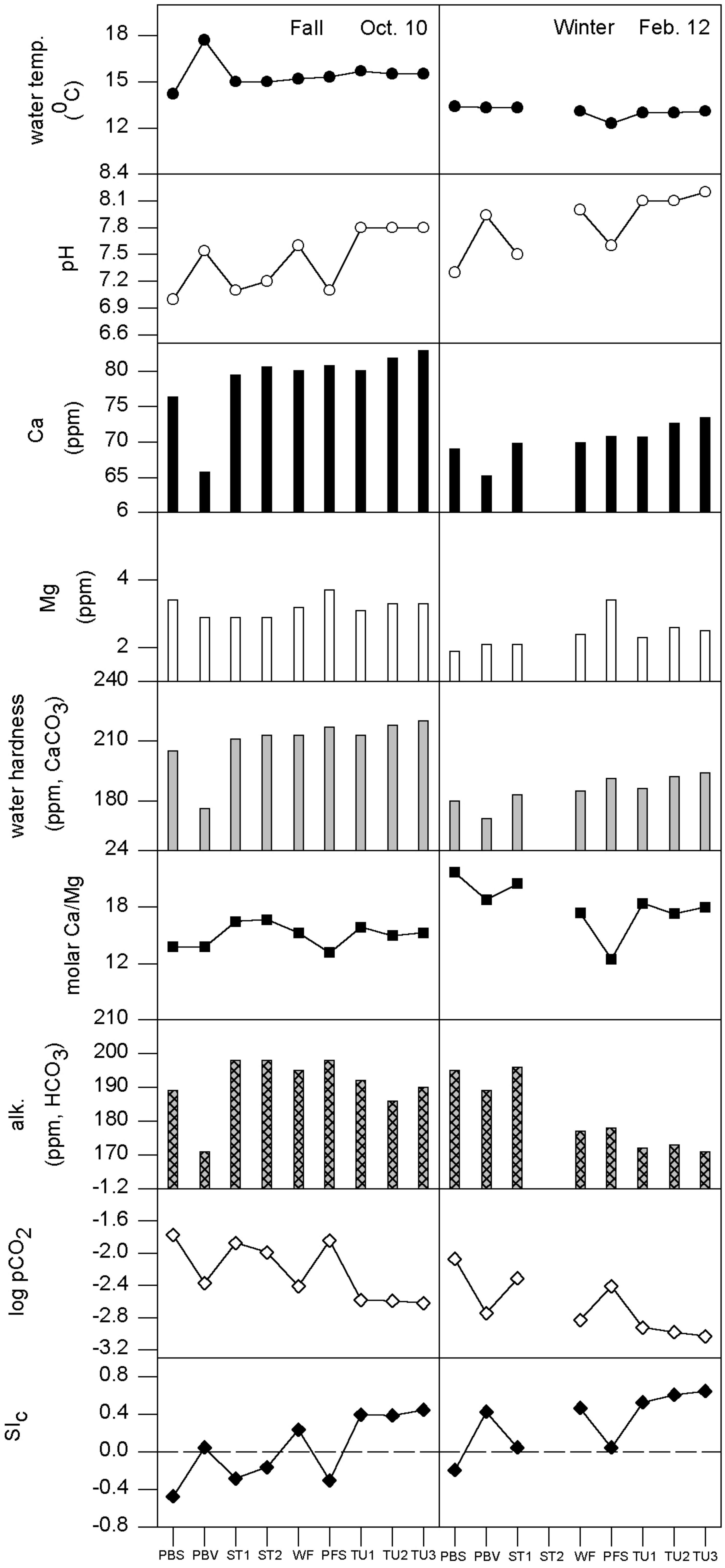

Figure 4.17. Spatial variations of water chemistry at Pocket Branch on Oct. 10 1999 and Feb. 12 2000.

CHAPTER 5

CONCLUSIONS

This chapter brings together the findings of Chapters 2 - 4 by comparing theory with empirical results. Water chemistry and denudation in karst terrains are influenced by temperature, rainfall, soil CO_2, runoff and aquifer type. The solubilities of CO_2 and limestone in water decrease as temperature increases. Although CO_2 and limestone are less soluble in warmer water, solution rates are faster and so the water is closer to saturation. Soil CO_2 is governed by temperature and rainfall. High temperature and high rainfall increase vegetation growth, producing high soil CO_2. Runoff also controls karst denudation; with denudation increasing with increasing runoff. Therefore, climate has long been regarded as the most important factor affecting water chemistry in karst areas. By contrast, the influence of aquifer type has not been fully studied. This research used both a theoretical and empirical approach to examine the influence of aquifer type on water hardness and karst denudation.

Aquifers in karst terrains are part of a continuous sequence, the end points being purely "open-system" (diffuse) and purely "closed-system" (conduit). Many, if not most, karst aquifers are intermediate between theses two extremes.

Theoretical data from Chapters 2 and 3 show that aquifer type may be extremely important in determining water hardness and karst denudation. Chapter 2 presents estimates of water hardness and denudation for "open" and "closed" ground water systems in tropical, temperate and cold regions with the water at "equilibrium".
The estimates were made using computer programs developed in FORTRAN language (Sheen, 2000). Chapter 3 goes a step further by presenting theoretical models for both

"equilibrium" and "disequilibrium" conditions in conduit and diffuse systems using PHREEQC (Parkhurst 1995).

The theoretical data of Chapters 2 and 3 support the argument that aquifer type is as important as temperature and soil CO_2 in influencing water hardness and karst denudation. The calculations show that water hardness should vary from 188 to 384 ppm in tropical karst, from114 to 297 ppm in temperate karst and from 61 to 231 ppm in cold karst. They also show that there are overlaps in water hardness between tropical, temperate and cold regions. This suggests that water hardness in cold and temperate regions can be greater than in tropical regions and implies that water hardness is not controlled by temperature and soil CO_2 alone.

The theoretical estimates of variations in water hardness and denudation in tropical, temperate and cold karst regions indicate the importance of aquifer type. According to theoretical calculations, aquifer conditions can produce a "within-region" change in water hardness of 170-200 ppm in tropical, temperate and cold regions, and can change denudation by 60-70 mm/ka (at a runoff of 1,000 mm). The "between-region" effect of temperature, and soil CO_2, on tropical, temperate and cold karsts is somewhat less, these variables causing a change of 100-180 ppm in hardness and 40-70 mm/ka in denudation.

These data indicate that aquifer type may have an equal or greater influence on water hardness and karst denudation than temperature and soil CO_2. This conclusion implies that global karst denudation patterns are also influenced as much by aquifer type as by temperature and soil CO_2. Aquifer type may explain some overlaps in water hardness and denudation rates in different climatic environments.

The empirical study outlined in Chapter 3 confirms that water hardness and karst denudation in the diffuse aquifer system (220 ppm and 39 mm/ka) of Pocket Branch, Georgia is significantly higher than in the conduit aquifer system (118 ppm and 30 mm/ka) of Lost Cove, Tennessee. Both are temperate regions with similar climate and geology. This research suggests that the difference in denudation between conduit-flow and diffuse-flow aquifers is substantial enough for aquifer type to be considered in any assessment of global denudation patterns.

The data from Chapter 3 show that karst denudation is highly seasonal being controlled by runoff (i.e. denudation is higher during the wet season), and is not controlled by temperature and/or soil CO_2, which we presume are higher in summer based on other studies in the region. However, in areas of similar runoff, denudation is controlled by aquifer type.

As tufa is deposited by some diffuse systems, and as this reduces denudation, a study was made of tufa deposition at Pocket Branch, Pigeon Mountain, Georgia. This study is outlined in Chapter 4. It showed that re-precipitation of Ca was minor (summer/fall: 9% and winter/spring: 4%) although it occurred throughout the study year. Heavy runoff diluted spring waters causing some erosion of tufa (and therefore higher denudation rates) during very short periods of the year. The detailed study found that although there is some minor re-precipitation of $CaCO_3$ in diffuse aquifer systems, denudation is still greater in them than in conduit systems.

The theoretical models are supported by the empirical data. The overall conclusion is that aquifer type should not be ignored in considering spatial variations in denudation rates and water chemistry around the world. In assessing factors responsible for karst landform morphology, denudation rates alone are not sufficient as these are not entirely climate dependent but are greatly influenced by aquifer type. What is needed in the field of karst landform studies are data on the frequency and spatial distribution of aquifer types. These data would allow us to determine if conduit aquifers are more common in tropical areas where rainfall intensities are high, and whether diffuse aquifers are more common in temperate areas where rainfall is generally less intense.

REFERENCES

Parkurst, DL. 1995. User s Guide to PHREEQC- A Computer Program for Speciation, Reaction-Path, Advective-Transport, and Inverse geochemical Calculations. Water-Resources Investigations Report 95-4227. U.S. Geological Survey, Lakewood,Colorado.

Sheen, SW. 2000. A world model of chemical denudation in karst terrains. *Professional Geographer* **52**: 397-406.

Smith, DI and Atkinson, TC. 1976. Process, landforms and climate in limestone regions. In *Geomorphology and climate*, ed. Derbyshire, E. 367-409. New York: John Wiley.